PROSTAGLANDIN Gβγ SIGNALING STIMULATES GASTRULATION MOVEMENTS BY LIMITING CELL ADHESION THROUGH SNAIL STABILIZATION

By

Christina Koo Yang Speirs

Dissertation

Submitted to the Faculty of the

Graduate School of Vanderbilt University

in partial fulfillment of the requirements

for the degree of

DOCTOR OF PHILOSOPHY

in

Biological Sciences

December, 2009

Nashville, Tennessee

Approved:

Professor Lilianna Solnica-Krezel

Professor James G. Patton

Assistant Professor Joshua T. Gamse

Assistant Professor Douglas P. Mortlock

Associate Professor Bruce Appel, University of Colorado, Denver

To my mother, Karen Kyungmo Koo Haas. Thank you for the constancy of your love and support. It overwhelms me still.

ACKNOWLEDGEMENTS

First, I would like to thank my mentor, Lila Solnica-Krezel. My best experiments often germinated in your mind, and you have shown me that the finest qualities of science are borne of collaboration, magnified and refined from one person to another. Your intelligence, unflagging commitment to science, unwavering integrity, grace, and diplomacy have rightfully earned you your flawless reputation. I have benefited from working with you and will continue to do so, for the rest of my career.

To my committee members, Drs. Bruce Appel, Josh Gamse, Doug Mortlock, and Jim Patton: you have selflessly offered me your expertise and creativity again and again disguised as "feedback." It has been a privilege to be under your tutelage.

To my lab members, both past and present: I have reaped so much from all of you throughout my time in the lab. The LSK lab has truly been like an adopted family to me. To Fang, my den mother: you are a force of nature, taking care of everyone (including me), raising a family, and still completing projects and papers with bravado. If they ever bottle up your energy, I'll be the first in line. Diane, you have mentored me both scientifically and emotionally through awful time-lapses and confusing results. Your encyclopedic knowledge of biology and your unending passion for the difficult, technically challenging questions have inspired me. Thank you, Adi, for your critical eye and your passion for science. You were one of the main reasons I joined the lab, and if I could be one-tenth as passionate about science and as logical about what is necessary to get to the heart of a scientific question, I would be very, very lucky.

To Xin-Xin and Dan, my lab 'bros,' I have enjoyed all of our lunches and squabbling, even if I deny it. I look forward to knowing you both for many more years to come. I want to thank Jen, Terry, Isa, and Yinzi, my benchmates over the years. My talks with all of you were welcome distractions to a bad day or unfertilized embryos. Seok-Hyung, you have been my outlet for practicing my toddler-like, rudimentary Korean, but other than your occasionally puzzled looks, you have never made fun of me. Thank you for that, and for being a scientist with awesome technical expertise, and the unfailing ability to pick out my (or anyone's) weakest piece of data. To the rest of the people I have met in the lab; Chunyue, Amayra, Encina, Xin, Atsushi, Jade, Simon, Aurelie, and Haiting, you have all been a pleasure for me to get to know. I am sure I will hear many exciting stories about your work in the future. I also thank the amazing "caretakers of the lab and the fish," Amy, Heidi, Nick and Maya. Were it not for you, I would still be stumbling over my first experiments, waiting for reagents to arrive.

Thanks to the Department of Biological Sciences. Not only were you always there when I had administrative issues to solve, but your generous funding and support allowed me to attend both a meeting in Amsterdam and a course in Woods Hole, MA. Those experiences enriched my graduate career in a way I will never forget.

Thanks to the Medical Scientist Training Program for their support throughout my seven years thus far. I especially thank Terry Dermody, Susan Wente, and Jim Bills for the leadership roles they perform astoundingly well.

Thanks to my friends in Nashville. I have known most of you since the beginning of medical school seven years ago. It's been a long road, and I have always enjoyed the company, whether it was to encourage, inspire, or complain.

To Ben: You are an amazing man, and I am lucky to have you in my life. Thank you for your love, your enthusiasm, your support, your generosity, and your pancakes. I love you.

Finally, to my family: I know I may be somewhat biased, but it seems like I have stumbled onto the best relatives in the world. I love love love all of you, and I will always be here for all of you. Steph, you are an amazing woman that I will probably call Ms. President someday. I have loved living with you and sharing our lives, even if it's just on the phone now. Andy, you are the sage in my life. Your brilliance, wit, humor, and generosity are something that will enrich anyone's life as soon as they meet you. Papa Joe, you are an excellent human being, and we are lucky to have your love, loyalty, integrity, honor, and your untouchable motorcycling skills. If you and I go on a road trip someday, please try not to leave me in the dust. And lastly, to Marmee: if at the end of my life, I have loved and protected and fought for my family as much as you have, living through difficult and seemingly insurmountable situations with as much intelligence, grace, energy, faith, and wacky humor, I will have everything I wanted. Thank you for everything you have sacrificed and have done for us. I love you so much.

TABLE OF CONTENTS

LIST OF FIGURES

LIST OF TABLES

LIST OF ABBREVIATIONS

μg	microgram
μL	microliter
μm	micrometer
A	Animal pole
AGM	Aorta/Gonad/Mesonephros region
ALM	Anterior lateral mesoderm
APC	Adenomatous polyposis coli
β-ARK	β-adrenergic receptor kinase
BCC	Basal cell carcinoma
CAT	Chloramphenicol Acetyltransferase
CHO	Chinese hamster ovary
CLASP	Cytoplasmic linker-associated proteins
CK	Casein kinase
DA	Dorsal aorta
dpf	Days post fertilization
ECM	Extracellular matrix
EGR1	Early growth response factor 1
EGF	Epidermal growth factor
ENU	*N*-ethyl *N*-nitrosourea
EVL	Enveloping layer
FAK	Focal adhesion kinase
FAP	Familial Adenomatous Polyposis

FCS	Fetal calf serum
GEF	Guanine nucleotide exchange factor
GFP	Green fluorescent protein
GPCR	G protein-coupled receptor
HCC	Hepatocellular carcinoma cells
HEK	Human embryonic kidney
HSPG	Heparan sulfate proteoglycan
HSC	Hematopoietic stem cell
HLA	Human leukocyte antigen
ICM	Intermediate cell mass
LEF/TCF	Lymphoid enhancer-binding factor/T cell-specific transcription factor
LPA	Lysophosphatidic acid
LRP	Lipoprotein receptor-related protein
MAPEG	Membrane-associated proteins involved in Eicosanoid and Glutathione metabolism
MMP	Matrix metalloproteinase
MO	Antisense morpholino oligonucleotide
MOMP	Mitochondrial outer membrane permeabilization
MT	Microtubule
MZ	Maternal zygotic
NET	Neuroendocrine tumor
NSAID	Non-steroidal anti-inflammatory drugs
NSCLC	Non-small cell lung cancer
PAF	Platelet Activating Factor
PAN	Puromycin Aminonucleoside Nephrosis

15-PGDH	15-hydroxyprostaglandin dehydrogenase
PKA	Protein kinase A
PKB	Protein kinase B
PKC	Protein kinase C
PCV	Posterior cardinal vein
PLM	Posterior lateral mesoderm
qRT-PCR	Quantitative real-time PCR
RGS	Regulator of G-protein signaling
shRNA	Small hairpin RNA
siRNA	Small interfering RNA
TILLING	Targeting induced local lesions in genomes
TGF-β	Tumor growth factor-β
YSL	Yolk syncytial layer
ZNR	Zebrafish nodal-related
ZO1	Zonula occludens 1

ABSTRACT

Prostaglandin E_2 (PGE_2) influences many processes in vertebrates, including development, homeostasis, and disease through its GPCRs EP receptors 1-4. PGE_2 regulates gastrulation movements during zebrafish embryogenesis, but how it does so was previously unclear, as PGE_2 can affect cell adhesion, motility, proliferation, and survival. Our studies reveal that the loss of PGE_2 synthesis impairs all gastrulation movements, epiboly, internalization, convergence, and extension, in part due to increased cell adhesion in the embryo. The increase of tight junctions (ZO1) and adherens junctions (E-cadherin) occurs in a germ layer-dependent fashion. In the mesendoderm, PGE_2 modulates E-cadherin by stabilizing Snail through the inhibition of Gsk3β by a novel interaction with the Gβγ subunits (in collaboration with K. Jernigan and E. Lee). Moreover, the reduction of PGE_2 synthesis results in an endoderm deficiency without significant effect on the mesoderm, possibly due to decreased Nodal signaling. Finally, we present preliminary characterization of a fish harboring a reverse genetics TILLING-generated *ep4a* nonsense mutation that strongly depletes function of the gene, but manifests no apparent phenotype. In conclusion, our findings suggest that PGE_2 signaling can coordinate cell fate specification and movement, in part through its negative regulation of cell adhesion in zebrafish gastrulae.

CHAPTER I

INTRODUCTION

Prostaglandins influence many aspects of cell behavior: proliferation, survival, fate specification and movement. The regulation of these processes downstream of prostaglandin signaling has been described during adult homeostasis and diseases such as cancer. Here, I will discuss these studies and introduce an emerging area in the prostaglandin field: the role of prostaglandins during developmental processes such as gastrulation, hematopoiesis, and vasculogenesis, involving conserved signaling mechanisms that have been implicated in other physiological and pathological contexts.

Lipids as Bioactive Mediators

Lipid mediators are secreted signaling molecules that contribute to the maintenance of homeostasis, which is underscored by their dysregulation in diseases such as metabolic syndromes, inflammatory dysfunction, and cancer. The importance of lipid mediators as signaling molecules is inferred from their evolutionary amplification in the phylum Chordata, particularly in vertebrates (Hla, 2005). Prior to the emergence of the chordates, lipids primarily functioned as structural components of the membrane. Lipids that have been evolutionally recruited as cell-cell signaling mediators include the eicosanoids, lysophospholipids, ether lipids, and endocannabinoids (**Fig. 1-1A**). These families collectively affect processes as diverse as cell proliferation, death, fate specification, differentiation, and migration (Hla, 2005). Additionally, whereas

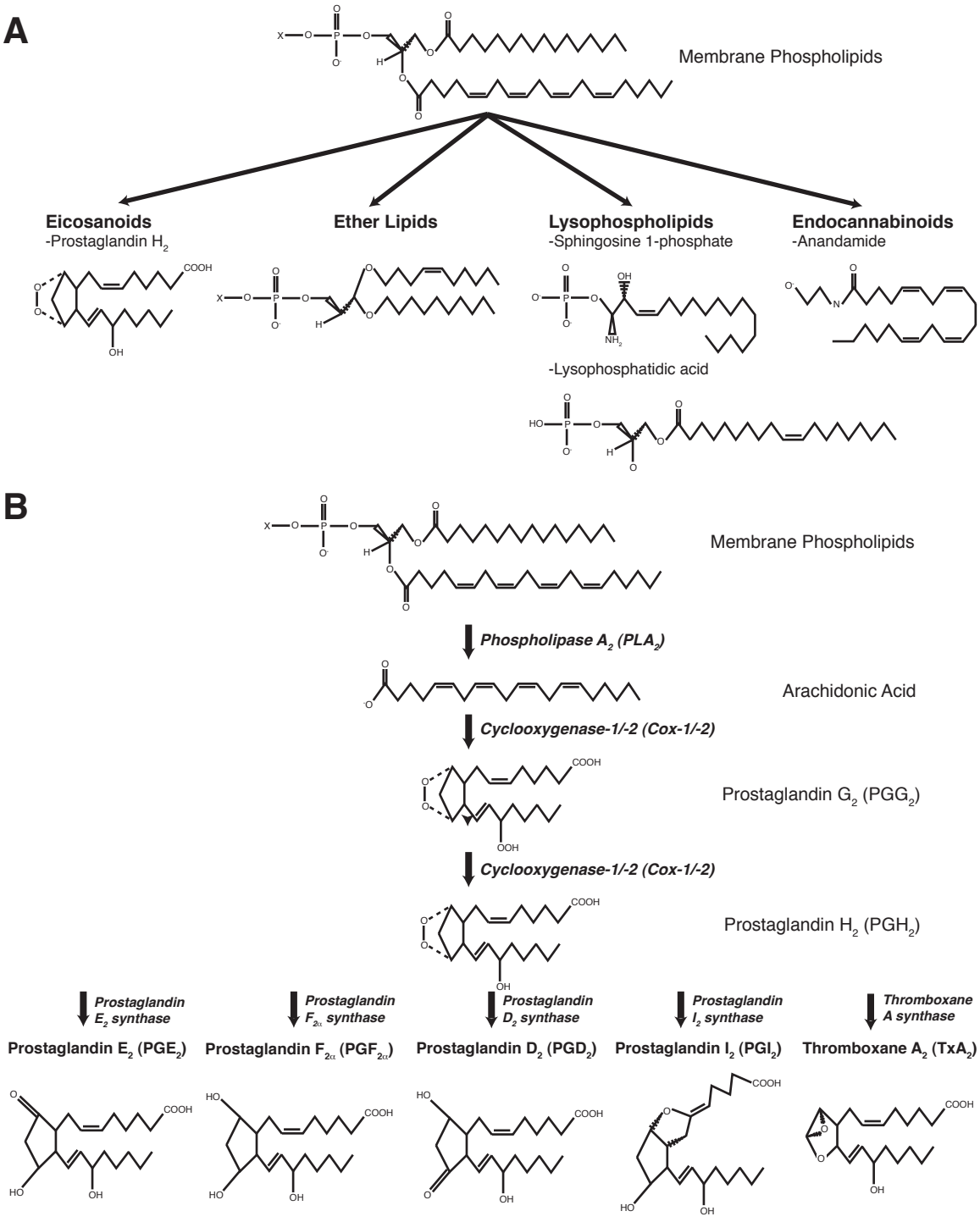

Figure 1-1. Lipid mediator and prostaglandin synthesis. (A) Four classes of lipid mediators are synthesized from membrane phospholipids. These lipids represent a chordate signaling repertoire that is mediated by G protein-coupled receptors (GPCRs). (B) Prostaglandin synthesis begins with the formation of Arachidonic Acid and Prostaglandin G_2/H_2, then the five active prostanoids are each synthesized by a specific synthase enzyme.

the same lipid can have many different effects, different families of lipid mediators often share downstream targets and effector molecules, resulting in an interconnected signaling network among the different ligands (Wymann and Schneiter, 2008).

The Synthesis and Signaling of Prostaglandins

The eicosanoid family is composed of the prostanoids (prostaglandins, prostacyclins, and thromboxanes) and the leukotrienes (Wymann and Schneiter, 2008). Eicosanoids arise from C20-polyunsaturated fatty acids that are liberated from membrane phospholipids or diacylglycerol, usually by the action of Phospholipase A_2 (**Fig. 1-1B**). Some of the C-20 fatty acids are synthesized by Lipoxygenase to form leukotrienes, whereas others are formed into the precursor prostaglandin PGG_2 by the Prostaglandin-Endoperoxide synthase (PTGS)/Cyclooxygenase (COX) enzymes (For the nomenclature of human, mouse and zebrafish genes and proteins, see **Table 1-1**). PGG_2 is then reduced to form PGH_2, which generates the five products PGE_2, PGD_2, $PGF_{2\alpha}$, Prostacyclin (PGI_2), and Thromboxane A_2 (TxA_2) through the action of prostanoid-specific synthases (**Table 1-1**) **(Fig. 1-1B)**. For example, PGE_2, our prostaglandin of interest, is synthesized by the Prostaglandin E synthase (PTGES) (**Table 1-1**). COX peroxidase enzymes are the rate-limiting step of prostaglandin synthesis. They are located in the lumen of the endoplasmic reticulum as well as in the inner and outer nuclear membranes (Hla, 2005; Zhu et al., 2006). There are two *COX* genes: *COX1*/*PTGS1* and *COX2*/*PTGS2* (**Table 1-1**). COX1 is considered to be a housekeeping enzyme that maintains homeostasis. In addition, it appears to be the preferred regulator of developmental events (Grosser et al., 2002; Cha et

Component	Human		Mouse		Zebrafish	
	G	P/L	G	P/L	G	P/L
Prostaglandin E2	--------	PGE_2	--------	PGE_2	--------	PGE_2
Prostaglandin F2 alpha	--------	$PGF_{2\alpha}$	--------	$PGF_{2\alpha}$	--------	$PGF_{2\alpha}$
Prostaglandin I2	--------	PGI_2	--------	PGI_2	--------	PGI_2
Prostaglandin D2	--------	PGD_2	--------	PGD_2	--------	PGD_2
Thromboxane A2	--------	TxA_2	--------	TxA_2	--------	TxA_2
Cyclooxygenase 1/Prostaglandin-endoperoxide synthase 1	*COX1/PTGS1*	COX1/PTGS1	*Cox1/Ptgs1*	COX1/PTGS1	*cox1/ptgs1*	Cox1/Ptgs1
Cyclooxygenase 2/Prostaglandin-endoperoxide synthase 2	*COX2/PTGS2*	COX2/PTGS2	*Cox2/Ptgs2*	COX2/PTGS2	*cox2/ptgs2*	Cox2/Ptgs2
Prostaglandin E synthase (m=microsomal; c=cytosolic)	*PTGES*	PTGES	*Ptges*	PTGES	*ptges*	Ptges
Prostaglandin E2 Receptor, Subtype EP1	*EP1/PTGER1*	EP1/PTGER1	*Ep1/Ptger1*	EP1/PTGER1	*ep1/ptger1*	Ep1/Ptger1
Prostaglandin E2 Receptor, Subtype EP2	*EP2/PTGER2*	EP2/PTGER2	*Ep2/Ptger2*	EP2/PTGER2	*ep2/ptger2*	Ep2/Ptger2
Prostaglandin E2 Receptor, Subtype EP3	*EP3/PTGER3*	EP3/PTGER3	*Ep3/Ptger3*	EP3/PTGER3	*ep3/ptger3*	Ep3/Ptger3
Prostaglandin E2 Receptor, Subtype EP4	*EP4/PTGER4*	EP4/PTGER4	*Ep4/Ptger4*	EP4/PTGER4	*ep4/ptger4*	Ep4/Ptger4
Snail Homolog 1	*SNAI1*	SNAI1	*Snai1*	SNAI1	*snai1a*	Snai1a
	--------	---------	--------	---------	*snai1b*	Snai1b
Snail homolog 2/Slug	*SNAI2*	SNAI2	*Snai2*	SNAI2	*snai2*	Snai2
E-cadherin/Cadherin 1/type 1, Epithelial cadherin	*CDH1*	CDH1	*Cdh1*	CDH1	*cdh1*	Cdh1
Phosphoinositide-3-kinase, alpha polypeptide	*PIK3α/PIK3CA*	PIK3α/PIK3CA	*Pik3α/Pik3ca*	PIK3α/PIK3CA	*pik3α/pik3CA*	Pik3α/Pik3ca
Phosphoinositide-3-kinase, gamma polypeptide	*PIK3γ/PIK3CG*	PIK3γ/PIK3CG	*Pik3γ/Pik3cg*	PIK3γ/PIK3CG	*pikγ/pik3CG*	Pik3γ/Pik3cg
Glycogen Synthase Kinase 3, alpha	*GSK3α*	GSK3α	*Gsk3α*	GSK3α	*gsk3α*	Gsk3α
Glycogen Synthase Kinase 3, beta	*GSK3β*	GSK3β	*Gsk3β*	GSK3β	*gsk3β*	Gsk3β
G protein, alpha stimulating	*$G\alpha_S$/GNAS*	$G\alpha_S$/GNAS	*$G\alpha_S$/Gnas*	$G\alpha_S$/GNAS	*$g\alpha_S$/gnas*	$G\alpha_S$/Gnas
G protein, alpha inhibiting	*$G\alpha_I$/GNAI*	$G\alpha_I$/GNAI	*$G\alpha_I$/Gnai*	$G\alpha_I$/GNAI	*$g\alpha_I$/gnai*	$G\alpha_I$/Gnai
G protein, beta 1 gamma 2.	*$G\beta_1\gamma_2$*	$G\beta_1\gamma_2$	*$G\beta_1\gamma_2$*	$G\beta_1\gamma_2$	*$g\beta_1\gamma_2$*	$G\beta_1\gamma_2$

(G) Gene: DNA, RNA (P/L) Protein or Lipid

Table 1-1. Nomenclature of relevant genes in human, mouse, and zebrafish.

al., 2006). By contrast, COX2 is upregulated during inflammation and is associated with tumorigenesis. COX1 and COX2 also interact with different substrates: COX1 prefers arachidonic acid, whereas COX2 can utilize 2-arachidonyl glycerol and anadamide as substrates (Hla, 2005). The COX enzymes are not widespread outside the phylum Chordata; no *COX* homologs have been identified in the *D. melanogaster*, *C. elegans*, *S. cerevesiae*, and *D. discoideum* genomes (Hla, 2005). When *COX* is present within older phyla, prostanoids are synthesized not for signaling purposes, but for specialized functions such as self-defense in some sea coral species (Hla, 2005).

The induction of bioactive lipids as signaling molecules that participate in cell-cell communication probably did not occur until the appearance of the lipid **G p**rotein-**C**oupled **R**eceptors (GPCRs) in the phylum Chordata. GPCRs link lipid mediators to second messenger systems within the cell, allowing lipid mediators to influence cell-cell communication (Hla, 2005). Therefore, the refinement of the vertebrate physiology; its immune, circulatory, nervous, and metabolic systems, and the increasing complexity of the ontogeny required to develop these sophisticated systems in vertebrates may have required the increasing recruitment of lipid mediators to expand the signaling repertoire already provided by protein signaling.

The prostanoid family acts upon physiological processes such as vascular smooth muscle contraction, platelet aggregation, pain, inflammation, fever, uterine contraction, and immune system modulation (Hla, 2005). Of all the prostaglandins, PGE_2 performs the greatest diversity of functions - regulating physiology, development, and disease progression. Specifically, PGE_2 has been shown to influence inflammation, pain, fever, reproductive fitness, bone

metabolism, urogenital tract function, atherosclerotic plaque rupture, and the progression of Alzheimer's disease (Regan, 2003; Hla, 2005).

Synthesis of PGE_2 requires the PTGES enzyme, which belongs to the **m**embrane-**a**ssociated **p**roteins involved in **E**icosanoid and **G**lutathione metabolism (MAPEG) family. Three genes code for three PTGES forms: the first, cPTGES, is found in the cytosol, but the other forms, mPTGES1 and mPTGES2, are isolated in the microsomal fraction. There are two biosynthetic PGE_2 arms; the COX-1-cPTGES and the COX2-mPTGES, which allow for the short-term and long-term induction of PGE_2 synthesis, respectively (Murakami et al., 2002; Regan, 2003). Which biosynthetic axis is initiated depends on the type of stimulation and the cell type being stimulated. Short-term PGE_2 synthesis (on the order of minutes) is needed for pain, gastric protection, and neuronal function. By contrast, sustained PGE_2 synthesis (on the order of hours) influences bone metabolism, inflammation, pregnancy, Alzheimer's disease, and tumorigenesis (Murakami et al., 2002). mPTGES2 is associated with the induction of *COX2* expression (Regan, 2003). Indeed, cotransfection of both *mPTGES* and *COX2* results in greater PGE_2 synthesis than either enzyme alone (Murakami et al., 2002). Interactions between mPTGES and COX2 may occur in the perinuclear region, where both components are localized. mPTGES likely plays a pro-inflammatory role, as it can be induced following *in vitro* and *in vivo* stimulation with Ca^{2+} mobilizers and proinflammatory and hormonal stimuli, such as IL-1β, TNFα, LPS, β-Amyloid, PMA, and Gonadotropin (Murakami et al., 2002). Therefore, the expression of mPTGES, like COX2, is induced as part of the inflammatory response. Lastly, the μ class of the microsomal **G**lutathione-**S**-

Transferase (GST) family of enzymes non-specifically catalyzes the conversion of PGH_2 to PGE_2, PGD_2, and $PGF_{2\alpha}$ in the cytosol. The GST-μ2 and -μ3 enzymes are expressed predominantly in the brain of rats and humans (Murakami et al., 2002). Therefore, PGE_2 synthesis is tightly regulated and can occur in a wide variety of physiological processes and tissue types.

Diversity of the effects of prostaglandin signaling, despite a limited number of ligands, results from the binding of prostaglandins to receptors of the GPCR Rhodopsin superfamily, the predominant receptor type for lipid mediators. The prostaglandin receptors are typical of the Rhodopsin superfamily, featuring an extracellular region, 7 transmembrane domains, and an intracellular domain that binds the Gα and Gβγ effector subunits (**Table 1-1**). The GPCRs downstream of PGE_2 are the Prostaglandin E Receptors (PTGER), subtypes E-prostanoid (EP) 1-4 (**Table 1-1**). Most of the receptors are integral cell membrane proteins, however, eicosanoids can also bind nuclear membrane receptors. EP receptors on the plasma membrane and nucleus appear to be identical; they have the same kinetic profiles, immunoreactivity, molecular weight, and are encoded by the same genetic loci (Zhu et al., 2006). However, in addition to location, post-translational modifications may distinguish the receptors, but this hypothesis awaits confirmation (Zhu et al., 2006). Nuclear EP receptors may regulate gene transcription, as PGE_2-, **P**latelet **A**ctivating **F**actor (PAF)-, and **L**yso**p**hosphatidic **A**cid (LPA)-associated nuclear receptor stimulation is linked to the calcium-dependent induction of pro-inflammatory genes such as *c-fos*, *eNOS*, *COX2*, and *iNOS* (Zhu et al., 2006).

The specific cellular outcome of stimulating a membrane-associated prostaglandin receptor is dependent on the GPCR subtype, cell type, and the signaling networks that are already activated. Furthermore, multiple prostaglandins can signal to the same second messengers. For example, Phosphatidylinositol-3-kinase (PIK3/PI3K) (**Table 1-1**) is activated downstream of PGE_2 and $PGF_{2\alpha}$ receptor activation, albeit through very different mechanisms. There are two $PGF_{2\alpha}$ receptors, FP_A and FP_B. FP_B is identical to the FP_A receptor, with the exception of a truncated carboxyl terminus. Interestingly, FP_B, but not FP_A, shows agonist-independent interaction with, as well as activation of, PIK3 with simultaneous internalization of the FP_B, PIK3, E-cadherin/Cadherin 1/Cdh1, and β-catenin proteins (Fujino and Regan, 2003) (**Table 1-1**). This receptor "conditioning" later supports the ligand-dependent increase of β-catenin and E-cadherin in areas of cell adhesion, which also occurs through the FP_B receptor. Although most of the cytoplasmic β-catenin is targeted by GSK3β (**Table 1-1**) to the proteasome, some escapes to potentiate *cdh1* transcription. Once stimulated by $PGF_{2\alpha}$, both receptor types result in filopodial retraction, cell rounding, and aggregation due to the activation of Rho and **p**rotein **k**inase **C** (PKC). But again, they do so by different mechanisms. Upon stimulation, the FP_A receptor activates PKC, which then causes clathrin-dependent internalization of FP_A when it phosphorylates the receptor's cytoplasmic tail. By contrast, the FP_B receptor activates Rho and PKC through G_q signaling. Furthermore, FP_B receptor activation also provides a positive feedback loop by activating *COX2* transcription, which generates more $PGF_{2\alpha}$.

Although the EP2 and EP4 receptors of PGE_2 do not share amino acid or structural identity, both can bind and be activated by PGE_2. The EP4 receptor is sensitive to ligand-dependent sensitization and internalization, but the EP2 receptor is not. Both were initially thought to activate adenylyl cyclase, however, the EP4 receptor is Pertussis toxin-sensitive, indicating that EP4 couples to $G\alpha_i$, which inhibits adenylyl cyclase, whereas liberation of $G\beta\gamma$ activates PIK3/ERK-dependent signaling (Fujino et al., 2003; Fujino and Regan, 2006). Like FP_B, EP4 receptor stimulation increases the expression of the COX2-mPTGES1 biosynthetic arm, setting up a positive feedback loop (Regan, 2003). Thus, though PGE_2 and $PGF_{2\alpha}$ both stimulate PI3K, the downstream effects differ because they bind to different receptors.

Many of the effects of PGE_2 signaling are conveyed by the EP4/PTGER4 receptor. *Ep4* genetic knockout mice demonstrate the signaling multiplicity of the EP4 receptors, as they have reduced immune lymphocytic responses, bone resorption and formation, and incidence of rheumatoid arthritis in a disease model, as well as failure of the ductus arteriosus to close after birth. The latter phenotype eventually results in the neonatal death of mutant mice (Segi et al., 1998; Regan, 2003).

The Developmental Roles of Prostaglandin E_2 Revealed in the Zebrafish

Beside the cardiac phenotype in the newborn *Ep4* mouse mutants, it has been difficult to conclude that the loss of prostaglandin signaling results in developmental phenotypes *de novo*. *Cox1* and *Cox2* knockout mice both show normal development, likely because maternal and littermate prostaglandin

synthesis compensate for the absence of prostaglandins in the mutants (Dinchuk et al., 1995; Langenbach et al., 1995). *Cox1* and *Cox2* knockout studies indicate that COX1 and COX2 contribute distinct functions to maternal reproductive fitness and parturition. *Cox1* is expressed in the uterine epithelium of adult mice, and is essential for normal parturition. *Cox2* is expressed in the placenta and fetal membrane, and appears to help initiate labor (Reese et al., 2000). *Cox1* mutant mice show some compensatory upregulation of *Cox2*, but this could not rescue the depletion of prostaglandin production, lengthened gestation, and parturition defects, suggesting that the COX forms are required tissue-autonomously. However, exogenous prostaglandin subcutaneous injection ($PGF_{2\alpha}$, PGE_2, or carbaprostacyclin, a stabilized form of PGI_2) prior to delivery or the transfer of wild-type donor blastocysts into *Cox* mutant mothers results in normal delivery, suggesting that the synthesis of prostaglandins by COX is required for parturition (Reese et al., 2000). Although the function of prostaglandins prior to, during, and following parturition appears to occur via autocrine or paracrine signaling due to the expression pattern of both *Cox1* and *Cox2* in the uterine and fetal tissue, very low levels of *Cox1* and *Cox2* were detected in the ductus arteriosus, suggesting that the closure of the ductus arteriosus relies on the endocrine signaling of prostaglandins. Indeed, though COX1- and COX2-deficient mice show normal ductus arteriosus closure, either COX1/COX2-deficient mice or treatment with COX inhibitors shows developmental defects of the closure of the ductus arteriosus, likely by reducing the level of prostaglandins in the circulation (Reese et al., 2000). Further studies to determine the signaling mechanisms that regulate fertility and delivery show that EP2-deficient mice have ovulation defects that ultimately lead to decreased

reproductive fitness (Hizaki et al., 1999), an effect that could account for the decreased fertility seen in *Cox2* mutant mice. In addition, $PGF_{2\alpha}$ is required for luteolysis, which initiates, then enhances parturition by contributing to uterine relaxation and contraction (Sugimoto et al., 1997; Cha et al., 2006). Therefore, prostaglandins are a critical regulator of maternal fertility and parturition.

These mutant mouse models, whereas revealing the importance of prostaglandins in reproductive fitness, left the developmental role of prostaglandins in question. The zebrafish model system has advantages that make it uniquely suitable for elucidating the role of prostaglandins during development. Embryos are externally fertilized, surmounting the effects of altered prostaglandin signaling on the mother's maintenance of the mouse fetus. This allows the genetic analysis of mutant embryos during development, but also makes the zebrafish model system unsuitable for studying mammalian implantation. In addition, zebrafish embryos develop rapidly and most organogenesis is significantly advanced by 5 **d**ays **p**ost-**f**ertilization (dpf). Embryos also remain optically transparent throughout early development, making them accessible for imaging of the internal features of live embryos, as well as the analysis of gene expression at the level of the transcript and the protein. Furthermore, many transgenic lines have been generated to monitor promoter-driven fluorescent cells. Zebrafish are also amenable to genetic manipulation. *N*-**e**thyl *N*-**n**itroso**u**rea (ENU) is an alkylating agent that often results in AT⇒TA transversions and AT⇒GC transitions. When zebrafish are mutagenized with ENU, point mutations are introduced into the male zebrafish germline and can be subsequently identified by phenotype-driven forward

genetic screens (Grunwald and Streisinger, 1992; Driever et al., 1996; Haffter et al., 1996) or molecularly detected in reverse genetics approaches, such as **T**argeting **I**nduced **L**ocal **L**esions **in G**enomes (TILLING) (Wienholds et al., 2003; Henikoff et al., 2004; Amsterdam and Hopkins, 2006). Antisense morpholino oligonucleotides (MO) are another loss-of-function tool that can be injected into zebrafish embryos at the one-cell stage to interfere with transcript splicing or translation of the target gene (**Fig. 1-2B**). MOs contain sequences that are complementary to the 5′ UTR, ATG, or splice site of the target gene, and are synthesized from nucleotides that have a stable morpholine ring substituting the ribose ring (Corey and Abrams, 2001) (**Fig. 1-2A**). The addition of the morpholine ring results in an uncharged backbone rather than the negatively charged nucleic acids, reducing the non-specific binding of these constructs to cellular proteins, and increasing stability. Most synthetic antisense oligonucleotides bind to the transcript and either induce steric hindrance of the mRNA or degrade the mRNA through RNase H. MO-RNA hybrids do not activate RNase H activity, and the morpholino backbone may bind more effectively to the target sequence (Corey and Abrams, 2001). Gain-of-function analyses can also be performed in zebrafish embryos when synthetic sense RNAs are injected into embryos at the one-cell stage for ubiquitous misexpression, or at later embryonic stages for mosaic misexpression. More recently, transgenic approaches have been successfully employed to drive gene expression in zebrafish embryos in a temporally- or spatially-controlled manner (Scheer and Campos-Ortega, 1999; Inbal et al., 2006; Davison et al., 2007). These tools allow the developmental roles of prostaglandins to be addressed in zebrafish.

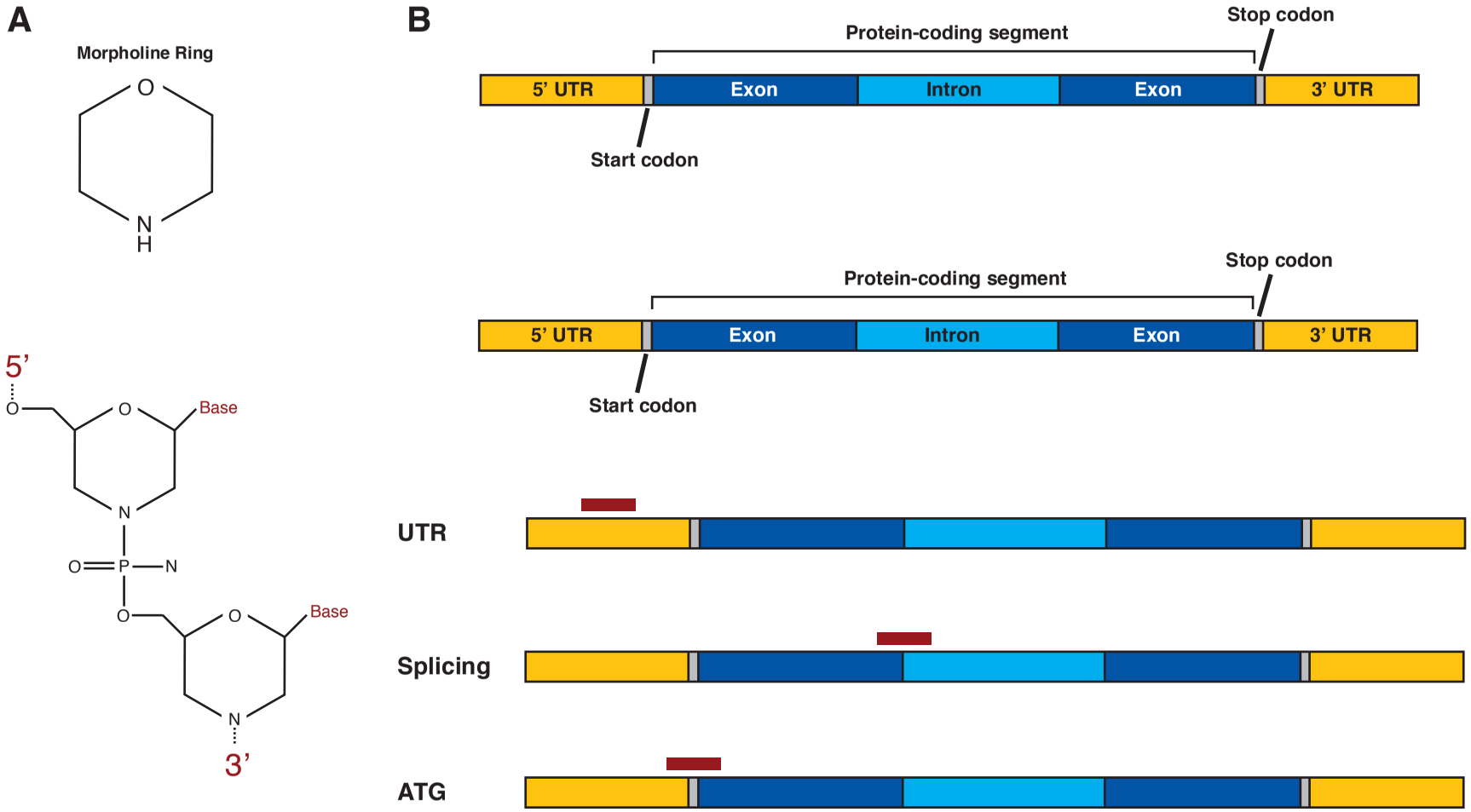

Figure 1-2. Morpholinos. (A) Antisense morpholino oligonucleotides (MOs) are constructed with a morpholine ring rather than the deoxyribose ring in DNA oligonucleotides, which may account for more effective binding and increased stability. *Figure is adapted from http://www.ncbi.nlm.nih.gov/projects/genome/probe/doc/TechMorpholino.shtml.* (B) Schematic of MO action. MOs can interfere with translation or splicing.

Zebrafish gastrulation

Gastrulation is a developmental process that transforms a blastula with a simple morphology and undetermined cells to an embryo with left-right, dorsal-ventral, and anterior-posterior polarity and three germ layers through cell specification, movements, and proliferation (**Fig. 1-3**). In zebrafish, gastrulation occurs between 5.3-10.3 hours post-fertilization (hpf) when embryos are incubated at 28°C. The blastula initially is composed of the surface **e**n**v**eloping **l**ayer (EVL), the non-epithelial layer of blastoderm cells, and the **y**olk **s**yncytial **l**ayer (YSL). The YSL forms at the 1000-cell stage when marginal blastomeres collapse and their nuclei move into the yolk cell. The YSL nuclei then divide to form a syncytium within the yolk that has important signaling properties (Kimmel and Law, 1985; Montero and Heisenberg, 2004).

Cell fate specification during gastrulation

The dorsal YSL and dorsal blastomeres in zebrafish are homologous to the frog Nieuwkoop center, the blastula organizing center that induces a secondary axis when transplanted into the ventral vegetal side of a donor blastula (Nieuwkoop, 1977; Gimlich and Gerhart, 1984). Although the first cleavage plane does not predict the dorsal-ventral pattern of the embryo (Abdelilah et al., 1994), loss of the yolk cell after the first cell cleavage severely ventralizes the embryo (Mizuno et al., 1999), suggesting that dorsal determinants are present in the egg. The Nieuwkoop center in frog and zebrafish is characterized by the nuclear localization of β-catenin, the effector molecule of the canonical Wnt, or Wnt-β-catenin pathway (**Fig. 1-4**). In the absence of Wnt stimulation, β-catenin is

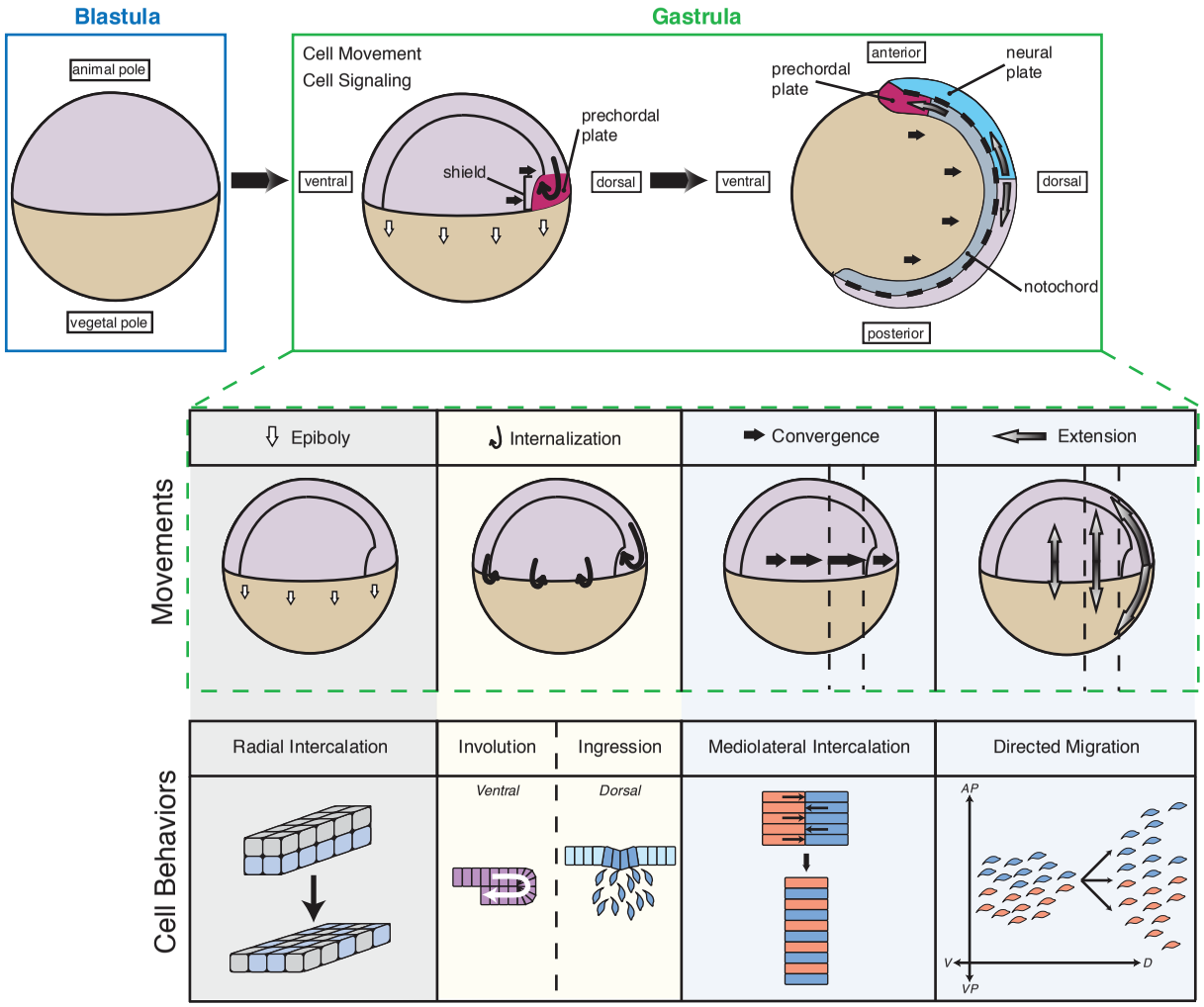

Figure 1-3. Gastrulation movements in zebrafish. The comprehensive movements are shown in the top panel, followed by the individual movements and the cell behaviors that contribute to each movement. Directed migration cell behavior also occurs during other types of cell migration in gastrulation, such as the anterior migration of mesendodermal cells following internalization. *Portions of figure adapted from Solnica-Krezel, Curr Biol, 2005.*

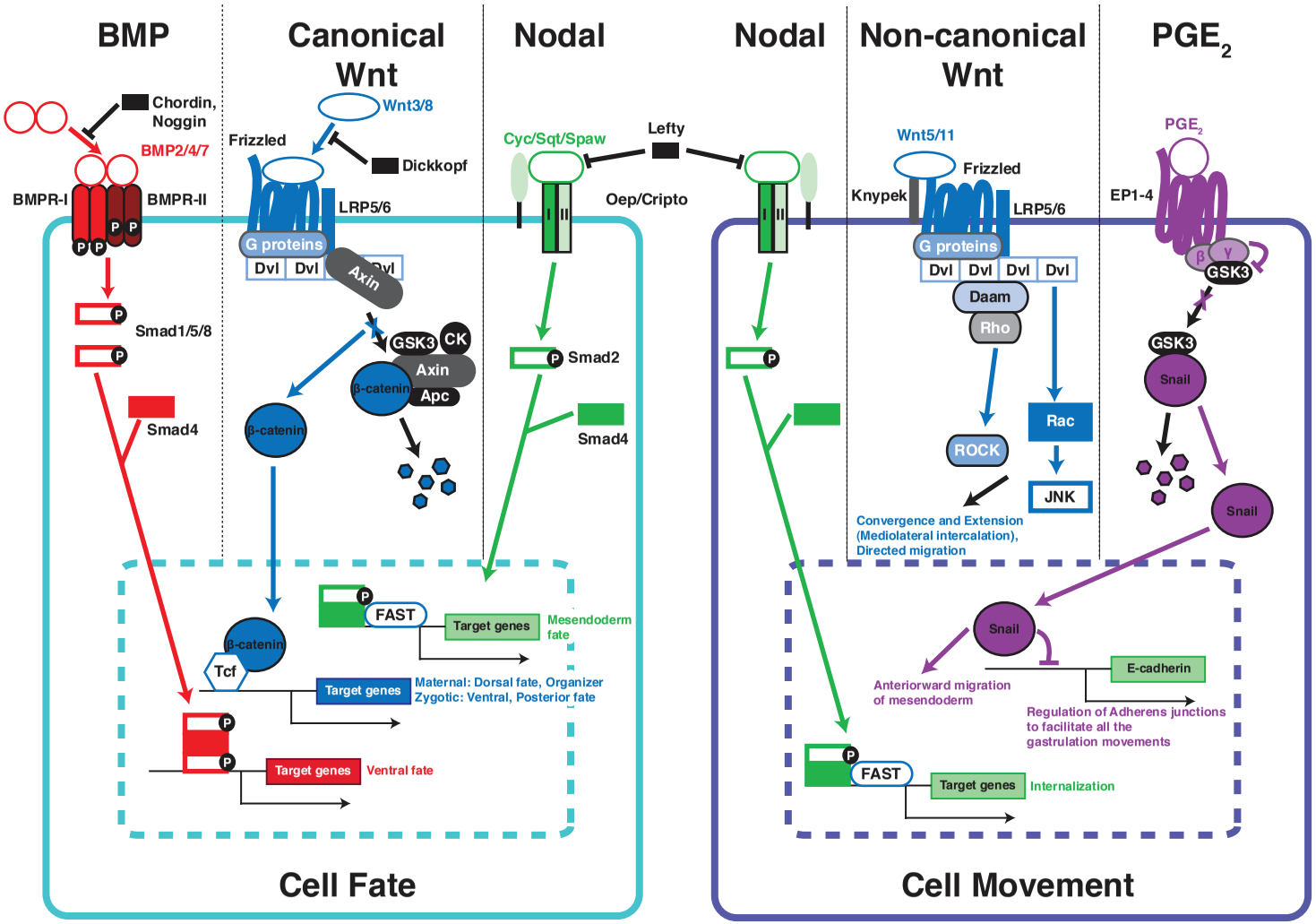

Figure 1-4. Signaling pathways that regulate cell fate and cell movement during gastrulation.

targeted to the proteasome by the degradation complex including Axin, Apc, **C**asein **K**inase (CK), and GSK3 (Logan and Nusse, 2004; Nusse, 2005). However, when the canonical Wnt ligands, e.g., Wnt1, Wnt3, or Wnt8, bind the Frizzled (Fz)/Low Density **L**ipoprotein **R**eceptor-related **P**rotein (LRP) receptor complex, the degradation complex is dispersed through the intracellular recruitment of Disheveled (Dsh) and Axin by LRP (Mao et al., 2001). Stabilized β-catenin then translocates to the nucleus to regulate transcription through cooperation with the **L**ymphoid **E**nhancer-Binding **F**actor (LEF)/**T** **c**ell-specific transcription **F**actor (TCF) (Logan and Nusse, 2004; Nusse, 2005).

The importance of β-catenin as the Organizing Signal of dorsal-ventral patterning is demonstrated by its nuclear expression in the future dorsal region of the embryo, and more tellingly, by its ability to induce a duplicated axis composed of neural tissue and dorsal mesoderm when β–catenin is overexpressed in the embryo (McCrea et al., 1993; Funayama et al., 1995; Kelly et al., 1995). Moreover, mutations in the genes encoding Ichabod or Tokkaebi, which maintain the expression of β–catenin, result in ventralized embryos that lack the head and notochord (Kelly et al., 2000; Nojima et al., 2004; Bellipanni et al., 2006). Once activated, β-catenin induces expression of the downstream genes *bozozok/dharma*, *chordin*, *dickkopf*, and *squint* (Yamanaka et al., 1998; Fekany et al., 1999).

Bozozok (Boz) is a transcriptional repressor that directly targets *bmp2b* and directly or indirectly targets *wnt8*, *vox/vega1*, *vent/vega2*, and *ved* (Koos and Ho, 1999; Fekany-Lee et al., 2000; Kawahara et al., 2000; Melby et al., 2000; Erter et al., 2001). Loss of Boz function in $boz^{m168/m168}$ mutants results in defective

anterior and dorsal structures, such as the brain, eyes, and notochord (Fekany et al., 1999). Misexpression of Boz induces partial secondary axes in embryos, and overexpression of Boz in the yolk syncytial layer of *boz*$^{m168/m168}$ mutants rescues the induction of dorsal tissues, indicating that Boz is one of the effectors of dorsal-ventral patterning (Yamanaka et al., 1998; Fekany et al., 1999). The *boz*$^{m168/m168}$ phenotype could not be rescued by *β-catenin*, suggesting that Boz functions downstream or parallel to maternal Wnt signaling (Fekany et al., 1999). Moreover, the promoter of *boz* contains consensus Tcf/Lef binding sequences, and thus its expression may be activated by β-catenin (Ryu et al., 2001). The *boz*$^{m168/m168}$ mutant phenotype, however, can be rescued with Nodal overexpression. Moreover, expression of nodal-related Cyclops (Cyc) in the organizer is reduced in *boz*$^{m168/m168}$ mutants (Sampath et al., 1998), suggesting that the Nodal pathway acts parallel to and downstream of Boz.

The function of the Nieuwkoop Center non-autonomously activates the function of the shield region in zebrafish, which is homologous to the Hensen's node in the avian embryo, the node in mammals, and the Spemann-Mangold Organizer in the frog. Like the Nieuwkoop Center, the transplantation of the Spemann-Mangold Organizer in the gastrula to the ventral side of a newt gastrula results in the duplication of the embryonic axis in the host embryo (Spemann and Mangold, 1924). Binding of Boz to the promoter region of *bmp2b* allows Spemann-Mangold Organizer formation (Leung et al., 2003). In addition, Vox and Vent may inhibit Hhex in the Nieuwkoop Center, and Hhex in turn may inhibit Bmp2b, further stabilizing the Spemann-Mangold Organizer (Bischof and Driever, 2004). Once established, the gastrula-organizing center patterns the axis

by inducing dorsal fates in the embryo, primarily by inhibiting ventral signaling pathways.

The ventralizing signaling pathways that function during gastrulation include the Bmp and Wnt-β-catenin signaling pathways. The secreted Bmp ligands Bmp2, Bmp4, and Bmp7, specify ventral fates such as the blood, heart, pronephros, and tail somites in a concentration-dependent manner, indicating that BMP acts as a morphogen during gastrulation (Mullins et al., 1996; Hwang et al., 1997; Kishimoto et al., 1997; Dick et al., 2000; Schmid et al., 2000; Stickney et al., 2007). *bmp2* and *bmp7* genes are expressed ubiquitously during the blastula stages, but their expression becomes limited to the ventral hemisphere of the embryo at the beginning of gastrulation (Martinez-Barbera et al., 1997; Wise and Stock, 2006). Loss of Bmps in the *bmp2b/swirl* and the *bmp7/snailhouse* mutants results in dorsalized embryos (Kishimoto et al., 1997; Dick et al., 2000); however, *swirl;snailhouse* double mutants do not show a more severe phenotype than either mutation alone, suggesting that Bmp2 and Bmp7 function as a heterodimer (Schmid et al., 2000), which has been confirmed by biochemical and genetic studies (Little and Mullins, 2009). Bmps bind the TGFβ-like type I and II Bmp receptors, activating intracellular serine/threonine kinase domains that phosphorylate Smad1, Smad5, and Smad8 (Anderson and Darshan, 2008) (**Fig. 1-4**). The intracellular Smads translocate to the nucleus and, together with Smad4, activate the expression of target genes (Schier and Talbot, 2005). Bmp signaling also has multiple extracellular modifiers, including Twisted gastrulation, a Bmp agonist, as well as Chordin, Ogon/Sizzled, and Follistatin, which are secreted Bmp antagonists. Consequently, the overexpression of Chordin produces a

dorsalized phenotype, whereas *chordin/dino* mutants are severely ventralized (Hammerschmidt et al., 1996; Miller-Bertoglio et al., 1997). Other modifiers that influence Bmp signaling include Tolloid, a metalloprotease that targets Chordin, Hhex, and ADMP (Blader et al., 1997; Ho et al., 1999; Dosch and Niehrs, 2000; Willot et al., 2002). These modifiers serve to refine the Bmp activity gradient that patterns the dorsal-ventral axis.

At the early blastula stages maternal β-catenin leads to formation of the Spemann-Mangold gastrula organizer/shield, but later Wnt-β-catenin signaling with zygotic Wnt3a and Wnt8 ventralizes and posteriorizes the embryonic tissue by inhibiting dorsal genes such as *gsc* and *chd* (Kelly et al., 1995; Kim et al., 2002; Braun et al., 2003). Thus, *wnt3a* and *wnt8* mutants have expanded axial mesoderm at the expense of the ventro-posterior and paraxial mesoderm, in contrast to the *bmp* mutants, which lack all ventral mesoderm (Kishimoto et al., 1997; Dick et al., 2000; Erter et al., 2001; Lekven et al., 2001), suggesting that these two pathways pattern mesoderm through distinct mechanisms. Antagonists that modulate the effects of canonical Wnt signaling include the SFRP Tlc, Wnt inhibitory factor, Dickkopf1/Dkk1, Naked1/Nkd1, and Naked2/Nkd2 (Houart et al., 2002; Caneparo et al., 2007; Roberts et al., 2007; Van Raay et al., 2007). Therefore, Wnt signaling is dynamically regulated during gastrulation and contributes to the dorsal-ventral and anterior-posterior axes.

Specification of the animal/blastoderm-vegetal/yolk cell axis also occurs during gastrulation. Fate map analysis in zebrafish was performed on single cells near the blastoderm margin that were labeled with lineage tracers between the 1000- and 4000-cell stage (Warga and Nusslein-Volhard, 1999). Clones of

labeled cells were plotted on an embryo map at 40% epiboly and shield stage, and analyzed for their lineage from 1 to 5 dpf. In this way, the fates of cells were correlated with their early position within the blastula. 71 clones were analyzed, and of those, 24% gave rise to only endoderm, 42% gave rise to only mesoderm, and 34% generated both mesoderm and endoderm. Cells that eventually give rise to mesoderm and endoderm are located in the margin of the blastula, however cells that reside more than 4 cells from the margin are mesodermal progenitors. Endodermal progenitors are most frequently found within 2 cell diameters of the margin, and never more than 4 cell diameters from the margin (Warga and Nusslein-Volhard, 1999). In addition, endodermal progenitors are biased towards dorsal locations, whereas mesodermal progenitors are more uniformly distributed on the ventral side of the embryo. Therefore, the position of cells along the animal-vegetal axis predicts its germ layer specification.

Initial specification of the mesendoderm occurs through Nodal signaling. Like Bmps, the Nodal secreted ligands belong to the **T**umor **G**rowth **F**actor-**β** (TGF-β) superfamily (**Fig. 1-4**). The Nodal signaling pathway in zebrafish involves the three **z**ebrafish **N**odal-**r**elated (ZNR) ligands Znr1/Cyclops (Cyc), Znr2/Squint (Sqt), and Znr3/Southpaw (Spaw), as well as the cofactor One-eyed pinhead (Oep), the zebrafish homologue to the human Cripto protein, a member of the **E**xtracellular **G**rowth Factor-like and/or Co-receptor-like (EGF-CFC) family (Erter et al., 1998; Feldman et al., 1998; Sampath et al., 1998; Feldman et al., 2000; Saloman et al., 2000; Schier and Shen, 2000; Long et al., 2003). Once the ligands bind the Type I and Type II activin-like receptors, Smad2 and Smad4 are activated to transcriptionally induce the downstream targets of Nodal signaling

(Schier and Shen, 2000).

In the frog, Nodal signaling is activated by a maternally deposited factor, VegT, as well as Wnt-β-catenin signaling (Zorn and Wells, 2007). What induces Nodal signaling in amniotes and zebrafish, however, remains unknown. This signal likely emanates from the YSL in zebrafish, because removal of the yolk cell and YSL results in defective mesendoderm development (Zorn and Wells, 2007). Indeed, *sqt* is initially maternally deposited and asymmetrically expressed (Gore et al., 2005). Subsequently, it is zygotically expressed in the dorsal blastomeres, then in the entire YSL by the oblong stage (3.7 hpf), suggesting that the expression of *sqt* in the yolk syncytial layer is activated by early, yolk-derived inductive signal(s) (Erter et al., 1998; Feldman et al., 1998). Nodal signaling through Cyc and Sqt contributes to the induction of mesendodermal patterning, evidenced by *cyc*;*sqt* double mutants that lack most mesendoderm (Feldman et al., 1998; Feldman et al., 2000). Sqt, in particular, appears to act as a morphogen to activate Nodal signaling, whereas Cyc can only activate Nodal signaling locally (Chen and Schier, 2001). Spaw, the third Nodal ligand, acts at the segmentation stages to pattern the left-right axis (Long et al., 2003). Misexpression of the consitutively active form of Activin A receptor, type IB/Taram-A/Tar (Acvr1b), a TGF-β-Related Type I receptor, in zebrafish embryos induces early mesendodermal markers such as *ntl* (mesoderm), *gata5*, and *mixer* (endoderm) (Aoki et al., 2002). MO-targeting of *lefty1*/*lft1* and *lefty2*/*lft2*, which encode for TGFβ-related secreted proteins that function as Nodal signaling feedback antagonists and are themselves activated by Nodal signaling (Meno et al., 1999; Cheng et al., 2000), results in the expansion of the

mesendoderm population due to constitutively active Nodal signaling during gastrulation (Feldman et al., 2002). Thus, Nodal signaling induces and patterns the mesendodermal germ layers.

Nodal signaling may also regulate the decision between mesodermal and endodermal fates in cells by the duration and strength of signaling (Grapin-Botton and Constam, 2007). Embryos with low Nodal signaling, such as zygotic *oep* mutants, lack all the endoderm but retain most of the mesoderm. Moreover, mosaic overexpression of a constitutively active form of Acvr1b/Taram-A induces Acvr1b-expressing cells to become endoderm. In addition, Acvr1b/Taram-A overexpression rescues endoderm formation in *oep* homozygotes, suggesting that conversion to the endodermal fate requires higher, sustained levels of Nodal signaling (Schier et al., 1997; Peyrieras et al., 1998). This model is consistent with the germ layer fate map, whereby endodermal cells reside closest to the margin, while mesodermal cells are specified within a broader marginal domain (Warga and Nusslein-Volhard, 1999).

Cell movements during gastrulation

There are four evolutionarily conserved gastrulation movements in vertebrates: epiboly, emboly/internalization, convergence, and extension (**Fig. 1-3**). In zebrafish, the first movement is epiboly, which entails the enveloping of the yolk cell by the EVL, YSL, and the blastodermal cells (**Fig. 1-3**). To spread over the yolk surface area, the blastodermal cells undergo radial intercalation (**Fig. 1-3**), the intermingling of superficial and deep blastodermal cells to thin the epibolizing cell layer as cells actively migrate towards the vegetal pole. Cell adhesion is required for this cell spreading, which is demonstrated by the severe

epiboly arrest in the E-cadherin mutant *half-baked*$^{vu44/vu44}$/*cdh1*$^{vu44/vu44}$ (*hab*$^{vu44/vu44}$) (Kane et al., 2005). Interestingly, in *hab*$^{vu44/vu44}$ mutant gastrulae, cells initially intercalate normally, but eventually delaminate back into the deeper layers, indicating that the E-cadherin is necessary for maintaining the position of epibolizing cells (Kane et al., 2005; Schier and Talbot, 2005; Solnica-Krezel, 2006). Another mutant, **M**aternal **Z**ygotic (MZ) *oct4/pou5/spiel ohne grenzen* (MZ*spg*) have altered cell adhesion and also show a severe epiboly defect with concomitant decoupling of epiboly of the EVL and deep blastodermal layers, similar to the *hab*$^{vu44/vu44}$ mutants (Lachnit et al., 2008). In a study by our group, embryos with increased $G\alpha_{12/13}$ signaling also show decoupling of the deep blastodermal layer and the EVL as they undergo epiboly, decreased cell scattering and adhesion, and dissociation of cells from the embryonic surface (Lin et al., 2009). Consistent with studies in mammalian cell culture (Kaplan et al., 2001; Meigs et al., 2001; Meigs et al., 2002), zebrafish $G\alpha_{13}$ binds the cytoplasmic domain of E-cadherin and is suggested to inhibit the function of E-cadherin because $G\alpha_{13}$ overexpression exacerbates, and reduced fuction ameliorates, the epiboly defects of *hab*$^{vu44/vu44}$ (Lin et al., 2009). Thus, E-cadherin-based cell adhesion is critical for the progression of epiboly.

Emboly, or internalization, is the gastrulation movement that generates the ectoderm and mesendoderm progenitor layers (**Fig. 1-3**). As cells undergo epiboly, marginal blastomeres actively migrate towards the interface between the blastoderm and the yolk cell, resulting in the marginal thickening that marks the "germ ring" stage of zebrafish development (5.6 hpf). Next, the marginal cells, the mesendodermal precursors, turn inwards towards the yolk cell surface, then

move underneath the epibolizing cells. Epibolizing cells are the ectodermal progenitors of the blastoderm and the internalized cells are mesendodermal progenitors. Frog mesendodermal precursors internalize by involution, when the cell sheet bends upon itself and moves inward, retaining its epithelial character. The amniote (mouse and chick) gastrulae mesendodermal progenitors ingress, or delaminate, from the embryonic epithelium at the blastopore lip (Solnica-Krezel, 2005). Interestingly, cells from the gastrulae of divergent organisms like sea urchins and spiders also ingress to create the mesendodermal germ layer (Kominami and Takata, 2004; Chaw et al., 2007). Zebrafish gastrulation uses both of these modes of internalization. The involution mechanism generates the ventral mesendoderm, whereas on the dorsal side of the embryo, the involuting cell layer bends upon itself as a sheet, then single cells delaminate into the deeper mesendodermal layer (Montero et al., 2005; Solnica-Krezel, 2005; Keller et al., 2008) (**Fig. 1-3**). Internalization in the zebrafish is greatest at the dorsal side of the embryo, forming a thickened domain called the "shield," which is the zebrafish equivalent to the frog Spemann-Mangold organizer (6 hpf). Following internalization, the earliest cells to internalize migrate actively towards the animal pole, eventually becoming the anterior mesendoderm underlying the head. Animalward migrating cells that will become the axial mesendoderm form dense, cohesive clusters, whereas paraxial cells retain looser, mesenchymal-like clusters (Heisenberg and Tada, 2002). After initially migrating towards the animal pole, internalizing cells will later migrate towards the vegetal pole, the future tail region of the embryo (Heisenberg and Tada, 2002; Keller et al., 2008).

In addition to its role in mesendoderm specification, Nodal signaling also regulates the internalization movements (**Fig. 1-4**) (Schier and Talbot, 2005). *sqt;cyc* double mutants show diminished internalization movements (Feldman et al., 2000). In the MZ*oep* mutants, marginal cells also fail to internalize, with ~60 internalizing cells in comparison to the ~1550 internalizing cells in wild-type embryos during the same time period (Carmany-Rampey and Schier, 2001; Keller et al., 2008). MO-targeting of *lft1* and *lft2* lengthens the phase of internalization (Feldman et al., 2002). MZ*oep* single cells in wild-type hosts initially internalize but do not ultimately contribute to the mesendoderm, instead retreating back to the superficial, epibolizing cell layer (Carmany-Rampey and Schier, 2001). These results indicate that cells can internalize as part of a mass movement due to interactions with their neighbors, but Nodal signaling maintains the cell's position within the mesendodermal progenitor layer. Contrastingly, single wild-type cells in MZ*oep* host embryos undergo internalization and subsequently contribute to the mesendoderm (Carmany-Rampey and Schier, 2001), emphasizing that Nodal signaling is required cell-autonomously in mesendodermal progenitors.

Dickkopf1, an antagonist of the Wnt-β-catenin pathway, is also implicated in the internalization movement. MO-mediated downregulation of *dickkopf1*/*dkk1* accelerates internalization and animalward migration without affecting epiboly (Caneparo et al., 2007). Increased Wnt-β-catenin signaling does not phenocopy the accelerated internalization of *dkk1* morphants, nor does the expression of dominant-negative Wnt8 rescue the movement defect (Caneparo et al., 2007). Therefore, the regulation of internalization movements by Dkk1 is

Wnt-β-catenin-independent. Dkk1 also activates the Wnt-**P**lanar **C**ell **P**olarity (PCP) signaling pathway through interaction with Knypek, a Glypican 4/6 **H**eparan **S**ulfate **P**roteo**g**lycan (HSPG), however, these effects could not contribute to the effects on internalization as Wnt-PCP signaling does not regulate this movement. Nodal signaling does repress *dkk1* expression (Trinh et al., 2003), suggesting that Dkk1 governs internalization movements via an unknown mechanism.

The last two movements, convergence and extension, narrow and lengthen the embryo body, respectively (**Fig. 1-3**). Three broad regions of the embryo can be defined with respect to the convergence and extension movements (Heisenberg and Tada, 2002; Myers et al., 2002) (**Fig. 1-3**). The ventral cells do not converge, but move over the yolk towards the vegetal pole. Dorsal cells elongate and intercalate mediolaterally, resulting in little convergence but fast extension (**Fig. 1-3**). Subdomains of cell behavior can be delineated within the third domain, the lateral region of the gastrula (Jessen et al., 2002; Sepich et al., 2005; Solnica-Krezel, 2006). Lateral cells in the subdomain distal to the dorsal pole move in meandering paths dorsally. Depending on their location along the animal-vegetal axis, lateral cells either migrate animally, vegetally, or equatorially (Solnica-Krezel, 2006) (**Fig. 1-3**). The spectrum of migration paths towards the future anterior-posterior poles of the embryo extends the embryo body (Solnica-Krezel, 2006). Cells migrate using the same behaviors in the subdomain of lateral cells proximal to the dorsal pole, but cells migrate dorsally with increasing speed and more directed cell paths. Lateral cells also show greater mediolateral elongation as they approach the dorsal side of the embryo (Jessen et al., 2002). All regions of convergence and extension

require Stat3 in a non-cell autonomous manner. Stat3 functions in part to activate Wnt-PCP signaling through the Dsh-RhoA pathway so that cells achieve the proper polarization for the convergence and extension movements (Miyagi et al., 2004; Habas and Dawid, 2005; Jessen and Solnica-Krezel, 2005; Pongracz and Stockley, 2006) (**Fig. 1-4**). The early convergence movements, which depend on Stat3 but are Wnt-PCP-independent, are impaired in *gna*$_{12/13}$ morphants, and cells are less polarized with inefficiently directed paths towards the dorsal midline (Lin et al., 2005). Therefore, a GPCR coupled to the G$\alpha_{12/13}$ mediators likely promotes cell polarization during early convergence movements. Later convergence and extension movements require Wnt-PCP signaling both autonomously and non-cell autonomously (**Figs. 1-3, 1-4**) (Jessen et al., 2002; Sepich et al., 2005; Solnica-Krezel, 2006).

Prostaglandin E_2 regulates zebrafish gastrulation movements

The first study of prostaglandins in zebrafish demonstrated the expression of *cox* and prostaglandins during later embryogenesis (8 dpf larvae) (Grosser et al., 2002). The homologs of *COX1* and *COX2* in zebrafish, designated *cox1* and *cox2*, contain 67% amino acid identity to the human genes, as well as conservation of the catalytic domains (Grosser et al., 2002). Like the mammalian Cox enzymes, Cox1 and Cox2 are distinguished by a 12-amino acid (aa) insertion in Cox1, as well as an 18-aa C-terminal motif and multiple AU-rich sequences in the 3′ UTR of *cox2* gene (Grosser et al., 2002). PGE_2 is the major prostaglandin expressed in adult zebrafish, though TxB_2 and a hydrolytic product of PGI_2 are also present. Adult zebrafish were treated with either indomethacin or NS-398, which function as a non-specific Cox inhibitor and a Cox2-specific inhibitor,

respectively, in cell culture and mammalian model systems. Although treated fish manifested no obvious phenotype, measurements of PGE_2 biosynthesis indicates the inhibitors act on the Cox isoforms in zebrafish as in cell culture and mammalian systems. *cox1* and *cox2* expression is observed in the carotid arteries, pharyngeal arches, intestinal arteries, and the gill vasculature (8 dpf), but *cox2* expression is limited to the vessel wall in the gill vasculature and is absent from the endothelium. *cox1* is expressed in the cranial vessels, the aorta, and the segmental and intestinal arteries. MO-targeting of *cox1* (MO1-*ptgs*) produced severe epiboly arrest and high lethality in early embryos. By contrast, the injection of *cox2* MO did not produce any morphological phenotype (Grosser et al., 2002). These data presented the first evidence that prostaglandin biosynthesis is essential for the normal progression of gastrulation movements in vertebrates.

Continued collaborative work from the Solnica-Krezel and the DuBois groups shows that PGE_2, $PGF_{2\alpha}$, and PGI_2 are produced during gastrulation, whereas TxA_2 is expressed at barely detectable levels (Cha et al., 2005). *cox2* transcripts are undetectable until early somitogenesis, which is consistent with the normal development that occurs in *cox2* morphants (Grosser et al., 2002; Cha et al., 2006). By contrast, *cox1* is maternally deposited and ubiquitously expressed during gastrulation, along with *ptges*/*mptges* and *ep4*. The receptor *ep2* is also expressed in zebrafish embryos, but not until the end of gastrulation. Thus, zebrafish gastrulae express the components for PGE_2 biosynthesis and signaling. The low-dose injection (2 ng) of MOs that interfere with Ptges translation (complementary to the 5′ UTR; MO1-*ptges*) and splicing (complementary to the first intron-exon boundary; MO2-*ptges*) delay epiboly and

shorten the anterior-posterior body axes by the end of gastrulation. Whole mount *in situ* hybridization analysis of tissue-specific markers showed that the distance between the forebrain (*six3b*) and the midbrain-hindbrain boundary (*pax2.1*) is closer in *ptges* morphants than the control (Cha et al., 2006). Furthermore, the width of the axial mesoderm (as revealed by the expression of *notail/brachyury*) was increased in *ptges* morphants, suggesting that these embryos suffer convergence and extension defects as well as delayed epiboly (Cha et al., 2006). PGE_2 rescued these defects, in contrast to PGI_2 and $PGF_{2\alpha}$, both of which had no effects on the phenotype. *ep4* morphants manifest gastrulation movement defects that are similar to those in *ptges* morphants. In addition, *ep4* morphants have normal gastrula expression of *gsc* and *bmp4* expression, suggesting that dorsal-ventral patterning is unaffected by diminished PGE_2 signaling. Notably, *ep4* morphant lateral mesodermal cells move more slowly without changes in cell shape or the path of migration. Thus, PGE_2-EP4 signaling regulates cell motility during gastrulation (Cha et al., 2006). *ptges* and *ep4* morphants also have reduced activation/phosphorylation of Akt, suggesting that as in cancer cells (Fujino and Regan, 2003), PGE_2 signaling activates Pik3 and Akt, which may contribute to coordination of the gastrulation movements (Cha et al., 2006).

Zebrafish hematopoiesis

Blood vessel development and hematopoiesis, the generation of blood cells, begin in the ventral mesoderm, which is specified during gastrulation by Bmp and Wnt signaling (Amatruda and Zon, 1999; Hsia and Zon, 2005; Schier and Talbot, 2005) (**Fig. 1-5**). Consequently, mutations that influence the

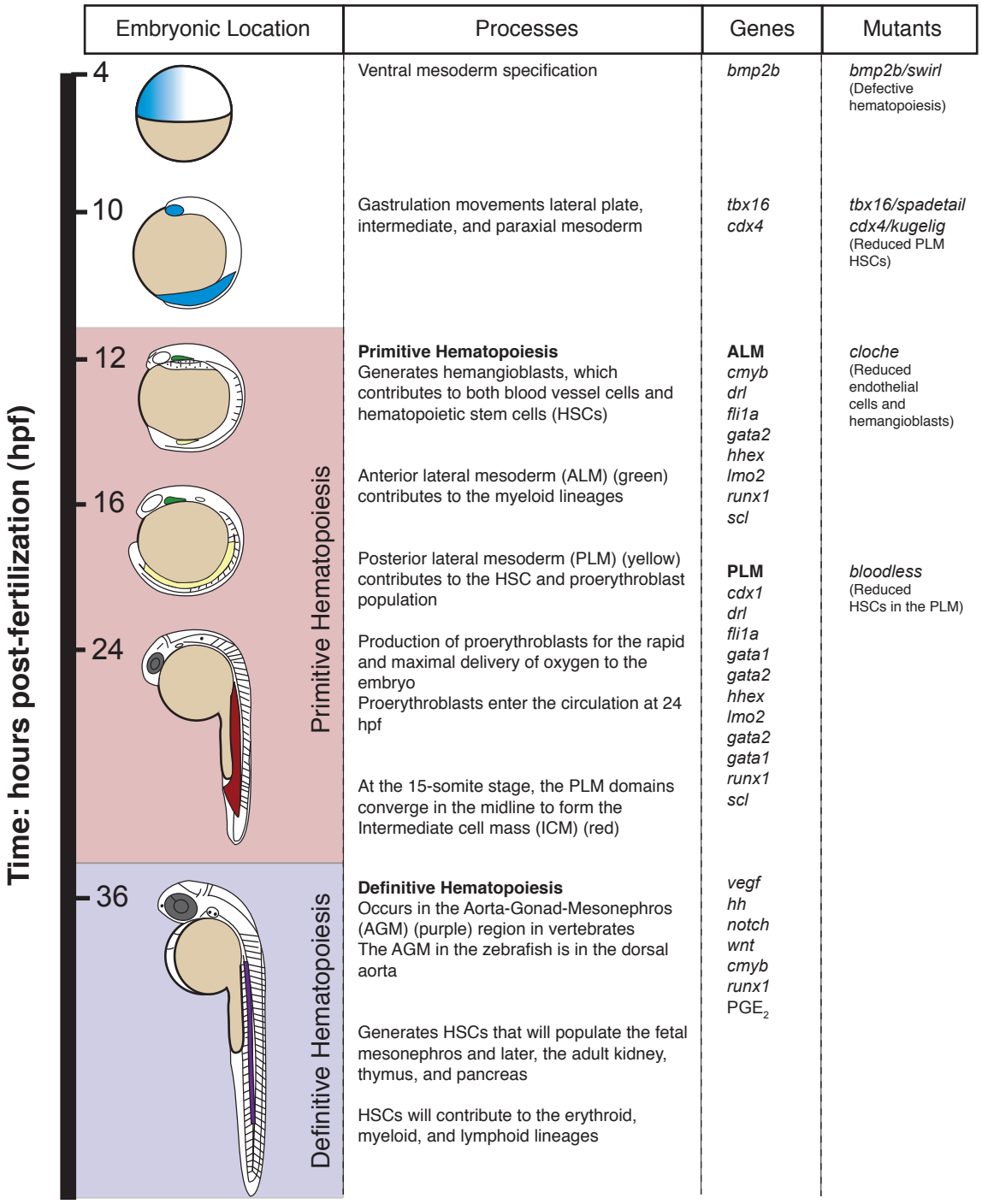

Figure 1-5. Hematopoiesis in zebrafish. There are two waves of hematopoiesis in vertebrates; primitive or embryonic hematopoiesis, which gives rise to primitive red blood cells called proerythroblasts, and definitive hematopoiesis, which gives rise to all of the blood types in the maturing organism.

specification of ventral mesoderm also result in hematopoietic defects. For example, *swirl/bmp2b* mutants show loss of the ventral mesoderm and a subsequent loss of hematopoiesis (Kishimoto et al., 1997) (**Fig. 1-5**). In addition, Spadetail/Tbx16 is a transcription factor that regulates convergence movements of the lateral plate, intermediate, and paraxial mesodermal during gastrulation (Ho and Kane, 1990). Thus, *spadetail* mutants also show defective hematopoiesis (Hsia and Zon, 2005).

Hematopoiesis occurs in two phases during development (**Fig. 1-5**). Embryonic, or primitive, hematopoiesis provides rapid and maximal oxygen to the developing embryo by generating the cells for blood vessel development as well as the embryonic erythroid cells, the proerythroblasts. Proerythroblasts are large and mature circulating cells remain nucleated, distinguishing them from adult erythroblasts in mammals. In addition, they synthesize embryonic globins rather than hemoglobin to carry oxygen (Zon, 1995; Bahary and Zon, 1998). Primitive hematopoiesis begins with the formation of the hemangioblasts, which are the putative common progenitor to the endothelium/blood vessels and the hematopoietic stem cells (HSCs) (Baldessari and Mione, 2008) (**Fig. 1-5**). The existence of the hemangioblasts is inferred from the *cloche* mutant in zebrafish, which has defective endothelial and blood development, suggesting that vasculogenesis and hematopoiesis share a common progenitor cell type (Stainier et al., 1995; Amatruda and Zon, 1999). Although the gene mutated in *cloche* remains unidentified, it is essential either for the maintenance or the differentiation of the hemangioblast identity (Orkin and Zon, 1997; Amatruda and Zon, 1999). In addition, a hemangioblast-like cell population demonstrated

in zebrafish by lineage tracing is the first *in vivo* evidence of hemangioblasts (Vogeli et al., 2006).

Primitive hematopoiesis usually takes place outside of the embryo, in the extraembryonic yolk sac of the mouse and chick and the ventral blood island in the frog (Orkin and Zon, 2002). In zebrafish, however, primary hematopoiesis occurs in the **a**nterior **l**ateral **m**esoderm (ALM) and the **p**osterior **l**ateral **m**esoderm (PLM). Interestingly, fate mapping in the zebrafish gastrula showed that dorsal marginal cells contributed to the ALM, whereas dorsal marginal cells contributed to the PLM (Warga et al., 2009). At the 2-somite stage (10.6 hpf), bilateral expression of *stem cell leukemia* (*scl*), the earliest marker of HSCs, occurs. From the 2-somite to the 4-somite stage, *scl* is co-expressed with *lmo2* and *gata2* in the PLM as well as the ALM (Amatruda and Zon, 1999; Hsia and Zon, 2005). *gata1* is expressed later in the PLM at the 5-somite stage, when erythropoiesis begins in the *scl+/gata1+* cells (Amatruda and Zon, 1999; Hsia and Zon, 2005). Cells in the ALM do not express *gata1*, and eventually become macrophages (Warga et al., 2009). At the 15-somite stage, the bilateral stripes of HSCs in the PLM converge to form the **I**ntermediate **C**ell **M**ass (ICM), which lies dorsal to the yolk extension (Orkin and Zon, 1997; Amatruda and Zon, 1999) (**Fig. 1-5**). Cells of the ICM are multipotential, in contrast to the ALM, and will become erythrocytes, neutrophils, and thrombocytes (Warga et al., 2009).

Shortly after proerythroblasts enter the circulation at 24 hpf, definitive hematopoiesis begins in zebrafish in the Aorta/Gonad/Mesonephros (AGM) region, common to all vertebrates (**Fig. 1-5**). Definitive hematopoiesis is initiated by Hedgehog, Vegf, and Notch signaling (Hsia and Zon, 2005). This wave of hematopoiesis generates HSCs that will populate the fetal and adult organism.

These HSCs have definitive characteristics: they can self-renew, maintain the hemopoetic lineages within the organism, and convert into all the differentiated lineages either following injury to the hemopoietic reservoir or when transplanted into an irradiated organism (Lord et al., 2007). Consequently, experimental assays of HSC development test the ability of an HSC population to recapitulate all of the blood lineages in the bone marrow following injury or irradiation (repopulation analysis). The HSCs later give rise to progenitor cells, which lack the capacity for self-renewal. These progenitors then differentiate into precursors that are committed to the myeloid, lymphoid, or erythroid lineage (Amatruda and Zon, 1999). Therefore, each step down the lineage path restricts the cell's developmental potential.

The process of differentiation does not occur in the AGM. Instead, HSCs differentiate in mammals in the fetal liver and spleen and later, in the adult bone marrow. Lymphoid progenitors will travel to the thymus to complete their commitment to the lymphoid lineage and terminally differentiate (Trede and Zon, 1998; Amatruda and Zon, 1999). In teleost fish, cells within the ventral wall of the dorsal aorta likely represent the AGM region (Orkin and Zon, 1997). These HSCs will migrate and differentiate in the fetal mesonephros, and later, in the adult kidney (Amatruda and Zon, 1999). Despite these regional differences, studies show that the generation, maintenance, and differentiation of HSCS, as well as the genes involved in these processes, are conserved between mammals and zebrafish, making zebrafish a useful model for the study of HSC development and generation (Amatruda and Zon, 1999).

Prostaglandin E_2 enhances hematopoiesis and stimulates HSC recovery following injury

The basis of hematopoiesis and HSC differentiation is currently under intense scrutiny because of the outstanding implications and therapeutic potential of this knowledge for devastating and incurable human diseases, such as leukemia and aplastic anemia. Even at the most prosaic level, understanding the factors that inhibit and support hematopoiesis could lead to improved stem cell replacement therapies for patients with congenital hematopoietic defects as well as those undergoing chemotherapy for cancer. This is particularly important given that current replacement protocols are fraught with insufficient numbers of stem cells, feasible storage issues, and graft-versus-host disease (Lord et al., 2007). Graft-versus-host disease is the most common cause of morbidity and mortality following allogeneic hematopoietic stem cell transplantation, and is due to mismatching of the **H**uman **L**eukocyte **A**ntigen (HLA) in the donor and the recipient. Consequently, the recipient's immune system rejects the transplanted cells, resulting in the acute or chronic destruction of the transplanted tissue (Pasquini, 2008). Therefore, studies that implicate PGE_2 during hematopoiesis contribute to the understanding of how lipid signaling regulates the generation and maintenance of the HSC population during development and in the adult organism.

Prostaglandin signaling supports lymphoid and myeloid differentiation in mice and zebrafish by enhancing proliferation and differentiation (Williams and Jackson, 1980; Rocca et al., 1999; Villablanca et al., 2007). Stimulating human leukemia THP-1 cells to form macrophages using phorbol ester increases COX1 expression and prostaglandin synthesis (Smith et al., 1993). Furthermore, *Cox2* knockout mice fail to recover from 5-fluorouracil-induced myelotoxicity with hematopoietic repopulation, in comparison with *Cox2* heterozygotes (Lorenz et

al., 1999). Together, these data imply that prostaglandin synthesis enhances HSC function in the adult animal.

PGE_2 also maintains the HSC population in developing zebrafish embryos. Chemicals were screened for their effects on the number of HSCs that express the diagnostic markers *runx1* and *cmyb* in zebrafish embryos (36 hpf) (**Fig. 1-5**). 10 compounds that affected PGE_2 synthesis all resulted in changes to the HSC population, suggesting that PGE_2 enhances HSC development in zebrafish embryos (North et al., 2007). $dmPGE_2$ treatment also increases HSCs in the dorsal aorta (the AGM in zebrafish). Contrastingly, Cox1 inhibition with SC-560, inhibition of Cox2 with either Celecoxib or NS-398, and injection with MOs targeted against *ep2* and *ep4* result in more HSCs. *cox1* and *cox2* are both expressed in the HSC domain of the AGM, though they show distinctive expression patterns. *cox1* is expressed in both the HSCs and the endothelial cells of the AGM, whereas *cox2* is only expressed in the HSCs. The effects of prostaglandin synthesis or signaling inhibition on the number of HSCs are suppressed with treatment using a stabilized derivative of PGE_2 ($dmPGE_2$). In addition, all four EP receptors are expressed on HSCs and differentiated cell populations in the bone marrow of the mouse and human (Hoggatt et al., 2009), suggesting that PGE_2 signaling occurs in this region. The effects of PGE_2 on the recovery of the HSC population following injury were tested in both zebrafish and mouse models. Kidney marrow recovery of irradiated fish is delayed with Indomethacin treatment, but enhanced with exposure to $dmPGE_2$. The precursor cell population was especially sensitive to changes in PGE_2. Embryoid colony formation of mouse stem cell lines also decreases with Indomethacin treatment and increases with $dmPGE_2$ exposure, with the exception of the highest dose (100

μM). The authors suggest that the high dose of PGE_2 results in the maintenance, or "freeze," of the stem cell fate, preventing the differentiation of cells and the formation of embryoid colonies. Lastly, repopulation analysis of both competitor cells and $dmPGE_2$-treated cells into congenic irradiated mice shows that PGE_2-treated cells form more short-term and long-term spleen colonies, which are each derived from one HSC. Furthermore, PGE_2-treated HSC clones contribute to the whole bone marrow more frequently than competitor cells (North et al., 2007; Hoggatt et al., 2009). Therefore, PGE_2 positively regulates the HSC population during development and promotes recovery following injury.

Although the Zon group did not find that decreased PGE_2 signaling results in changes in HSC homing to the bone marrow, another study shows that $dmPGE_2$ treatment can enhance the homing capacity of HSC cells, possibly by upregulating CXCR4 levels (North et al., 2007; Hoggatt et al., 2009). The stromal cell-derived factor-1α (SDF-1α), a ligand for CXCR4, is an important chemoattractant that mediates the homing efficiency of cells to the bone marrow. In addition, $dmPGE_2$-treated cell migration is more sensitive to a SDF-1 gradient, though this increased chemoattraction is inhibited by AMD3100, a CXCR4 antagonist. $dmPGE_2$-treated HSCs also show decreased apoptosis and upregulated expression of Survivin, which facilitates entry into the cell cycle. Indeed, $dmPGE_2$-treated HSCs proliferate more rapidly (Hoggatt et al., 2009). Thus, these results suggest that PGE_2 signaling enhances the homing and survivability of HSCs.

Zebrafish vasculogenesis (blood vessel development)

Hemangioblasts differentiate into angioblasts, the progenitors to the blood vessels by the 4-somite stage (Hsia and Zon, 2005). Angioblasts express *scl*, *vegf*, *flk1*, *fli1*, *radar/gdf5*, *tie1*, and *tie2*. The inducing factor for differentiation is still unknown, however, according to one report, FGF-2 signaling is sufficient for the differentiation of epithelial quail somitic cells into angioblasts in both embryos and explant culture (Poole et al., 2001; Baldessari and Mione, 2008). Following specification, angioblasts migrate in two waves to the midline; first at 14 hpf, then again at 16 hpf, to form the **d**orsal **a**orta (DA) and the **p**osterior **c**ardinal **v**ein (PCV), as wells as the vascular plexuses surrounding the nerves and the yolk sac (Amatruda and Zon, 1999; Jin et al., 2005; Baldessari and Mione, 2008). The **e**xtra**c**ellular **m**atrix (ECM), which includes Fibronectin, is required for the migration of hemangioblasts to the midline to form the vascular cord at 16 hpf (22-somite stage), as are cytoskeletal components such as Cdc42. The assembly of cell-cell junctions happens later, at 17 hpf, and involves the adhesion components **Z**ona **O**ccludens **1** (ZO1), β-catenin, and Claudin 5 (Baldessari and Mione, 2008). Cells in the vascular cord differentiate by the 26-somite stage into the DA and the PCV, which are distinguished by *ephrin b2a* (*efnb2a*) and *fms-related tyrosine kinase* (*flt4*) expression, respectively (Thompson et al., 1998; Lawson et al., 2001; Baldessari and Mione, 2008).

Prostaglandin E_2 regulates the formation of the vascular tube during development

Our group provided the first evidence that Cox1 functions during vertebrate vascular tube development (Cha et al., 2005). Following its ubiquitous expression during gastrulation, *cox1* transcript is detected in bilateral stripes in the developing lateral plate and intermediate mesoderm during the 7-somite

stage and overlaps with the *fli1* (endothelial marker) and *pax2.1* (nephrogenic marker) expression domains (Cha et al., 2005). During late segmentation, *cox1* expression is enriched in the posterior mesoderm, which contributes to the distal nephric duct, notochord, hypochord, and vasculature. Embryos treated with either Indomethacin or Cox1-specific inhibitor SC-560 and embryos injected with *cox1* MO are arrested during gastrulation at higher doses, consistent with the results of the FitzGerald group (Grosser et al., 2002; Cha et al., 2005). At lower doses, treated embryos complete gastrulation, but also manifest other phenotypes that reflect the function of *cox1* in the posterior mesoderm. For example, *cox1* morphants have more *pax2.1* staining, indicating an increase of the distal neprhric duct. The predominant late phenotypes, however, are vascular developmental defects. Blood pools accumulate in the posterior body because of a single distended vessel rather than distinct DA and PCV structures. Cox1 inhibitor-treated embryos and *cox1* morphants also do not have normal vessel boundaries, as indicated by *fli1* expression. Arterial markers (*ephB2*) are normal in *cox-1* morphants, but expression of the venous marker *flt4* in the PCV as well as in the posterior venous plexus is reduced. To establish when Cox1 is required for posterior vessel formation, embryos were treated with the nonspecific NSAID Indomethacin for overlapping periods ranging from the 5 somite stage to 38 hpf. When Indomethacin is removed before the 25 somite stage, none of the embryos show the posterior vessel defect. When Cox1 function is inhibited after the 25 somite stage, the posterior vascular defects are present. Interestingly, the vascular tube forms from the vascular cord at the 26 somite stage (Parker et al., 2004). Therefore, Cox1 mediates the transition from the vascular cord to the vascular tube during the 24-26 somite stages, though the precise mechanism by

which Cox1 inhibition causes venous defects remains unclear (Cha et al., 2005). Indomethacin-treated embryos also show intersomitic vessel defects without changes to the somite structure or organization. Angiogenesis of the intersomitic vessels from the DA requires Vegf and is inhibited by Notch signaling (Baldessari and Mione, 2008). Embryos treated with Indomethacin, however, showed no change in the expression of *vegf*, indicating that prostaglandin signaling influences intersomitic vessel development in a Vegf-independent manner. The effects of Indomethacin treatment could be rescued by PGE_2 as well as $PGF_{2\alpha}$, albeit less efficiently, suggesting that these two prostaglandins function during vascular tube development.

Although many studies implicate prostaglandins in promoting angiogenesis during tumorigenesis, this data provided the first indication that prostaglandins influenced vascular formation during normal vertebrate development (Cha et al., 2005). It remains to be determined how prostaglandin signaling regulates intersomitic vessel development and the formation of the vascular tube from the vascular cord during vasculogenesis.

The Role of Prostaglandin E_2 during Tumorigenesis

Many studies correlate PGE_2 with human cancers (Buchanan and Dubois, 2006; Buchanan et al., 2006; Wang and Dubois, 2006; Wu, 2006). Multiple components of prostaglandin biosynthesis, catalysis, and signaling change the course of tumorigenesis. Use of NSAIDs reduces colorectal cancer and associated mortality by 40-50% (Sheng et al., 2001). *COX1* expression is not correlated with cancer metastasis (Backlund et al., 2005), reflecting its role in homeostatic processes. COX2, however, is thought to promote cancer cell

growth, survival, and invasiveness. *COX2* expression increases in colon adenomas and adenocarcinomas in comparison with the normal colonic mucosa (Yoshimatsu et al., 2001). COX2 synthesis is also increased in hepatocellular carcinoma (HCC), whereas COX2 inhibitor treatment results in HCC cell growth inhibition (Wu, 2006).

These data convincingly correlate increased PGE2 biosynthesis with multiple cancer types, but how does PGE_2 signaling enhance or influence tumor properties? PGE_2 has been shown to inhibit immune responses to cancer cells as well as apoptosis by inducing BCL-2 and NF-κB (Sheng et al., 1998; Wang and Dubois, 2006). In contrast, PGE_2 stimulates cancer cell proliferation, angiogenesis via VEGF and bFGF regulation, and invasion through activation of the EGFR-PIK3-AKT signaling axis. Colorectal carcinoma cell treatment with PGE_2 stimulates cell migration, DNA synthesis, and the formation of actin stress fibers as well as the focal adhesion complex components, **f**ocal **a**dhesion **k**inase (FAK) and paxillin (Sheng et al., 2001). Low-dose PGE_2 treatment stimulates the growth of both colon adenomas and adenocarcinomas. Contrastingly, high-dose PGE_2 treatment inhibits the growth of colon adenomas but stimulates the growth of colon adenocarcinomas (Chell et al., 2006). Interestingly, EP4 expression is higher in adenocarcinomas than adenomas, which suggests that, unless increased PGE_2 levels are accompanied by increased EP4 receptor expression, increased PGE_2 inhibits growth, most likely through an EP4-independent signaling pathway. Thus, increasing cancer cell malignancy is correlated with accelerated PGE_2–mediated cell growth (Chell et al., 2006).

Catalysis of PGE_2 occurs by NAD^+-dependent **15**-hydroxy**p**rosta**g**landin **d**e**h**ydrogenase (15-PGDH). 15-PGDH expression is decreased in medullary

thyroid cancer, transitional bladder cancer, and colorectal cancer (Backlund et al., 2005; Repasky et al., 2007; Backlund et al., 2008). In particular, 15-PGDH expression is depressed in *Apc*^{min} mouse tumors relative to the normal colonic mucosa. Therefore, PGE_2 signaling in cancer cells not only increases PGE_2 synthesis, but also decreases PGE_2 degradation, stabilizing the existing lipid pool.

Expression of the PGE_2 GPCRs is also associated with tumorigenesis. EP2 signaling increases *COX2* expression in cell culture. Notably, EP4 expression in gallbladder and colorectal cancer is increased in 100% of tumors relative to the normal colonic mucosa. EP4 signaling also activates **E**arly **G**rowth **R**esponse Factor **1** (EGR1) through an ERK- and PIK3-dependent mechanism. The expression of EGR1 increases *PTGES* gene expression, thereby resulting in a positive feedback loop for PGE_2 signaling in cells (Fujino and Regan, 2003; Fujino et al., 2003; Regan, 2003). EGR-1 activation also regulates the cell cycle by activating *CYCLIN D1*/*CCND1* (Fujino and Regan, 2003). PIK3 activation downstream of EP4 receptor binding also promotes cell survival and proliferation by activating Peroxisome Proliferator Activated Receptor δ) PPARδ, a member of the nuclear hormone receptor superfamily. In addition, EP4 transfection into cell culture confers anchorage independence, a measure of tumor invasiveness (Chell et al., 2006). *Ep4* knockout mice show decreased aberrant crypt foci formation in comparison to wild-type mice, when animals are exposed the carcinogen azoxymethane, suggesting that EP4 signaling is important for tumor formation. Furthermore, the treatment of *Apc*^{min} mice, which have a confluence of intestinal tumors due to constitutively active β-catenin, with

an EP4 antagonist results in decreased intestinal polyps (Backlund et al., 2005). Therefore, PGE_2 signaling enhances tumorigenesis through multiple effector genes.

The studies reviewed here demonstrate that PGE_2 impacts on multiple processes during development and disease. But many open questions remain: does PGE_2 regulate development and disease using conserved mechanisms? What are the cell properties and the cell behaviors that are altered by PGE_2 signaling? Previous work from our group and the FitzGerald group has shown that decreased prostaglandin synthesis impairs gastrulation movements. Therefore, I am also interested in the following questions. Does PGE_2 only interact with one Ep receptor during gastrulation? Are there any effects of PGE_2 signaling during early development that do not occur in other cellular contexts? Are other cell populations affected in Ptges-deficient gastrula? Are epiboly, convergence, and extension the only gastrulation movements that are regulated by PGE_2 signaling? How does PGE_2 regulate the epiboly movement? How does PGE_2 affect lateral cell motility during the convergence and extension movements of lateral cells?

In the following chapters, I will discuss the effects of *ptges* MO high-dose injection on all the gastrulation movements (**Chapter 2**). Our data shows that cell adhesion and cell motility are affected in Ptges-deficient embryos, and we present a mechanism by which PGE_2 signaling modulates cell adhesion by inhibiting Gsk3β (**Chapter 2**). I also demonstrate that Ptges-deficient embryos have decreased endodermal cell specification, possibly due to effects on Nodal signaling (**Chapter 3**). Next, I present preliminary characterization of a nonsense mutation in the gene encoding Ep4a, a mutant that our group has generated in a

reverse genetics screen (**Chapter 4**). Lastly, I will discuss the conserved mechanisms that are regulated by PGE_2, as well as the future directions projected for this work and the prostaglandin signaling field (**Chapter 5**).

CHAPTER II

PROSTAGLANDIN Gβγ SIGNALING STIMULATES GASTRULATION MOVEMENTS BY LIMITING CELL ADHESION THROUGH SNAIL STABILIZATION

This chapter has been submitted as an article by the same title to *Nature Cell Biology*.

C.K. Speirs[1], K.K. Jernigan[2], S.-H. Kim[1], Y.I. Cha[3], F. Lin[1,4], D.S. Sepich[1], R.N. DuBois[3,5], E. Lee[2], and L. Solnica-Krezel[1]

[1]Department of Biological Sciences, Vanderbilt University, Nashville, TN 37232.

[2]Department of Cell and Developmental Biology, Vanderbilt University Medical Center, Nashville, TN 37232.

[3]Department of Medicine and Cancer Biology, Cell and Developmental Biology, Vanderbilt University Medical Center and Vanderbilt Ingram Cancer Center, Nashville, TN 37232. [4]Department of Anatomy and Cell Biology, Carver College of Medicine, University of Iowa, Iowa City, IA 52242.

[5]M.D. Anderson Cancer Center, University of Texas, Houston, TX 77030.

Summary

Gastrulation movements fabricate the germ layers and shape them into the vertebrate body. Prostaglandin E_2 (PGE_2) promotes gastrulation movements and cancer cell invasiveness, but how it regulates cell motility remains unclear. We show that PGE_2 signaling curbs cell adhesion by limiting E-cadherin transcript and protein, in part by promoting Snail stability. We delineate a β-catenin-independent pathway downstream of PGE_2, whereby the G protein βγ subunits inhibit the Gsk3β-mediated proteasomal degradation of Snail. In the prospective ectoderm, PGE_2 regulates E-cadherin via Snail-independent mechanisms. Our findings reveal the multi-pronged repression of E-cadherin by PGE_2 that enables the precise and rapid regulation of cell adhesion during gastrulation movements. PGE_2 likely employs these mechanisms in other contexts, such as when cancer cells exploit the PGE_2 signaling pathway to spread and advance disease.

Prostaglandin signaling is important to human physiology and contributes to digestion, reproduction, pain, immunity, cardiovascular function, and stem cell recovery (Wang and Dubois, 2006). PGE_2 synthesis begins when arachidonic acid, synthesized from membrane phospholipids, becomes PGG_2, then PGH_2, through the action of Prostaglandin-endoperoxide synthases (Ptgs)/Prostaglandin G/H synthase (Pghs)/Cyclooxygenases (Cox) 1 and 2. PGH_2 is converted by Prostaglandin E synthase (Ptges) to PGE_2, which binds and signals via its downstream **G P**rotein **C**oupled **R**eceptors (GPCRs) Prostaglandin E receptor (Ptger)/E-prostanoid (EP) 1-4 receptors (**Fig. 2-S1A**) (Regan, 2003; Wu, 2006).

Normal fertility and gestation require prostaglandins, confounding the interpretation of the mutant phenotypes in mice (Cha et al., 2006). However, studies in externally developing zebrafish showed that prostaglandins are required for early vertebrate embryogenesis, specifically gastrulation, a key process of cell signaling and cell movement that elaborates the body plan (Grosser et al., 2002; Solnica-Krezel, 2005; Cha et al., 2006). There are four evolutionarily conserved gastrulation movements; epiboly, internalization, convergence, and extension (**Fig. 2-S1B-C**). Epiboly is the initial movement of zebrafish gastrulation that thins and spreads embryonic tissues over the yolk cell. Internalization is the movement of mesendodermal progenitors underneath the prospective ectoderm. Following internalization, mesendodermal cells migrate towards the animal pole, the future head of the embryo. The movements of convergence and extension narrow the germ layers and embryonic body mediolaterally, while extension movements elongate the embryonic tissues head to tail (7).

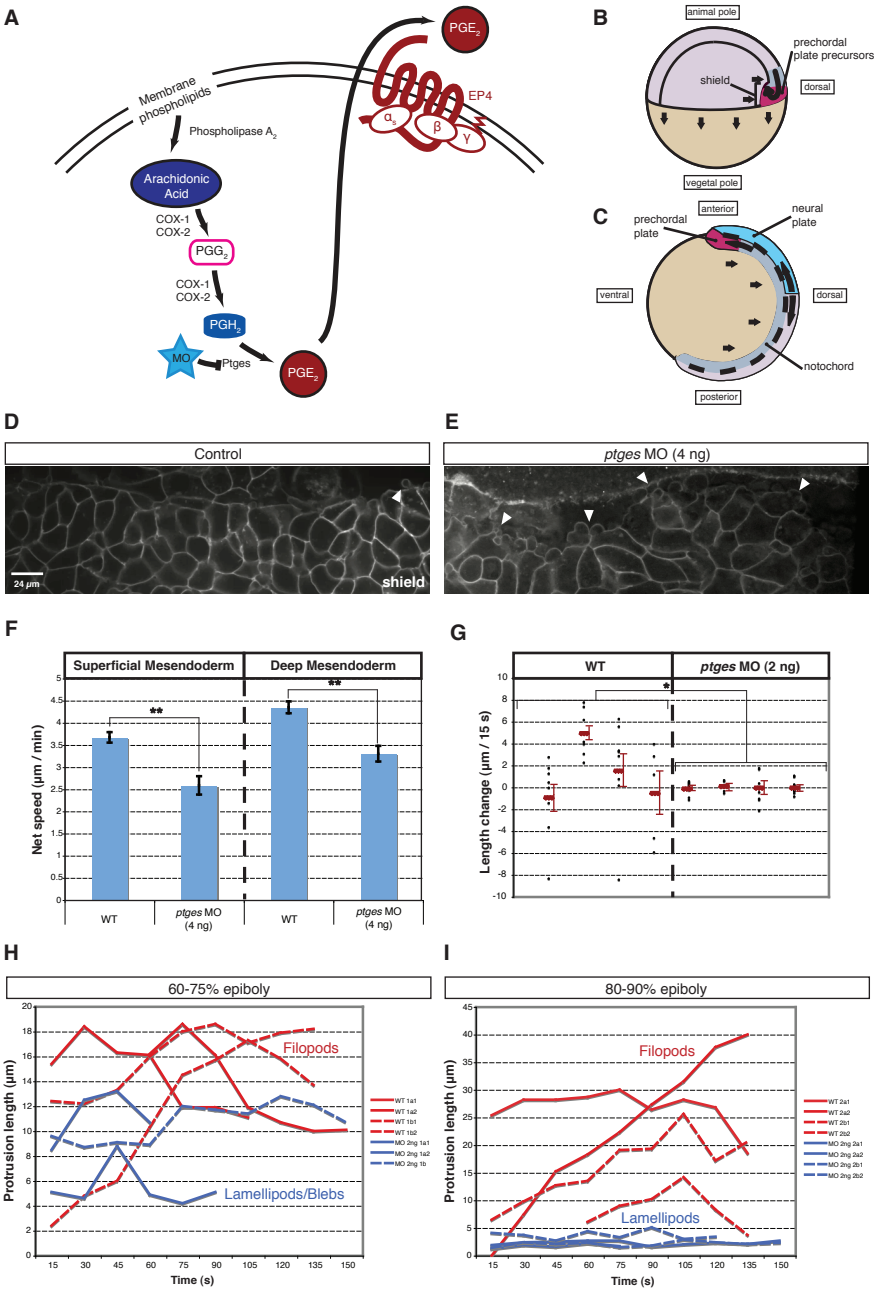

Figure 2-S1. (A) Schematic of PGE_2 synthesis. COX: Cyclooxygenase-/Prostaglandin -endoperoxide synthase type-1 and -2; PGG_2: Prostaglandin G_2; PGH_2: Prostaglandin H_2; PGE_2: Prostaglandin E_2; MO: antisense morpholino oligonucleotide; Ptges: Prostaglandin E synthase; EP4: E-prostanoid 4. Blue star: location of pathway inhibition by MO. (B, C) Schematic of gastrulation movements in zebrafish at the shield (B) and tailbud (C) stage embryos. (D, E) Protrusive activity of axial mesodermal cells undergoing epiboly (yolk cell-embryonic cell margin) in control (D) and tailbud (E) embryos. Arrowhead: blebbing activity. (F) The net speed (μm/min) of superficial and deep mesendodermal cells in wild-type embryos and ptges morphants. p-value(**)< 1x10-4. (G) Quantitation of the length changes (μm/15 sec) of four prechordal mesoderm cell protrusions per sample during the time-lapse. Cellular protrusions from *ptges* morphants show less extension and retraction than those from wild-type embryos (p-value(*)= 0.03). Red line: average protrusion length. (H, I) Protrusion length in prechordal mesoderm cells migrating anteriorly towards the animal pole. Four protrusions (Embryo 1: solid lines; Embryo 2: dashed lines) were analyzed in control (red) and *ptges* (blue) morphant gastrulae at 60-75% (H) and 80-90% (I) epiboly during time-lapse imaging. Control morphant protrusions are filopodia (Length>width; diameter<2 μm), whereas *ptges* morphant protrusions exhibit lamellipodial (Width>length; length>2 μm) or bleb-like characteristics (Montero, et al., 2003).

Previously, prostaglandin synthesis in zebrafish embryos was reduced with either enzymatic inhibitors of Cox1 or antisense morpholino oligonucleotides (MO), which inhibit the translation of Cox1 (*cox1* MO/MO1-*ptgs*) or Ptges (*ptges* MO/MO2-*ptges*) (Grosser et al., 2002; Solnica-Krezel, 2005; Cha et al., 2006). These manipulations resulted in an epiboly delay or arrest, largely due to reduced levels of PGE_2, the predominant prostaglandin in zebrafish gastrulae (Grosser et al., 2002). We have also shown that lowering PGE_2 signaling with a low dose of *ptges* MO (2 ng) resulted in a convergence and extension defect due to the decreased speed of dorsally-migrating lateral mesodermal cells (Cha et al., 2006).

To delineate the mechanisms by which PGE_2 regulates gastrulation, we focused on *ptges* morphant embryos, injected with a higher dose (4 ng) of MOs that displayed strong and global gastrulation defects (**Fig. 2-1A-C**). These defects were suppressed by supplementing the embryo medium with PGE_2 and were not observed when a control five-bp mismatch MO (control MO) was injected. Ptges- and Cox1-deficient gastrulae showed arrested epiboly and an uneven surface associated with cell clumping (**Figs. 2-1A, 2-S2A**). Whereas chordamesoderm cells expressing *no tail* (*ntl*)/*brachyury* were in the deeper, mesedodermal layer of control morphant gastrulae, Ptges-deficient gastrulae had *ntl*-expressing cells in the superficial layer, indicating that internalization was defective in the most strongly affected embryos (**Fig. 2-1B**). In less severely affected Ptges-deficient gastrulae, internalization occurred. However, the subsequent movement of mesodermal cells, animalward migration, was impaired relative to control gastrulae, as indicated by the posteriorly-shifted position of *frizzled homolog 8b* (*fzd8b*)-expressing prechordal mesoderm cells (**Fig. 2-1C**). All of these movement

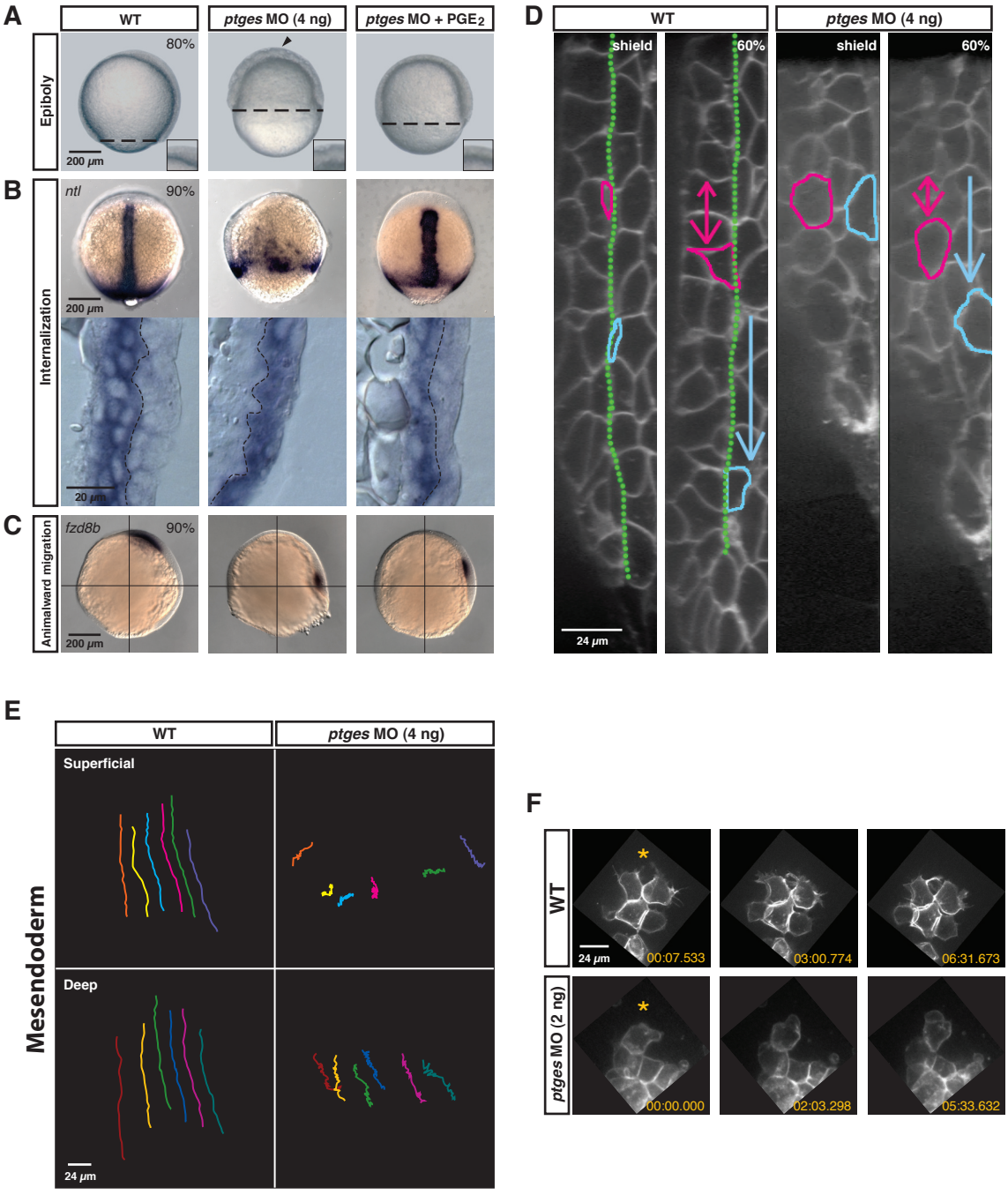

Figure 2-1. The depletion of PGE_2 causes global gastrulation defects. *ptges* MO-injected embryos (4 ng) were evaluated for gastrulation movement defects. (A) Live embryos (80% epiboly). WT: uninjected wild-type; *ptges* MO (4 ng): Ptges-deficient; *ptges* MO (4 ng) + PGE_2: Ptges-deficient embryos treated with 10 μM PGE_2. Dashed line: progress of epiboly; arrowhead: uneven surface of the blastoderm; inset: magnified blastoderm surface. (B) Deficit of internalized, *notail*-expressing axial mesodermal cells in *ptges* morphants (top)(90% epiboly; dorsal views). Lateral views of cryosections through the dorsal side of the embryo (bottom). Yolk cell, left; external surface, right; dashed line, germ layer boundary. (C) Animalward migration of *frizzled homolog 8b*-expressing prechordal mesoderm cells (90% epiboly; lateral views). (D) Confocal images of the lateral view of the dorsal midline in membrane EGFP-labeled embryos (shield stage; yolk cell, left; external surface, right). The green line marks the boundary between the superficial (blue cell) and deep layers (pink cell) of the gastrula (arrows: vector of movement). (E) Paths of six cells in the superficial and deep layers of the mesendoderm in wild-type and *ptges* morphant embryos. Vegetal pole, top; animal pole, bottom. (F) Confocal images of prechordal mesoderm cells (70% epiboly). Three frames from a time-lapse movie are shown. Orange asterisks: towards the animal pole.

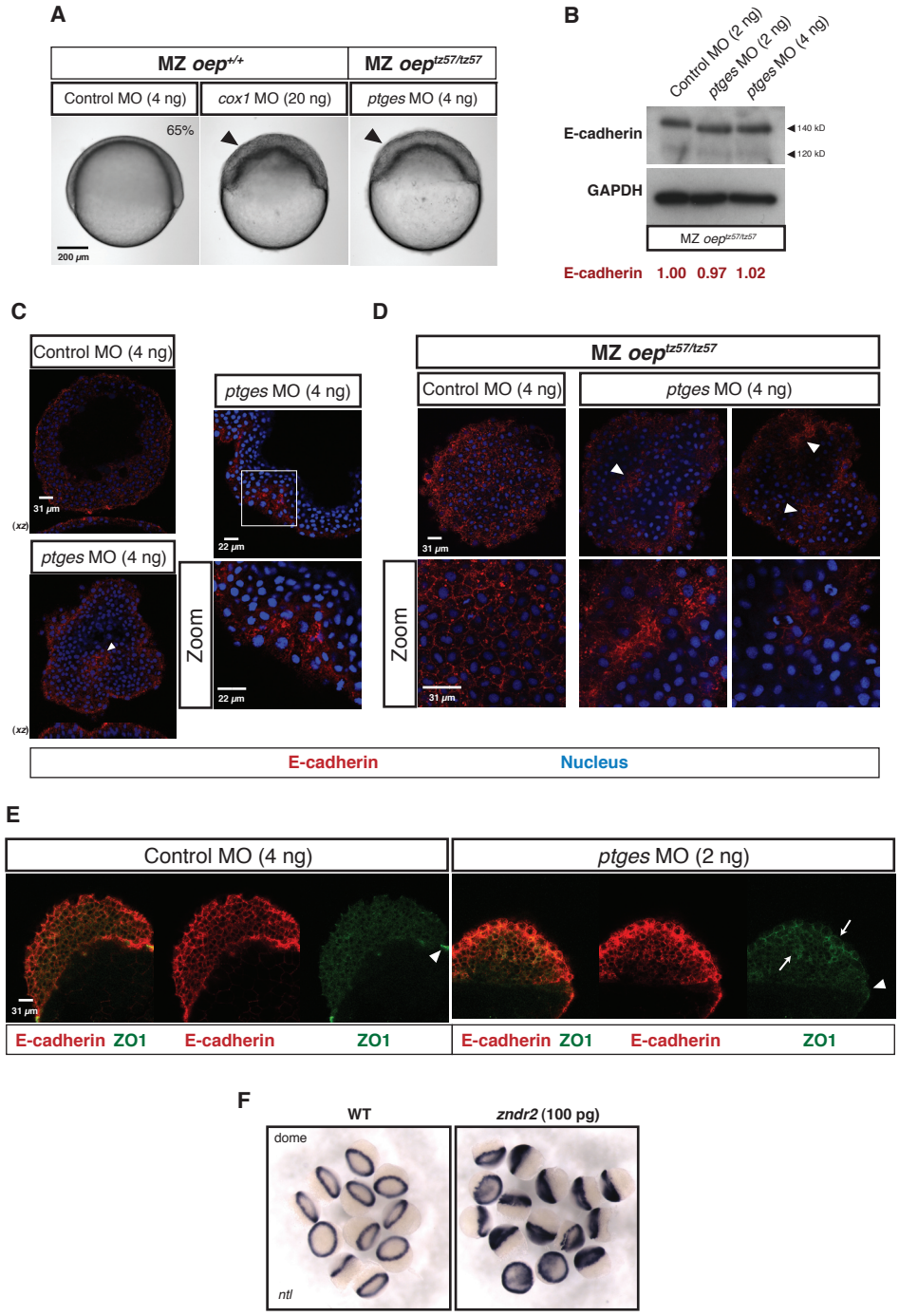

Figure 2-S2. (A) The cell clumping phenotype in *cox1* morphants and MZ *oep*$^{tz57/tz57}$ *ptges* morphants (arrowheads). (B) Immunoblotting and quantitation of total levels of E-cadherin in MZ *oep*$^{tz57/tz57}$ mutants injected with *ptges* MO (E-cadherin, top; GAPDH, bottom). (C) Confocal images of E-cadherin immunostaining in the ectoderm of control and *ptges* morphants at the shield stage (animal pole view; E-cadherin: red; Nuclei: blue). Boxed area in the right panel is shown below in the zoom view. Arrowhead: focal upregulation of E-cadherin. (D) Confocal images of E-cadherin immunostaining in the ectoderm of MZ *oep*$^{tz57/tz57}$ mutant gastrulae injected with *ptges* MO (bottom: zoom view). Arrowheads: foci of upregulation of E-cadherin that correlate with the uneven surface of the blastoderm (boxed, top panel) (E-cadherin: red; Nuclei: blue). (E) Immunostaining for ZO1 and E-cadherin in embryos injected with control or *ptges* MOs (E-cadherin: red; ZO1: green). Arrowhead: point of contact between the superficial enveloping layer and the yolk cell in the gastrulae, arrow: areas of increased E-cadherin and ZO1 expression. (F) Whole mount in situ hybridization showing that *cyclops* RNA-injected (100 pg) embryos form excess mesendoderm (dome stage).

defects were partially suppressed with synthetic PGE_2 treatment, confirming the specific and essential role of PGE_2 in gastrulation movements. Defective gastrulation movements, cell paths, and net speed were also revealed by time-lapse analysis of the dorsal shield, the homolog to the Spemann-Mangold amphibian organizer (**Figs. 2-1D-E, 2-S1F**). In addition, the boundary (Brachet's cleft) between the internalized mesendodermal cells and the superficial layer was distinct in the control but absent in Ptges-deficient gastrulae. Therefore, PGE_2 signaling regulates epiboly and internalization in addition to convergence and extension movements during gastrulation.

The cell properties that regulate cell movement include protrusive activity, cell adhesion, cytoskeleton dynamics, and cell polarity. Defects in these cell properties impair cell migration and rearrangements during gastrulation (Montero et al., 2003; Montero and Heisenberg, 2004; Solnica-Krezel, 2005; Ulrich et al., 2005). To evaluate protrusive activity, we analyzed the time-lapse imaging of membrane EGFP-labeled cells (**Fig. 2-1F**). At the interface of the blastoderm with the yolk cell at early gastrulation, cells exhibited protrusions with few blebs in the control morphants (**Fig. 2-S1D**). *ptges* morphant cells, however, showed increased blebbing (**Fig. 2-S1E**). From 60-90% epiboly, the protrusions of the prechordal mesodermal cells migrating towards the animal pole in control gastrulae were active and dynamic with filopodial characteristics, and all protrusions localized to the leading edge of the cell (**Figs. 2-1F, 2-S1G-I**). In contrast, the protrusions of the prechordal mesodermal cells in gastrulae with reduced Ptges function (2 ng MO) were blunted with lamellipodial, sometimes bleb-like, characteristics (Montero et al., 2003), and protrusions localized to all

edges of the cell. Therefore, impaired gastrulation movements in PGE_2-depleted embryos are associated with abnormal protrusive activity.

Because of the cell clumping in Ptges-deficient gastrulae (**Fig. 2-1A**), we hypothesized that increased cell adhesion contributed to the gastrulation movement phenotype. In all animals, normal gastrulation requires appropriate levels of E-cadherin/Cadherin 1, epithelial (Cdh1) (Solnica-Krezel, 2006; Hammerschmidt and Wedlich, 2008), a component of the adherens junction that binds β-catenin (Drees et al., 2005). Moreover, zebrafish *cdh1*$^{dtv43/dtv43}$/*half baked* (*hab*) mutants manifest defects in epiboly, internalization, convergence, and extension (Babb and Marrs, 2004; Kane et al., 2005; McFarland et al., 2005; Montero et al., 2005; Shimizu et al., 2005; von der Hardt et al., 2007). Using **q**uantitative **r**eal-**t**ime **PCR** (qRTPCR), we found that *cdh1* transcript levels relative to *β-actin* increased two-fold in Ptges-deficient embryos compared with controls (**Fig. 2-2A**). Consistently, the immunoblotting analysis showed that the protein levels of E-cadherin were increased two-fold relative to the controls (Fig. 2B). Interestingly, the whole mount immunohistochemistry revealed two patterns of E-cadherin protein expression in the Ptges-deficient gastrulae. In the mesendoderm, E-cadherin expression was uniformly increased (**Fig. 2-2C**), whereas, in the ectoderm, we observed foci of increased E-cadherin levels, surrounded by areas of relatively lower protein levels (**Figs. 2-2C, 2-S2C**). This pattern of ectodermal E-cadherin staining was not associated with a quantifiable increase of E-cadherin protein levels (**Fig. 2-S2B**). Consistently, the ectodermal E-cadherin staining and the cell clumping phenotype were also seen in Ptges-deficient MZ*oep*$^{tz57/tz57}$ mutants, which predominantly contain ectoderm (**Fig. 2-**

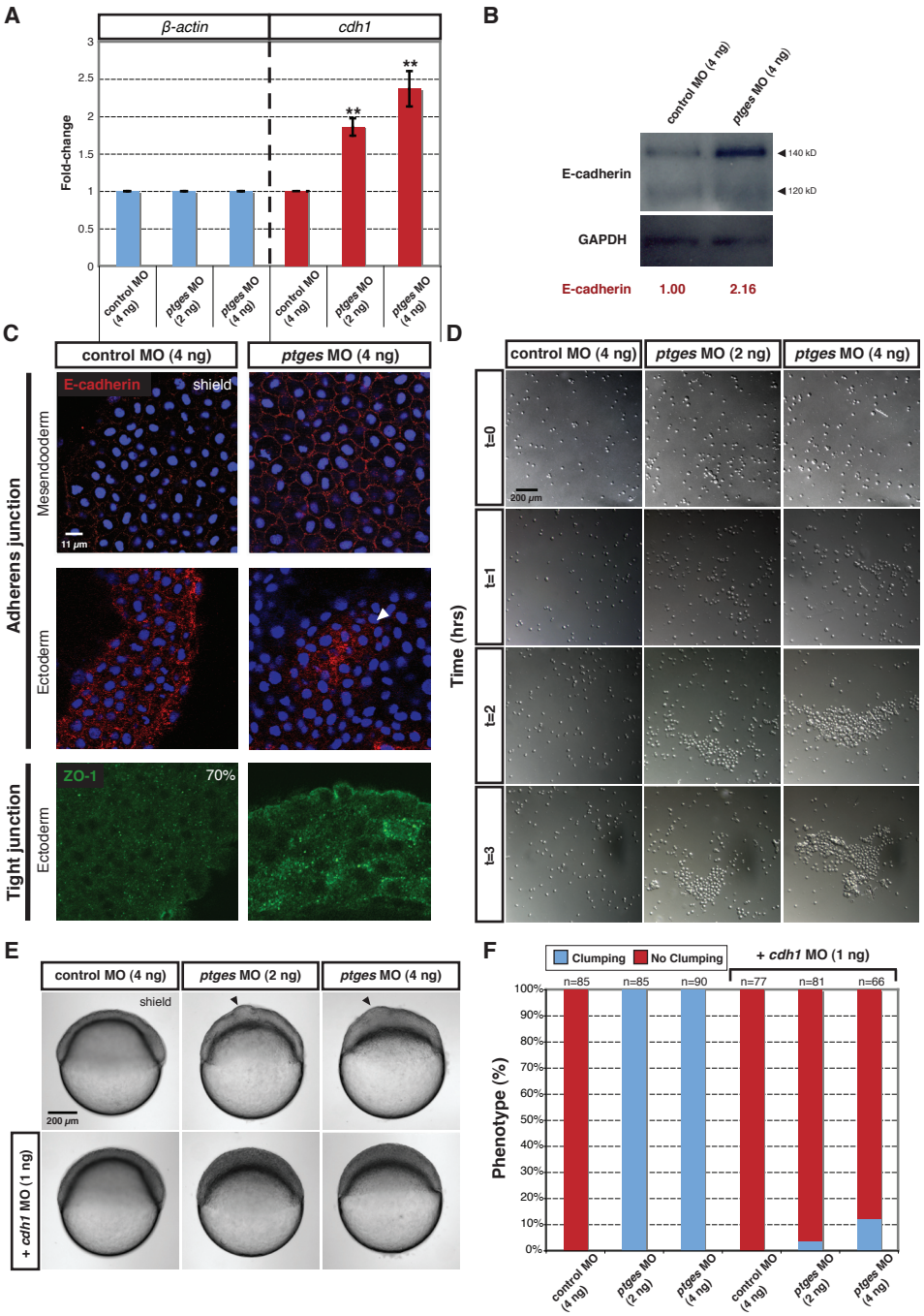

Figure 2-2. PGE_2 governs cell adhesion by decreasing *cdh1/e-cadherin* transcript and protein levels. (A) Quantitative real-time PCR (qRTPCR) of *β-actin* (left) and *cdh1* (right) transcript levels in control and *ptges* morphants at 60% epiboly. p-value(**)<0.005. (B) Western blot of E-cadherin (top) and GAPDH (bottom, loading control) from shield stage embryos injected with control and *ptges* MOs. Protein levels were quantified using Adobe Photoshop. (C) Confocal images of whole-mount immunostaining of adherens and tight junction components. E-cadherin protein expression at the shield stage in the mesoderm (top) and ectoderm (middle). Mesoderm: lateral view; ectoderm: animal pole view; Red: E-cadherin; Blue: Nuclear stain. Arrowhead points to the foci of increased E-cadherin in the ectoderm. ZO1 (bottom) in the ectoderm at 70% epiboly (lateral view). (D) Cell adhesion assay of cells from dissociated control and *ptges* morphant gastrulae. Images of dissociated blastomeres on Fibronectin substrate were taken every hour for three hours. (E) Suppression of the cell clumping phenotype in *ptges* morphants by *cdh1* MO injection. Images of embryos at the shield stage (arrowhead: cell clumping). (F) Graphical compilation of two experiments in which control and *ptges* morphant embryos were co-injected with *cdh1* MO (1 ng) and evaluated at 60% epiboly for the cell clumping phenotype.

S2A, D) (Gritsman et al., 1999). Thus, two distinct patterns of E-cadherin upregulation in Ptges-deficient embryos may account for the discrepancy between the strong cell clumping phenotype and the modest increase of total E-cadherin protein levels quantified in whole embryo extracts.

The assembly of adherens junctions precedes tight junctions at cell-cell contacts (Yap et al., 2007; Hartsock and Nelson, 2008), so the increase of E-cadherin levels in Ptges-deficient embryos may promote tight junction assembly. Accordingly, a component of tight junctions, **Z**onula **O**ccludens **1** (ZO1) (Yap et al., 2007; Hartsock and Nelson, 2008), was also found to be upregulated in Ptges-deficient gastrulae in areas of the ectoderm that correlated with increased E-cadherin expression (**Figs. 2-2C, 2-S2E**). Interestingly, the contact points of the superficial enveloping layer with the yolk cell contain tight junctions that are strengthened during epiboly (Trinkaus, 1984), however, this domain of ZO1 expression was decreased in Ptges-deficient gastrulae. Therefore, PGE_2 regulates components of tight junctions in addition to adherens junctions, thereby regulating cell adhesion through multiple types of cell-cell contact.

The expression of cell adhesion components in Ptges-deficient gastrulae might result in increased cell-cell adhesion, thereby contributing to the gastrulation phenotype. To evaluate cell adhesion in Ptges-deficient embryos, we carried out cell adhesion assays (Ulrich et al., 2005). First, we induced mesendodermal fates in embryonic cells by injection with synthetic *nodal-related 2* (*ndr2*)/*cyclops* RNA (**Fig. 2-S2F**) and co-injected *ptges* or control MOs. The resulting embryos were dissociated into single cells at the dome stage, then seeded into Fibronectin-coated wells for a three hour time-course to determine whether cells had formed aggregates. Cells from control morphants showed

clumps of two or three cells at the end of the three-hour time-course. Strikingly, the *ptges* MO injection increased cell clumping in a dose-dependent manner, with large three-dimensional clumps formed by cells from embryos injected with the high MO dose (**Fig. 2-2D**). We conclude that cell adhesion is increased in Ptges-deficient gastrulae, likely because of upregulated adherens and tight junction components, indicating that PGE_2 signaling regulates gastrulation movements by limiting cell adhesion. To investigate whether disrupting E-cadherin translation could suppress aspects of the gastrulation phenotype in PGE_2-deficient gastrulae, we co-injected *cdh1*/MO3-*cdh1* and *ptges* MOs. Downregulation of E-cadherin suppressed the cell clumping phenotype, but did not significantly improve the epiboly defect (**Fig. 2-2E-F**). Thus, enhanced cell adhesion contributes in part to the gastrulation defects seen in Ptges-deficient embryos.

The increase of *cdh1* transcripts in the Ptges-deficient embryos suggested that PGE_2 signaling positively regulates a transcriptional inhibitor of the *cdh1* gene. Snail/Snai1 (**Table 1-1**), the best characterized of these, binds E-boxes in the E-cadherin gene promoter to inhibit its transcription (Barrallo-Gimeno and Nieto, 2005). Two zebrafish *snail* genes, *snail homolog 1a*/*snai1a* and *snail homolog 1b*/*snai1b* (**Table 1-1**), are expressed in the internalizing mesendoderm during gastrulation and are required for the animalward migration of anterior mesendodermal cells (Hammerschmidt and Nusslein-Volhard, 1993; Yamashita et al., 2004; Blanco et al., 2007). Recent work in cell culture has shown that chemical or antisense interference with the prostaglandin signaling pathway resulted in decreased *SNAI1* transcription and increased E-cadherin protein (Dohadwala et al., 2006; Brouxhon et al., 2007). However, our qRT-PCR and whole-mount *in situ* hybridization analyses showed that *snai1a* and *snai1b* levels

were not significantly different in *ptges* versus control morphants (**Figs. 2-3A, 2-S3A-B**) until 60% epiboly, when the Ptges-deficient gastrulation phenotype is already apparent (**Fig. 2-S3B**). Therefore, we conclude that the regulation of *snai1a* transcription by PGE_2 could not cause the gastrulation phenotype in this developmental context. In contrast, the Snai1 protein level was significantly decreased in embryos injected with *ptges* MO in a dose-dependent manner (**Fig. 2-3B**), revealing the posttranscriptional regulation of Snail by prostaglandins.

To determine if the localization or stability of Snai1a was affected in Ptges-deficient gastrulae, we analyzed the expression of the Snai1a-YFP fusion protein (Yamashita et al., 2004) in live embryos. We injected synthetic *snai1a-yfp*, *membrane egfp*, and *yfp* RNA constructs into one-cell stage zebrafish embryos and analyzed the resulting proteins by confocal microscopy at the shield stage. The injection of *ptges* MO resulted in the dramatic and dose-dependent reduction or loss of Snai1a-YFP expression compared to control embryos (**Fig. 2-3C**). Residual cells expressing Snai1a-YFP still showed its nuclear localization, whereas YFP and mEGFP expression were unchanged. Loss of Snai1a-YFP expression in Ptges-deficient gastrulae was suppressed by PGE_2 treatment. Furthermore, *cox1* morphants also showed decreased Snai1a-YFP expression (**Fig. 2-S4B**). These results demonstrate that PGE_2 signaling can regulate the protein expression of Snai1a. To test whether the increased *cdh1* transcripts and E-cadherin protein levels were an outcome of reduced Snai1a expression, *snai1a-HA* RNA was injected mosaically at the 8-cell stage in embryos injected with *ptges* MO at the one-cell stage (**Fig. 2-3D**). The quantification of E-cadherin immunostaining showed that Snai1a-HA-expressing cells had significantly lower E-cadherin levels than surrounding HA-negative cells in these Ptges-deficient gastrulae (**Fig.**

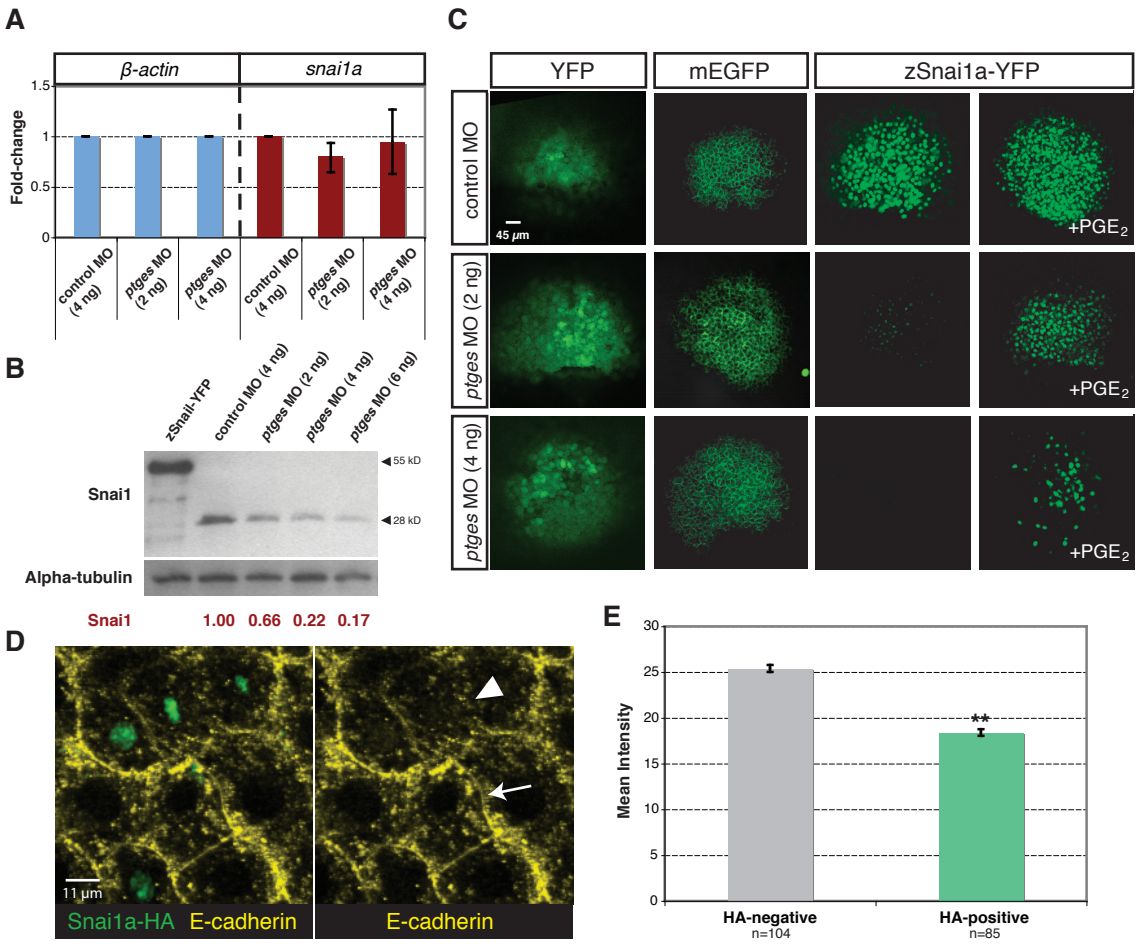

Figure 2-3. PGE_2 deficiency destabilizes Snai1 protein. (A) qRTPCR of *β-actin* (left) and *snai1a* (right) transcript levels in control and *ptges* morphants at 60% epiboly. (B) Immunoblotting using antibodies against Snai1 (top) and α-tubulin (loading control: bottom) in control and *ptges* morphants. The first lane shows embryos that were injected with *snai1a-yfp* (Molecular weight: 55 kD). (C) Confocal microscope images of Snai1a-YFP, YFP, and membrane EGFP expression in control and *ptges* morphants, and *ptges* morphants incubated with PGE_2 (shield stage). (D) Confocal images of *ptges* morphant gastrulae (shield stage) stained with anti-HA (green) and anti-E-cadherin (yellow) that were mosaically injected with *snai1a-ha* RNA (3 pg) at the 8-16 cell stage. Compare the membrane intensity of E-cadherin at the membranes between two HA-positive cells (arrowhead) to that between two HA-negative cells (arrow). (E) Quantitation of E-cadherin immunostaining intensity (Mean Intensity) of Snai1a-HA-negative and Snai1a-HA-positive cells in *ptges* morphant gastrulae. p-value(**)=1.16 x 10-10.

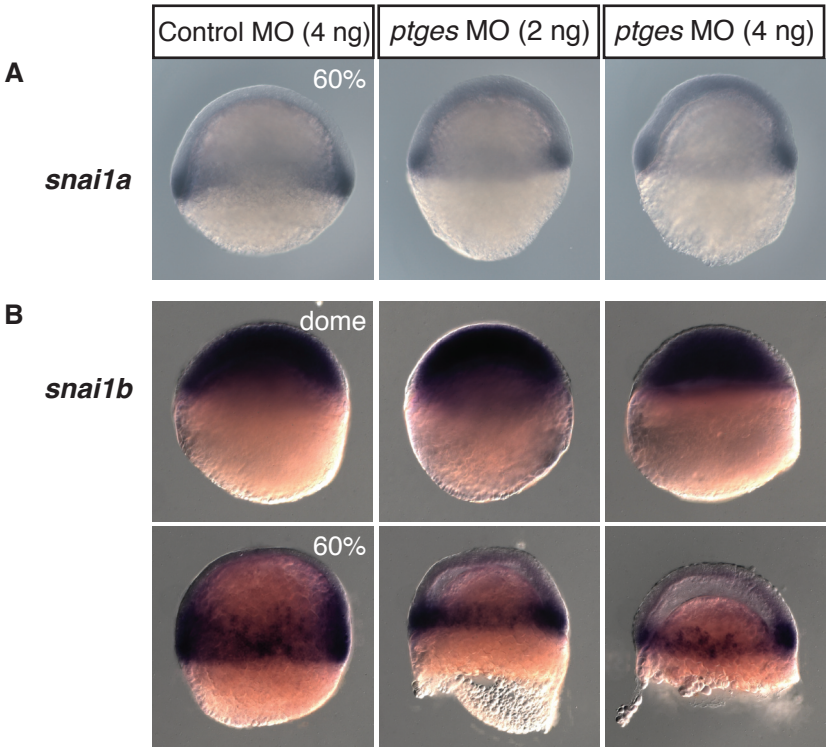

Figure 2-S3. *snai1a* and *snai1b* transcript levels during gastrulation. (A) *snai1a* transcripts shown by in situ hybridization at 60% epiboly. (B) *snai1b* transcripts revealed by *in situ* hybridization at dome and 60% epiboly. Control and *ptges* morphants have indistinguishable expression until 60% epiboly, when the expression domain remains the same but fewer internalized *snai1b*-positive cells are present in the *ptges* morphants.

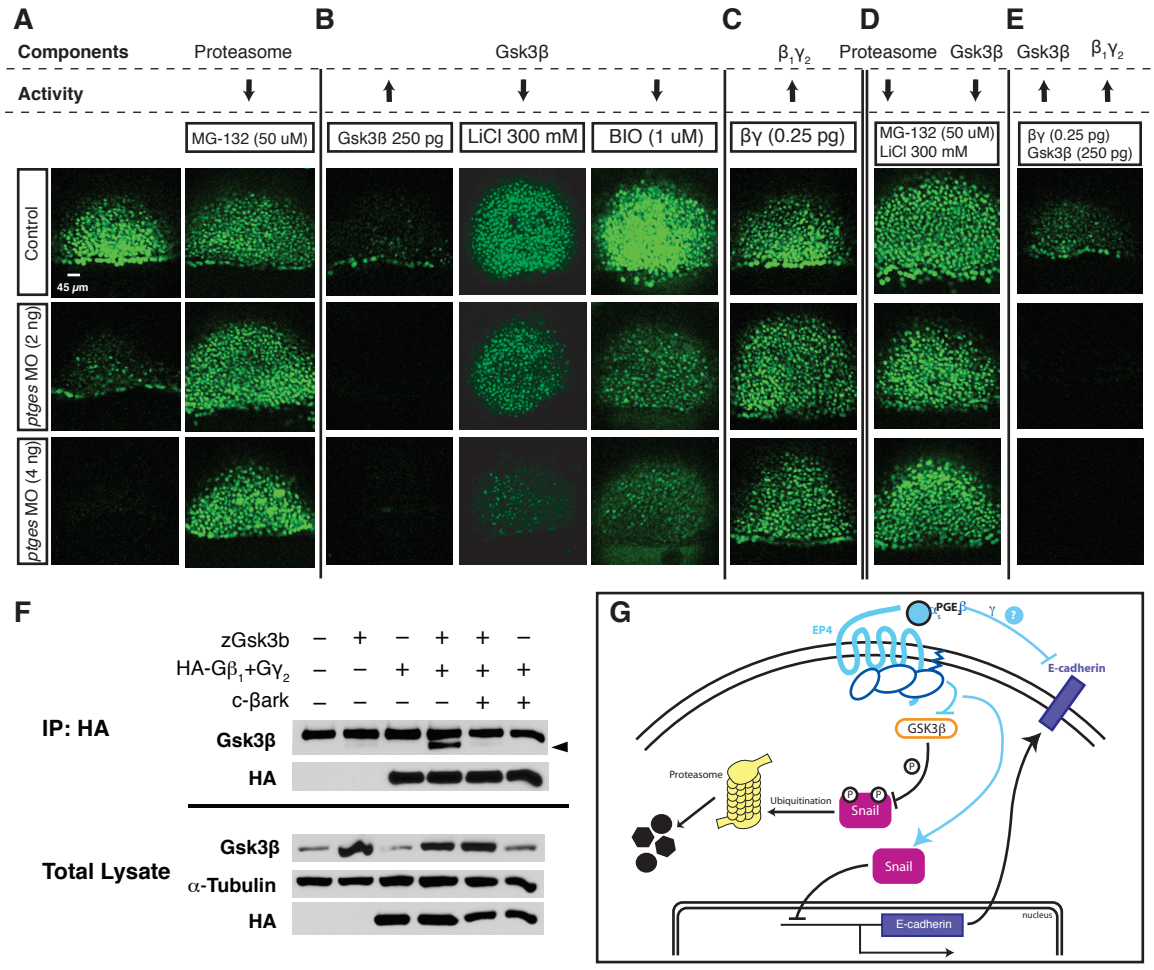

Figure 2-4. PGE_2 Gβγ signaling stabilizes Snai1a by inhibiting Gsk3β-mediated proteasomal degradation. Confocal microscope images of embryos in which the Snai1a-YFP assay was used to test downstream components of PGE_2 signaling for their ability to affect levels of Snai1a in control (top) and ptges morphants (middle, bottom). (A) Treatment with the proteasomal inhibitor, MG132. (B) Injection of *zgsk3β* RNA; treatment with LiCl and BIO, Gsk3β inhibitors. (C) Injection of *hgβ1* and *hgγ2* RNA. (D) Inhibition of both Gsk3β and the proteasome (MG132 treatment). (E) *hgβ1γ2* and *gsk3β* RNA co-injection. (F) Immunoblotting of Gsk3β following immunoprecipitation with hβ1γ2. Zebrafish *gsk3β* and HA-tagged *hβ1/γ2* were transfected into 293T cells. Cell extracts were immunoprecipitated with anti-HA, then immunoblotted with anti-Gsk3β (Gsk3β indicated by arrowhead). The interaction between Gsk3β and hβ1γ2 could be blocked by the addition of c-βark (top). Total lysate Western blots (bottom). (G) Model of the mechanism by which PGE_2 regulates E-cadherin using a Snail-dependent mechanism. (Blue arrows: pathway mechanism following PGE_2 signaling activation)

2-3E). Therefore, we conclude that PGE_2 signaling stabilizes Snai1a protein to limit E-cadherin expression during gastrulation.

To delineate the molecular mechanism by which PGE_2 promotes Snail stability, we evaluated the outcome of manipulating possible targets of PGE_2 signaling on misexpressed Snai1a-YFP protein levels. First, we tested if proteolysis contributed to the loss of Snai1a-YFP expression in Ptges-deficient embryos (Dominguez et al., 2003; Zhou et al., 2004). Remarkably, the treatment of Ptges-deficient embryos with a proteasomal inhibitor, MG132 (Zhou et al., 2004), fully suppressed the loss of Snai1a-YFP expression, indicating that proteasomal degradation decreased levels of Snai1a protein (**Fig. 2-4A**). Cell culture studies have shown that PGE_2 can regulate Glycogen synthase kinase 3β (Gsk3β) (Fujino et al., 2002; Fujino and Regan, 2003). Furthermore, Gsk3β can phosphorylate SNAI1, thereby targeting it to proteasomal degradation (Zhou et al., 2004; Yook et al., 2006), so we investigated whether this kinase regulated Snai1a expression downstream of PGE_2 signaling. Consistent with this notion, the injection of *gsk3β* RNA significantly decreased the level of misexpressed Snai1a-YFP in a dose-dependent manner in control embryos, and caused the complete loss of Snai1a-YFP in Ptges-deficient gastrulae (**Fig. 2-4B**). Conversely, Gsk3β inhibition through either LiCl (Stachel et al., 1993) or 6-bromoindirubin-3-oxime/BIO (Goessling et al., 2009) treatment suppressed the loss of Snai1a-YFP in Ptges-deficient gastrulae. Blocking the function of both Gsk3β and the proteasome resulted in the full restoration of Snai1a-YFP levels in Ptges-deficient embryos similar to those treated with proteasomal inhibitor alone (**Fig 2-3D**). Thus, PGE_2

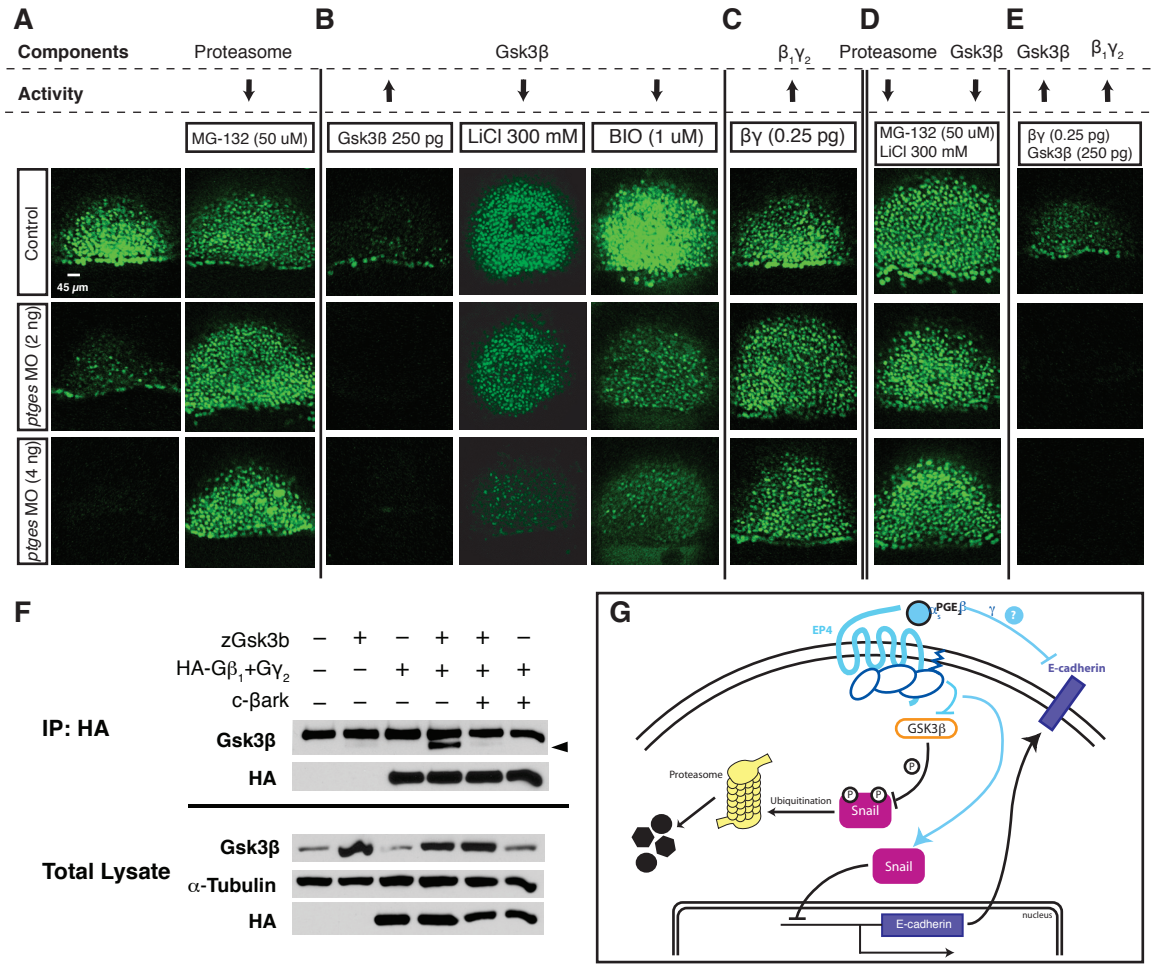

Figure 2-4. PGE_2 Gβγ signaling stabilizes Snai1a by inhibiting Gsk3β-mediated proteasomal degradation. Confocal microscope images of embryos in which the Snai1a-YFP assay was used to test downstream components of PGE_2 signaling for their ability to affect levels of Snai1a in control (top) and ptges morphants (middle, bottom). (A) Treatment with the proteasomal inhibitor, MG132. (B) Injection of *zgsk3β* RNA; treatment with LiCl and BIO, Gsk3β inhibitors. (C) Injection of *hgβ1* and *hgγ2* RNA. (D) Inhibition of both Gsk3β and the proteasome (MG132 treatment). (E) *hgβ1γ2* and *gsk3β* RNA co-injection. (F) Immunoblotting of Gsk3β following immunoprecipitation with hβ1γ2. Zebrafish *gsk3β* and HA-tagged *hβ1/γ2* were transfected into 293T cells. Cell extracts were immunoprecipitated with anti-HA, then immunoblotted with anti-Gsk3β (Gsk3β indicated by arrowhead). The interaction between Gsk3β and hβ1γ2 could be blocked by the addition of c-βark (top). Total lysate Western blots (bottom). (G) Model of the mechanism by which PGE_2 regulates E-cadherin using a Snail-dependent mechanism. (Blue arrows: pathway mechanism following PGE_2 signaling activation)

signaling functions to stabilize Snail by inhibiting its proteasomal degradation, which is regulated by Gsk3β.

Previous studies suggest that PGE_2 signaling acts in part through heterotrimeric Guanine nucleotide binding proteins (G proteins) (Buchanan and Dubois, 2006). Following activation, both G protein α and βγ subunits stimulate separate downstream effectors. Gβγ protein subunits have been shown in cell culture to regulate Gsk3β downstream of PGE_2 signaling by the activation of Phosphoinositide-3-kinase (Pik3) (Fujino et al., 2002; Fujino and Regan, 2003; Cha et al., 2006). We found that overexpression of the $G\beta_1\gamma_2$/(Gnb1, Gng2) subunits elevated the Snail-YFP levels in Ptges-deficient embryos, suggesting that the Gβγ subunits activated by the Ep receptors were responsible for conveying the effects of PGE_2 on Snai1a (**Fig. 2-4C**). Co-injection of RNAs encoding $G\beta_1\gamma_2$ and Gsk3β into Ptges-deficient embryos, however, blocked the rescue of Snai1a-YFP seen with $g\beta_1\gamma_2$ RNA alone, suggesting that Gsk3β regulated Snail downstream of the Gβγ subunits to inhibit Snail proteasomal degradation (**Fig. 2-4E, G**). Accordingly, Gsk3β can be detected following the immunoprecipitation of anti-HA in 293T cells co-transfected with zebrafish Gsk3β and HA-h$G\beta_1\gamma_2$. This interaction can be inhibited by expressing the C-terminal domain of the b-adrenergic receptor kinase (β-ark), which competes for $G\beta_1\gamma_2$ binding, thereby revealing Gsk3b as a potential new Gβγ effector protein (**Fig. 2-4F**) (Jernigan et al., ; Jernigan and Lee). This interaction between the Gβγ subunits and Gsk3β provides a novel mechanism for the regulation of the Snail protein downstream of PGE_2 signaling.

Next, to determine if the decreased regulation of Gsk3β by Pik3 contributed to the loss of Snai1a, we overexpressed the zebrafish Pik3γ, the form that acts downstream of Gβγ signaling (Leopoldt et al., 1998). We also used a Pik3 inhibitor, LY294002, which has been shown to impair zebrafish gastrulation (Montero et al., 2003), to investigate the effects of Pik3 downregulation on Snai1a-YFP levels. We found that neither treatment significantly altered Snai1a-YFP expression in control embryos or Ptges-deficient embryos (**Fig. 2-S5**). Thus, the interaction between Gβγ and Gsk3β to regulate Snail likely does not involve the regulation of Gsk3β by Pik3.

The regulation of Gsk3β presents a possible junction between PGE_2 signaling and Wnt signaling, lending insight into the finding that Cox inhibitors (NSAIDs) decreased the intestinal tumor load of *Adenomatous Polyposis Coli* (*Apc*)^{min} mice mutants with unmitigated β-catenin signaling (Buchanan and Dubois, 2006). Wnt8, which activates β-catenin, is expressed in the nascent mesendoderm during gastrulation, similarly to Snai1a (Hammerschmidt and Nusslein-Volhard, 1993; Kelly et al., 1995; Zohn et al., 2006). Therefore, these two pathways could cooperate to repress cell adhesion by regulating Snail through the inhibition of Gsk3β function. Previous data has shown that in cell culture, PGE_2 can bind Axin through its EP2-associated G protein α_s to displace GSK3β, preventing it from inhibiting β-catenin by proteasomal degradation (Castellone et al., 2005). Moreover, recent work indicates that the Prostaglandin and Wnt pathways converge on Gsk3β to enhance β-catenin levels and contribute to hematopoietic stem cell recovery (Goessling et al., 2009). However, we found that the

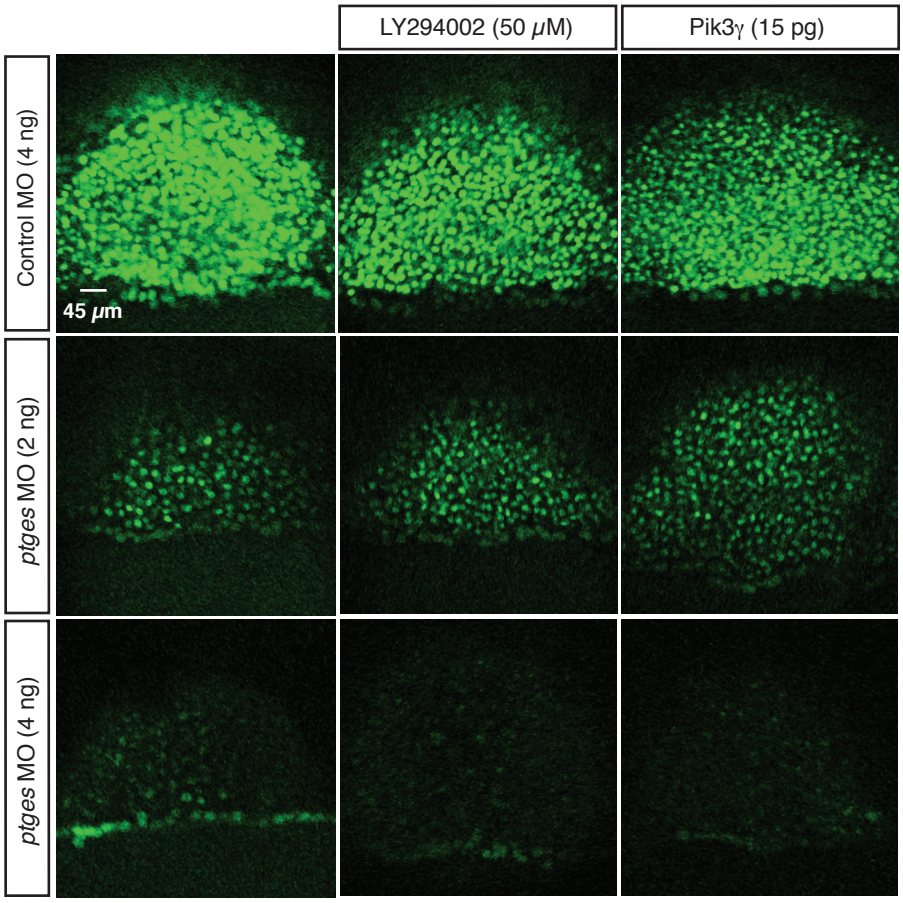

Figure 2-S5. Pik3γ does not significantly affect Snai1a stability. (A) Confocal images of embryos expressing Snai1a-YFP at the shield stage injected with either control or *ptges* MO that were either co-injected with RNA encoding Pik3γ (15 pg) at the one-cell stage or treated with Pik3 inhibitor (LY294002, 50 μM) from the dome to the shield stage (Montero, et al., 2003).

overexpression of ΔNβ-catenin, a constitutively active form, had no effect on Snai1a-YFP expression, either alone or when co-injected with the *ptges* MO (**Fig. 2-S4A**). Hence, the effect of PGE_2 stabilizing Snai1a through Gsk3β is β-catenin-independent.

Unbalanced cell adhesion, either in excess or deficit, cripples the cell movement of primordial germ cells in zebrafish, border cells in *D. melanogaster*, and during gastrulation in many animals (Blaser et al., 2005; Pacquelet and Rorth, 2005; Hammerschmidt and Wedlich, 2008). The presence of several direct and indirect inhibitors of E-cadherin; $G_{\alpha 12/13}$, Wnt11, and p38, underscores the significance of the precise and diverse regulation of cell adhesion for normal gastrulation movements (Lin et al., 2005; Ulrich et al., 2005; Zohn et al., 2006).

We suggest that divergent mechanisms to regulate cell adhesion also occur downstream of PGE_2 signaling. Snai1a-HA overexpression was unable to rescue the gastrulation phenotype in Ptges-deficient embryos. In addition, there were foci of increased levels of E-cadherin in the ectoderm, where Snai1a is absent or weakly expressed (Hammerschmidt and Nusslein-Volhard, 1993). These data suggest that a Snai1a-independent mechanism regulated by PGE_2 leads to increased E-cadherin in the ectoderm. We therefore conclude that PGE_2 employs multiple, germ layer-dependent mechanisms to inhibit E-cadherin expression. Furthermore, we hypothesize that PGE_2, ubiquitously produced during gastrulation (Grosser et al., 2002; Cha et al., 2006), constantly inhibits E-cadherin expression to ensure the dynamic and precise modulation of E-cadherin levels that is necessary for the massive and rapid gastrulation cell movements.

In conclusion, we have shown that PGE_2 signaling negatively regulates E-cadherin transcript and protein levels, thereby limiting cell adhesion. This effect of PGE_2 occurs in part through the stabilization of Snai1a by preventing its Gsk3β-mediated proteasomal degradation (**Fig. 2-4G**). PGE_2 signaling inhibits Gsk3β via its downstream G protein βγ subunits, a novel molecular mechanism by which PGE_2 can promote Snai1a function and limit cell adhesion to influence motility. Whereas the mechanism by which Gβg inhibits Gsk3β remains to be elucidated, the work by Jernigan, et al. (Jernigan et al., ; Jernigan and Lee) suggests that Gβg binds GSK3β, sequestering it to the membrane to activate its kinase activity on the co-receptor LRP6, which leads to the inhibition of β-catenin degradation and potentiation of β-catenin/TCF-mediated transcription. In addition, in breast cancer cells, the presence of GSK3β in the nucleus is essential for its silencing of SNAI1 activity. When AXIN2 acted as a nucleocytoplasmic chaperone for GSK3β, exporting it from the nucleus, SNAI1 remained active (Yook et al., 2006). Therefore, we speculate that following activation by PGE2, Gβg binds Gsk3β at the membrane to prevent it from inhibiting Snai1a activity in the nucleus.

SNAI1 expression is increased in multiple tumor types (Barrallo-Gimeno and Nieto, 2005; Yook et al., 2006), and promoted recurrence of breast cancer *in vivo* (Moody et al., 2005). In addition, the activation of EGF signaling, which plays a major role in multiple cancers, increased the expression of SNAI1, emphasizing its role during tumorigenesis (Lu et al., 2003; Mann et al., 2006; Backlund et al., 2008). PGE_2 signaling has been correlated with increased cancer cell invasiveness, angiogenesis, and anchorage independence (Wang and Dubois,

2006), properties that allow cancer cells to exit the primary tumor and migrate to secondary sites. The increased expression of the EP4 receptor was also reported in colon and breast cancer cells (Chell et al., 2006), indicating that in a pathological context, cancer cells may exploit PGE_2's native regulation of the cell motility machinery. Therefore, our discovery of the Snail-dependent and -independent repression of cell adhesion by PGE_2 may lend insight into the mechanism by which prostaglandins promote tumor cell motility, leading to more advanced disease states. As Wnt signaling also inhibits Gsk3β activity, Wnt and PGE_2 pathways can converge to promote hematopoietic stem cell survival via β-catenin (North et al., 2007; Goessling et al., 2009), and we suggest that this cooperation may also promote cell motility by inhibiting cell adhesion. We also speculate that the multi-pronged repression of E-cadherin by PGE_2 may apply to the other demonstrated roles of prostaglandins/PGE_2 in inflammation and hematopoietic stem cell recovery.

Experimental Procedures

Zebrafish strains and maintenance

Embryos were obtained from natural mating and staged according to morphology as described (Kimmel et al., 1995). With the exception of experiments using the MZ*oep*$^{tz57/tz57}$ (Gritsman et al., 1999) and the Tg(*gsc*:GFP)$^{+/+}$ (Doitsidou et al., 2002), all experiments were done using wild-type embryos.

Embryo injection

Zebrafish embryos were injected at the one-cell stage, 15-45 minutes post-fertilization. The MO constructs that were injected included the control MO/5bp mismatch MO2-*ptges* (GTTTTATCCTGTTAGGTC), *ptges* MO/MO2-*ptges* (Cha et al., 2006), *cox1* MO/MO1-*ptgs* (Grosser et al., 2002), and *cdh1* MO/MO3-*cdh1* (Babb and Marrs, 2004). RNA constructs that were used for injection included *megfp*, *yfp*, *zsnai1a-yfp* (T. Hirano Lab; Osaka University, Osaka, Japan) (Yamashita et al., 2004), *zgsk3β* (M. Hibi; Riken Center for Developmental Biology, Kobe, Japan), *hβ*$_1$, *hγ*$_2$, *ΔNβ-catenin*, and *znr1/cyclops* (C.V. Wright Lab; Vanderbilt University, Nashville, TN) (Erter et al., 1998). Embryos were injected with *zsnai1a-ha* at the 8-16 cell stage. All RNA constructs were in the pCS2 vector.

zSnai1a-YFP assay.

Injected embryos were chemically treated as described below and incubated at 28°C until they reached the shield stage. All experiments were performed at least three times as described, with at least 30 injected embryos per sample (per experiment). Live embryos were oriented using the shield as a morphological landmark in 2% Methylcellulose/0.3X Danieau. Representative embryos were imaged on a LSM 510® Confocal microscope (Carl Zeiss MicroImaging, Inc.; Thornwood, NY), using the 10X objective. Experiments were performed in part through the use of the VUMC Cell Imaging Shared Resource. Images were prepared for publication using Volocity® software (Improvision; Coventry, UK) and Adobe Photoshop (Adobe, San Jose, CA).

Embryo treatment

PGE_2. Embryos were treated with synthetic PGE2 (10 mM; Cayman Chemical; Ann Arbor, MI) following injection and later, at the dome stage, in 1% DMSO/embryo medium.

Proteasomal inhibitor. Embryos were treated with Z-Leu-Leu-Leu-H/MG-132 (Peptide Institute, Inc.; Japan) (50 mM) (Zhou et al., 2004) from the 128-256 cell stage in 1% DMSO/embryo medium until the embryos were imaged at the shield stage.

Gsk3β inhibitor. LiCl treatment was performed as previously described (Stachel et al., 1993). LiCl (Sigma-Aldrich Co.; St. Louis, MO) (0.3 M) was added to the embryo medium at the 256-cell stage for 10 minutes, then rinsed three times in

0.3X Danieau, to incubate until the shield stage. Gsk3β BIO (Stemgent; Cambridge, MA) (1 μM) was added at the 1000-cell stage and left until the shield stage.

Pik3 inhibitor. Embryos were incubated in 30-50 μM LY294002 (Caymen Chemical) in embryo medium from the dome stage until the shield stage.

Cell adhesion Assays

Assays were performed as described (Ulrich et al., 2005). Embryos were injected with 100 pg of *cyclops* RNA at the one-cell stage to induce mesendodermal fates. Whole mount *in situ* hybridization at the dome stage using *notail* was done to confirm that the *cyclops*-injected embryos consisted of predominantly mesendodermal cells. At the dome stage, 40 embryos from each sample were dechorionated in and rinsed with E2 medium (0.5 mM KCl, 15 mM NaCl, 2.7 mM $CaCl_2$, 1 mM $MGSO_4$, 0.7 mM $NaHCO_3$, 10 mM HEPES, soln pH 6.5), then 1 mL prewarmed (37°C) 0.05% Trypsin with 4Na EDTA (Invitrogen Corp.; Carlsbad, CA) was added to the embryos and shaken until the embryonic tissue was dissociated. The suspension was incubated at 37°C for 3 minutes, then 100 μL of fetal calf serum was added to stop the reaction. Embryonic cells were centrifuged for 3 minutes at 4°C at 1000 rpm. The resulting pellet was resuspended in E3 medium (62.5 mL DMEM, 1 mL Penicillin/Streptomycin (GIBCO Invitrogen; Carlsbad, CA), 1 mL L-Glutamine (GIBCO Invitrogen), 1 mL Insulin-Transferrin-Selenium X (GIBCO Invitrogen), then cells were counted the using a hemocytometer. The cells were diluted to 50,000 cells/mL and plated in

a Fibronectin-coated 96-well plate (5000 cells/well). Images were taken on a SteREO Discovery.V12® Dissecting Microscope (Carl Zeiss MicroImaging, Inc.) every hour for 3 hours.

Quantitative real-time PCR

RNA was extracted from 20 injected embryos per sample at 60% epiboly using 200 μL Trizol (Tingaud-Sequeira et al., 2004). Following RNA extraction, the samples were diluted to 50 ng/μL. Primers used included *β-actin* (Tingaud-Sequeira et al., 2004), *cdh1* (left: TGAAGGCTGCAGATAACGAC; right: GTGTTGAGGGAGCTGAGTGA), and *snai1a* (left: GAGCTGGAATGTCAGAACGA; right: GTGAAGGGAAGGTAGCAAGC). Samples were prepared for qRT-PCR using the iScript One-Step RT-PCR kit with SYBR-Green® (Bio-Rad; Hercules, CA). 100 ng of template DNA was used for each sample, and water was used as a negative control for the RT reaction. The qRT-PCR was performed on an iCycler iQ Multicolor machine® (Bio-Rad; Hercules, CA) at the VUMC Molecular Biology Resource Core. The annealing temperature was set for 60°C without a temperature gradient. The data shown represents three separate experiments with duplicate samples. The data were analyzed iQ5 Optical System Software, Version 2.0® (Bio-Rad; Hercules, CA).

Time-lapse imaging

Shield time-lapse. Embryos were injected with *membrane egfp* at the one-cell stage. At the shield stage, embryos were dechorionated in 0.3X Danieau and oriented in

plastic dishes using 0.8% SeaPlaque Low Melt Agarose (Lonza; Rockland, ME)/0.3X Danieau. Images were taken of the shield on a Zeiss Axiovert 200 inverted microscope® (Carl Zeiss MicroImaging, Inc.) with a ERS Spinning Disk Confocal system® (PerkinElmer; Fremont, CA) using the 40X oil-immersion (NA=1.3) objective. Z-sections were 0.5 μm in thickness, with images taken every minute. The resulting data points were orthogonally reconstructed using Volocity® software (Improvision). Time-lapse movies were processed using Volocity®, Adobe Photoshop® (Adobe) and Quicktime Pro® software (Apple; Cupertino, CA).

Protrusion movie analysis. *membrane egfp* or *membrane rfp* RNA was injected into Tg(*gsc*:GFP)$^{+/+}$ zebrafish embryos (labeled donor embryos) at the one-cell stage. Fewer than 10 cells were transplanted from donor embryos to unlabeled host embryos at the shield stage. Host embryos containing transplanted cells that were *gsc*:GFP-positive were mounted at 70-80% epiboly in 0.8% Low Melt Agarose (Co)/0.3X Danieau in plastic dishes, with the shield facing downward. Images were taken on a Zeiss Axiovert 200 inverted microscope® (Carl Zeiss MicroImaging, Inc.) with an ERS Spinning Disk Confocal system® (PerkinElmer) using the 40X oil-immersion (NA=1.3) objective for 5-10 minutes, with 2-3 z-planes taken every 10 seconds (z-plane thickness: 2.8-5 μm). Time-lapse movies were processed using Volocity®, Adobe Photoshop®, and Quicktime Pro® software.

Whole mount ISH

Embryos were collected at the indicated stage and fixed with 4% paraformaldehyde overnight at 4°C. Whole mount ISH was performed as previously described. Probes used included *snal1a*, *snai1b*, *frizzled 8b*, and *no tail*.

Western blotting

Embryos were homogenized with RIPA buffer (10 mM Tris pH 7.4, 150 mM NaCl, 1 mM EDTA, 0.1% SDS, 1% Triton X-100, 1% Na Deoxycholate), then frozen at -20°C. Embryo homogenates were lysed with 2X Lysis buffer (62.5 mM Tris-HCl pH 6.8, 10% Glycerol, 2% SDS, 0.5% Beta-mercaptoethanol, 0.01% Bromophenol blue) and heated at 100°C for 5 minutes. Extracts were resolved in a 4-15% polyacrylamide gel and transferred to a PVDF membrane using the Criterion System® (Bio-Rad). The antibodies used were anti-zSnai1 (1:500; Hammerschmidt Lab, Max-Planck-Institute of Immunobiology; Freiburg, Germany) (Hammerschmidt and Nusslein-Volhard, 1993) , anti-zE-cadherin (1:1000; J.A. Marrs Lab; Indiana University Medical Center, Indianapolis, IN) (Babb and Marrs, 2004), anti-Gsk3β (1:1000; Cell Signaling Technology; Danvers, MA), anti-Phospho-Gsk3β (1:1000; Cell Signaling Technology), and anti-GAPDH (1:500; RDI Division of Fitzgerald Industries; Concord, MA).

Whole-mount immunohistochemistry

Zebrafish embryos were collected at the indicated stage and fixed with a 1:1 solution 8% paraformaldehyde and 2X fix buffer (8% Sucrose, 0.3 mM CaCl2/PBS pH 7.3). Embryos were rinsed four times using PBS with 0.1% Tween. Antibodies used were anti-zE-cadherin (1:1000; J.A. Marrs Lab) and anti-ZO1 (1:200; Zymed Laboratories; San Francisco, CA). To visualize nuclei, samples were stained with SYTO®59 (Invitrogen) for 30 minutes prior to imaging, then rinsed twice with PBS with 0.1% Tween and 2% DMSO.

Cell culture, transfection, and immunoprecipitation

HEK-293 cells were cultured in DMEM (Cellgro; Manassas, VA) media supplemented with 100 units/mL Penicillin, 100 units/mL Streptomycin (Gibco Invitrogen) and 10% FBS (Gibco Invitrogen). Lipofectamine 2000 (Invitrogen) transfection reagent was used for tranfections following the manufacturer's suggested protocol. HEK-293 cells were plated in 30 mm dishes and transfected with 1 μg zGsk3, 1 μg HA-$G\beta_1$, 1 μg $G\gamma_2$, and 2 μg c-βark DNA pCS2-based constructs. Transfected cells were cultured for 48 hours, then cells were washed 1x with cold PBS and lysed for 30 minutes on ice in Non-Denaturing Lysis buffer (NDLB)(50mm Tris pH 7.4, 300mM NaCl, 5mM EDTA, 1%w/v Triton X-100, Protease inhibitors (1mg/ml leupeptin, Pepstatin, and Chymostatin). 750 μg of lysate were diluted to 1 mg/mL with the NDLB. Rat anti-HA (Roche Diagnostics GmbH; Mannheim, Germany) was crosslinked to the Protein G magnetic beads (New England BioLabs; Ipswich, MA) following the manufacturer's instructions.

anti-HA protein G beads were added to the lysate and incubated for 2-3 hours with rotation at 4°C. Beads were then washed 3x with NDLB and 1x with PBS. Protein was eluted from the beads with Sample Buffer. Samples, as well as 10 μg of the total protein lysate, were resolved on an SDS-Page gel and transferred to a Nitrocellulose membrane. Membranes were blocked in 5% milk solution (1 hour at room temperature) and probed with mouse anti-HA (1:1000, AbCam, Cambridge, MA), mouse anti-α-tubulin (1:3000, Sigma-Aldrich), and mouse anti-Gsk3 (1:1000, BD Biosciences; San Jose, CA). HRP conjugated anti-mouse antibodies were used to detect the primary antibody by chemiluminescence.

CHAPTER III

DEFICIT OF PROSTAGLANDIN E_2 SIGNALING DURING BLASTULA STAGES IMPAIRS DEVELOPMENT OF ENDODERMAL PRECURSORS

Summary

The endoderm and mesoderm are initially specified by Nodal signaling in blastulas. Following internalization at the onset of gastrulation, the endoderm is distinguished from the mesoderm by inductive signals that lead to endoderm-specific differentiation. Reduced PGE_2 signaling in zebrafish embryos resulted in the deficiency of *cas*- and *sox17*-expressing endodermal cells by the end of gastrulation. Nodal signaling was slightly decreased in *ptges* morphants (MO2-*ptges*) at the beginning of gastrulation, as evidenced by reduced expression of *lft2*. By contrast, mesodermal cells seem to be correctly specified, though their internalization and other gastrulation movements were impaired. These data suggest that PGE_2 enhances Nodal signaling to promote endodermal fates or influences endodermal differentiation directly.

Introduction

Endodermal derivatives contribute to an organism's ability to digest and absorb nutrients (pancreas and intestine), respire (lungs), and remove waste (liver and intestine). The mesoderm and endoderm arise from a common cell population in vertebrates (**Fig. 3-1A**). This was confirmed in zebrafish by fate map analysis that was performed on single cells labeled with lineage tracers between the 1000- and 4000-cell stage (Warga and Nusslein-Volhard, 1999). Clones of labeled cells were plotted on an embryo map at 40% epiboly and shield stage, and analyzed for their lineage from 1 to 5 dpf. In this manner, cell fates of cells were correlated with their early position within the blastula. 71 clonal cells were analyzed, and of those, 24% gave rise to only endoderm, 42% gave rise to only mesoderm, and 34% generated both mesoderm and endoderm. Cells that eventually give rise to mesoderm and endoderm are located in the margin of the blastula, however mesodermal cells reside within 4 cells of the margin (**Fig. 3-1A**). Endodermal progenitors were most frequently found within 2 cell diameters, and never more than 4 cell diameters, from the margin (Warga and Nusslein-Volhard, 1999) (**Fig. 3-1A**). In addition, endodermal progenitors are biased towards dorsal locations, whereas mesodermal progenitors are more uniformly distributed on the ventral side of the embryo. Fate map studies in the frog confirm these results, suggesting that the mesoderm and endoderm initially arise from a common cell population, but that inductive signals specify cells to the endodermal fate by the beginning of gastrulation. Additional inductive signals to these cells occur at mid-gastrulation to further differentiate these cells, patterning the future endodermal organs of the organism (Zorn and Wells, 2007).

The initial specification of the mesendoderm occurs through Nodal

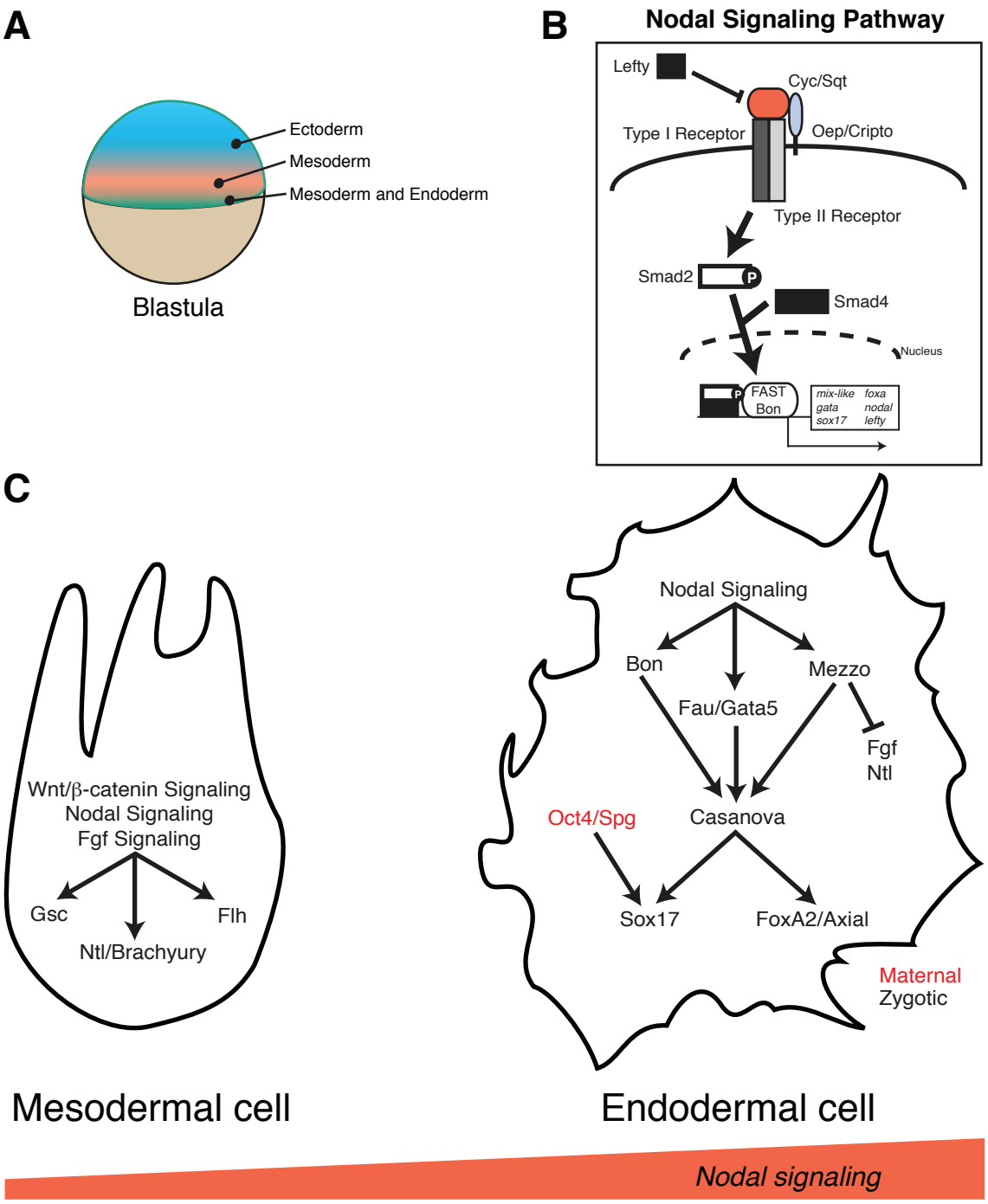

Figure 3-1. Endodermal specification in zebrafish. (A) Fate map of the zebrafish blastula showing the ectoderm, mesoderm, and endoderm domains. (B) The Nodal signaling pathway specifies the mesendoderm. (C) Mesodermal and endodermal cells require distinct levels of Nodal signaling for their differentiation. Mesodermal cells are more sensitive to Nodal signaling, whereas endodermal cells require higher levels of Nodal signaling to induce the endodermal specification pathway. In addition, mesodermal cells are rounder and smaller than endodermal cells, which have flat cell bodies with protrusions around the circumference of the cell.

signaling (**Fig. 3-1B**). Nodal secreted ligands belong to the Tumor Growth Factor-β (TGF-β) superfamily. The Nodal signaling pathway in zebrafish involves the three **z**ebrafish **N**odal-**r**elated (ZNR) ligands Znr1/Cyclops (Cyc), Znr2/Squint (Sqt), and Znr3/Southpaw (Spaw) as well as the cofactor One-eyed pinhead (Oep), which is the zebrafish homolog of the human Cripto protein, a member of the Extracellular Growth Factor-like and/or Co-receptor-like (EGF-CFC) family (Feldman et al., 1998; Sampath et al., 1998; Feldman et al., 2000; Saloman et al., 2000; Long et al., 2003). Once the ligands bind to the Type I and Type II activin-like receptors, the Smad2 and Smad4 signal transducers are activated to transcriptionally induce the downstream targets of Nodal signaling (Schier and Shen, 2000).

In the frog, Nodal signaling is activated by a maternally deposited factor, VegT, as well as Wnt-β-catenin signaling (Zorn and Wells, 2007). What induces Nodal signaling in amniotes and zebrafish, however, remains unknown. This signal, however, likely arises from the YSL in zebrafish, as removal of the yolk cell and YSL results in defective mesendoderm development (Zorn and Wells, 2007). Indeed, *sqt* is initially expressed from the zygotic genome in the dorsal blastomeres, then in the YSL by the oblong stage (3.7 hpf), suggesting that its expression in the YSL is activated by this early inductive signal(s) (Erter et al., 1998; Feldman et al., 1998).

In contrast to Spaw, which acts later during development to pattern the left-right axis (Long et al., 2003), Nodal signaling through Cyc and Sqt instructs the mesendodermal pattern. Indeed, the importance of Cyc and Sqt is evidenced by *cyc;sqt* double mutants, which lack mesendoderm (Feldman et al., 1998;

Feldman et al., 2000). Also, misexpression of Activin A receptor, type IB/Acvr1b/Taram-A/Tar, a TGF-β-Related Type I receptor, in zebrafish embryos induces early mesendodermal markers such as *ntl* (mesoderm), *gata5*, and *mixer* (endoderm) (Aoki et al., 2002).

Interestingly, the mosaic expression of either Cyc or Sqt induces downstream mesendodermal genes. However, Sqt could activate mesendodermal genes in cells distant (up to 8 cell diameters away) to the misexpression domain, whereas Cyc could only act within a short range (less than 2 cell diameters), suggesting that these activating ligands have distinct properties (Chen and Schier, 2001)). Inhibition of *lefty/lft*, which encodes TGFβ-related secreted proteins that function as Nodal signaling antagonists but are themselves activated by Nodal signaling (Meno et al., 1999; Cheng et al., 2000), by MO resulted in an expansion of Nodal expression and signaling at the margin, indicating that Lft limits the range of Nodal signaling (Chen and Schier, 2002). Interestingly, the function of Lft is dependent on Sqt, as the expansion of Nodal signaling in *lft* morphants was abolished in $sqt^{-/-}$ mutants but not $cyc^{-/-}$ mutant embryos (Chen and Schier, 2002). In addition, Lft misexpression at the animal pole inhibits the expression of the Nodal target gene *bhikhari* (*bik*) at the margin (Chen and Schier, 2002), suggesting that Lft acts as a long-range inhibitor. Therefore, Nodal-dependent Lft inhibits Nodal signaling by diminishing the activating effects of Sqt at a distance, as predicted by the reaction diffusion model theorized to be a mechanism for pattern formation (Solnica-Krezel, 2003).

Nodal signaling also may regulate the decision between mesodermal and endodermal fates in cells by the duration and strength of the signal (Grapin-

Botton and Constam, 2007) (**Fig. 3-1C**). Embryos with low Nodal signaling, such as zygotic *oep* mutants, lack all the endoderm but retain most of the mesoderm, suggesting that conversion to the endodermal fate requires sustained and higher levels of Nodal signaling (Schier et al., 1997). This model is consistent with the fate map that suggests that endodermal cells are those closest to the margin, and thus would receive the highest levels of Nodal signal.

Once Nodal signaling is stimulated, Smad2 and Fast1/Foxh1 activate downstream endodermal genes such as the *mix*-like homeodomain gene *bon*, *gata5*, and *foxa2*/*axial* (**Fig. 3-1C**). Gata5 maintains the expression of *foxa2* and *sox17*, which are endodermal-specific markers. The Mix-like factors activate *sry-like* ***h****igh* ***m****obility* ***g****rowth (HMG) domain box factor 32*/*sox32*/*casanova* (*cas*), an important transcriptional activator of *sox17*, to initiate *cas* expression in the dorsal YSL and also in the endodermal progenitors prior to internalization (Alexander and Stainier, 1999; Kikuchi et al., 2001; Grapin-Botton and Constam, 2007). Pou2/Oct4 is required cell-autonomously for the specification of endodermal fates, and possibly also functions to activate *sox17* transcription (Reim et al., 2004). Accordingly, MZ*pou5fl*/*pou2*/*oct4*/*spiel ohne grenzen* (*spg*) mutants show markedly reduced endoderm with few *sox17*-expressing cells (Lunde et al., 2004; Reim et al., 2004). Overexpression of Cas could not rescue *sox17*-expressing cells in MZ*spg*, nor could Pou2 rescue the endoderm defect in *casanova* mutants, suggesting that both Pou2 and Cas regulate *sox17* transcription in parallel (Reim et al., 2004).

Expression of *sox17* begins in zebrafish in the prospective dorsal forerunner cells at 50% epiboly (Alexander and Stainier, 1999). *sox17* expression starts in the endodermal progenitors at the shield stage, and is maintained

throughout gastrulation (Alexander and Stainier, 1999). The importance of Sox17 during endoderm specification is demonstrated by the effects of misexpressing xSox17 in the A tier of the 32-cell stage frog embryo (Clements and Woodland, 2000). Although the A tier blastomeres usually contribute to the ectoderm and nervous system, xSox17-expressing cells instead contribute to the endoderm or gradually disappear. The authors concluded that cells that did not contribute to the endoderm underwent apoptosis, though there was no increased TUNEL staining during gastrulation (Clements and Woodland, 2000). These data reveal the inductive ability of Nodal signaling to convert cells to the endodermal fate through Sox17 function.

The loss of the Nodal ligands also results in defects to the internalization gastrulation movement that generates the mesendodermal layer, internalization. No internalization movements occur in *cyc;sqt* mutant embryos (Feldman et al., 1998; Feldman et al., 2000). The transplantation of MZ*oep* mutant cells into wild-type hosts results in internalization, likely due to interactions between MZ*oep* mutant cells and their wild-type neighbors, however, the mutant cells eventually fall back to the ectodermal progenitor layer (Carmany-Rampey and Schier, 2001). By contrast, MO-targeting of *lft1* and *lft2* results in an expanded mesendoderm population as a consequence of constitutively active Nodal signaling during gastrulation (Feldman et al., 2002). Taken together, these data suggest that Nodal signaling is required cell-autonomously for mesendodermal specification and in internalizing cells to maintain their position within the deeper, mesendodermal layer. During internalization, the first cells to internalize are the endoderm progenitors, followed by the prechordal plate precursors, which eventually contribute to both mesodermal and endodermal structures, such as

the hatching gland and the pharynx.

Following internalization, endodermal cells use "random walk" behavior to spread over the yolk surface towards the animal pole, in contrast to the directed migration of mesodermal cells (Sepich et al., 2005; Pezeron et al., 2008). This "random walk" of endodermal cells is activated by Nodal signaling, and requires the function of Cas, as MO-targeting of *cas* abolishes this cell behavior (Pezeron et al., 2008). By mid-gastrulation, endodermal cells converge towards the the dorsal side of the embryo, possibly because of extracellular cues. This notion was supported by heterochronic transplantations, in which cells transplanted from early to late gastrulae embryos immediately started to converge towards the future midline (Pezeron et al., 2008), suggesting that inductive signals are present in the embryo at this time. A possible inductive signal that contributes to the anterior spreading of endodermal cells via the "random walk" behavior is the chemokine Cxcl12b and its receptor Cxcr4a (Nair and Schilling, 2008). *cxcr4a* expression in endodermal cells is induced by Mixer and Sox17 activity (Dickinson et al., 2006). *cxcl12b* is expressed in the mesoderm, while *cxcr4a* is present in endodermal cells, suggesting that mesoderm-endoderm interactions contribute to anterior movement of the endodermal cells (Nair and Schilling, 2008). *cxcl12b* and *cxcr4a* morphants both show *viscera bifida*, or duplicated endodermal organs, of the liver and pancreas. *cxcl12b* and *cxcr4a* morphant endodermal cells migrate farther anteriorly at early gastrulation, which culminates with the later defects. Defects in the adhesion of morphant endodermal cells to Fibronectin is also observed, suggesting that Integrin-mediated adhesion is involved. Accordingly, inhibition of Integrin with RGD peptides phenocopies the enhanced endodermal migration and the *viscera bifida*

phenotype, whereas misexpression of Integrin β 1b (Itgb1b) suppresses the *viscera bifida* phenotype in *cxcl12b* morphant embryos. In a model resulting from these studies, Cxcl12b-Cxcr4a signaling is critical for the tethering of the endodermal cells to the mesoderm, so that endodermal cells migrate further in the absence of Cxcl12b-Cxcr4a function because of decoupling from the mesodermal cell population (Nair and Schilling, 2008).

Morphological changes occur by mid-gastrulation (70-80% epiboly), distinguishing mesodermal and endodermal cells (Warga and Nusslein-Volhard, 1999). Endodermal cells become flattened, taking on a tear-drop shape and filopodial protrusions at the periphery of the cell's margin as they migrate over the yolk cell (Warga and Nusslein-Volhard, 1999). In contrast, mesodermal cells retain a rounder morphology throughout gastrulation, and reside in a cell layer superficial to the endodermal cells (Warga and Nusslein-Volhard, 1999) (**Fig. 3-1C**).

We show here that Ptges-deficient embryos have decreased numbers of endodermal cells without the parallel loss of *ntl*-expressing mesodermal cells. Furthermore, we demonstrate that these embryos have decreased Nodal signaling prior to the beginning of gastrulation, suggesting that PGE_2 signaling contributes to endodermal specification in addition to its movements.

Experimental Procedures

Embryo injection

Zebrafish embryos were injected at the one-cell stage, 15-45 minutes post-fertilization. The MO constructs that were injected included the control MO/5bp mismatch MO2-*ptges* (GTTTTATCCTGTTAGGTC) and *ptges* MO/MO2-*ptges* (Cha et al., 2006).

Whole-mount ISH

Embryos were collected at the indicated stage and fixed with 4% paraformaldehyde overnight at 4°C. Whole mount ISH was performed as previously described. Probes used included *lft2*, *sox17*, and *cas*.

Phalloidin/F-actin Staining

Control and *ptges* MOs were injected into wild-type or MZ*oep*$^{tz57/tz57}$ embryos were fixed at 65% or 85% epiboly with 4% paraformaldehyde overnight at 4°C. Embryos were incubated in block solution (5% goat serum, 5 mg/mL BSA in 2% DMSO-PBT solution), then incubated with Alexa Fluor® 546-Phalloidin, diluted 1:40 in block solution, (#A22283, Invitrogen Corp.; Carlsbad, CA) for 30 minutes at room temperature. Embryos were rinsed three times in succession with DMSO-PBT solution, then imaged in 80% glycerol on the LSM 510® Confocal microscope (Carl Zeiss MicroImaging, Inc.; Thornwood, NY), using the 10X

objective. Images were processed using Volocity® software (Improvision; Coventry, UK).

Results

Ptges-deficient embryos showed decreased endodermal cell numbers without the parallel loss of mesodermal cells

Embryos injected with the *ptges* MO/MO2-*ptges* at the one-cell stage showed fewer *sox17*-expressing cells than control morphants at the tailbud stage (TB) (10 hpf) (**Fig. 3-2**). In addition, the level of transcript in *sox17*-expressing cells was also decreased in *ptges* morphants. Analysis of *ptges* morphants showed that *sox17* expression was decreased from its inception at the shield stage (6 hpf) (Alexander and Stainier, 1999), and expression was not recovered throughout gastrulation (70% epiboly and TB stages). As *sox17* expression is regulated in part by the function of Cas (Alexander and Stainier, 1999), we next analyzed the expression of *cas* in the control and *ptges* morphant embryos (**Fig. 3-2**). *cas* expression was similarly decreased in *ptges* morphants at the shield and 70% epiboly stages, suggesting that endodermal specification was impaired in these embryos upstream of Sox17.

Nodal signaling is the inducer of the endodermal specification pathway, so next we analyzed control and *ptges* embryos using *lft2* expression as an output of Nodal signaling at 40% epiboly (**Fig. 3-3**). The *lft2* expression level was slightly decreased in *ptges* morphants in comparison with control morphants, especially in the dorsal side of the embryo (**Fig. 3-3**).

Ptges may affect the localization of F-actin in the gastrulae

Nodal signaling can influence cortical tension as well as mesendodermal specification, and the former may affect sorting of the germ layers (Krieg et al.,

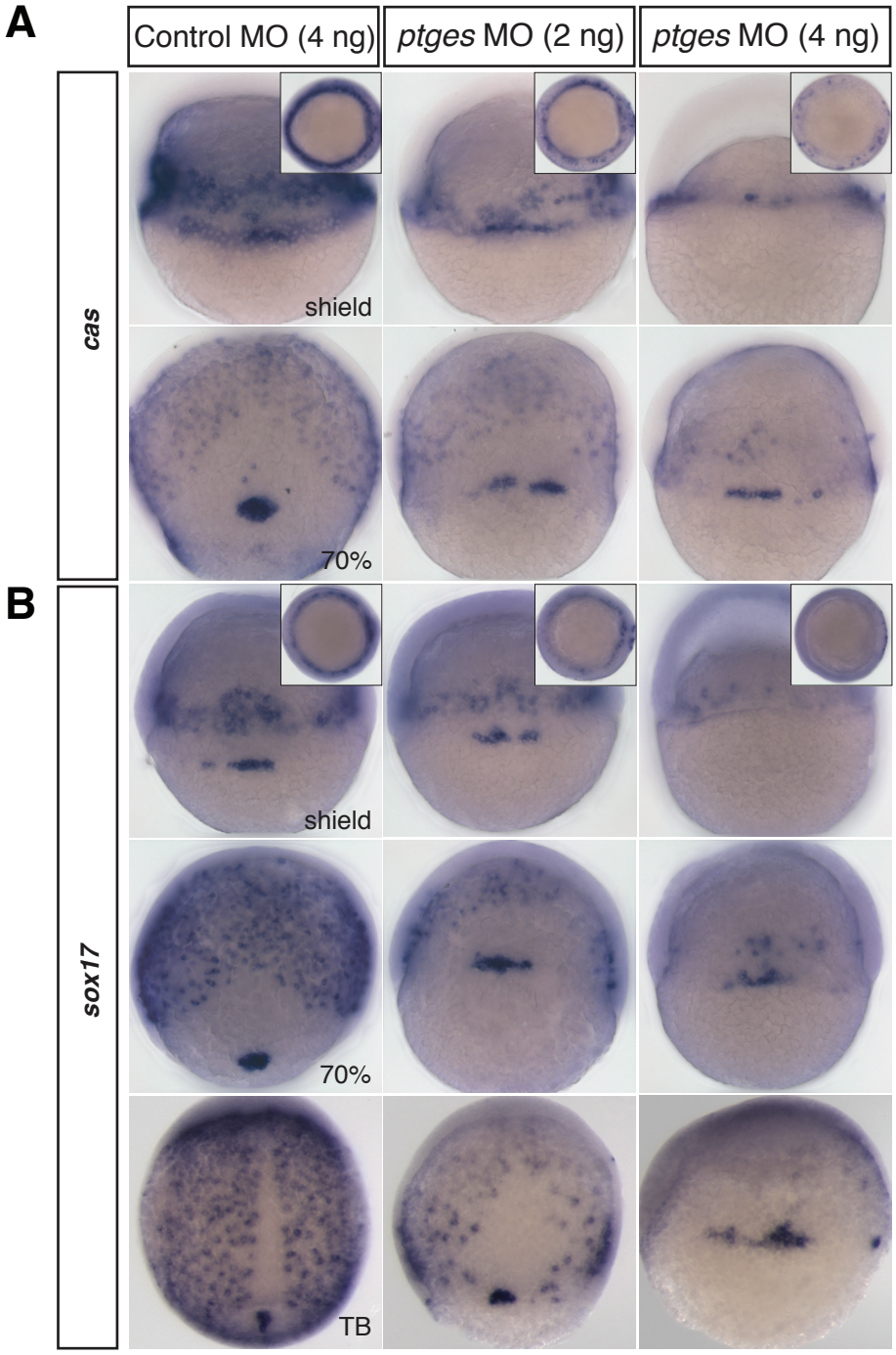

Figure 3-2. *ptges* morphants show reduced endodermal cells. Cas/Sox32 and Sox17 are endodermal proteins. *cas* (A) and *sox17* (B) expression in *ptges* morphants.

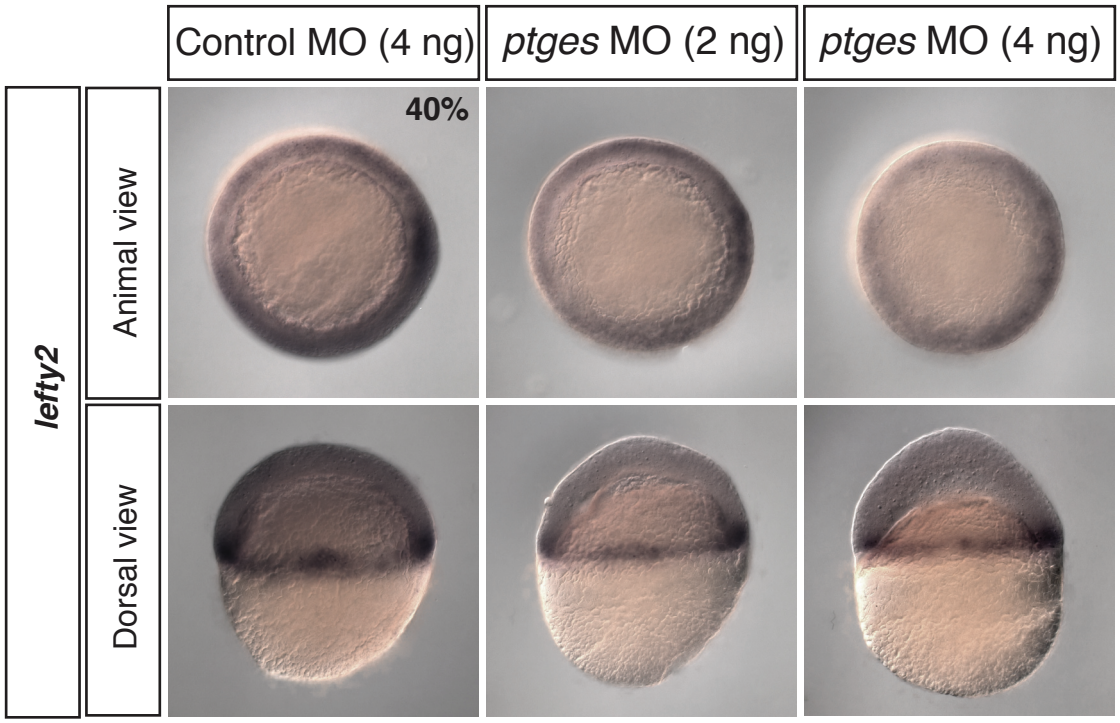

Figure 3-3. Nodal signaling is abrogated in the *ptges* morphants. Although Lft2 is an inhibitor of Nodals, *lft2* expression is induced by activation of the Nodal signaling pathway. *lft2* expression was analyzed in control and *ptges* MO-injected embryos at 40% epiboly by whole-mount *in situ* hybridization.

2008). Therefore, if Nodal signaling is diminished as a result of reduced PGE_2 signaling, it is also possible that the organization of the actin cytoskeleton is affected, which may contribute to some of the movement defects in the *ptges* morphants. To survey the actin cytoskeleton, we analyzed F-actin localization with Phalloidin staining in control and *ptges* morphant embryos (**Fig. 3-4**). *ptges* morphants stained with Phalloidin showed the defects in epiboly described previously (**Chapter 2**). In addition, in the EVL and deep cells, the F-actin organization in the yolk appeared unaffected by reduced PGE_2 synthesis, however, F-actin localization seemed to be elevated at the membrane and depressed in the cell cytoplasm, relative to the control morphants (**Fig. 3-4A**). Increased F-actin at the cell membrane could be indicative of increased cortical tension, so we analyzed Phalloidin staining in *ptges* MO-injected MZ*oep*$^{tz57/tz57}$ mutants (**Fig. 3-4B**). If the effects of PGE_2 on F-actin localization are entirely dependent on Nodal signaling, say by regulating cortical tension, one would predict that reducing PGE_2 in the absence or severe loss of Nodal signaling would not affect F-actin localization further. Therefore, our preliminary data indicates that the level of F-actin at the membrane is increased in *ptges* morphants, even with declined Nodal signaling.

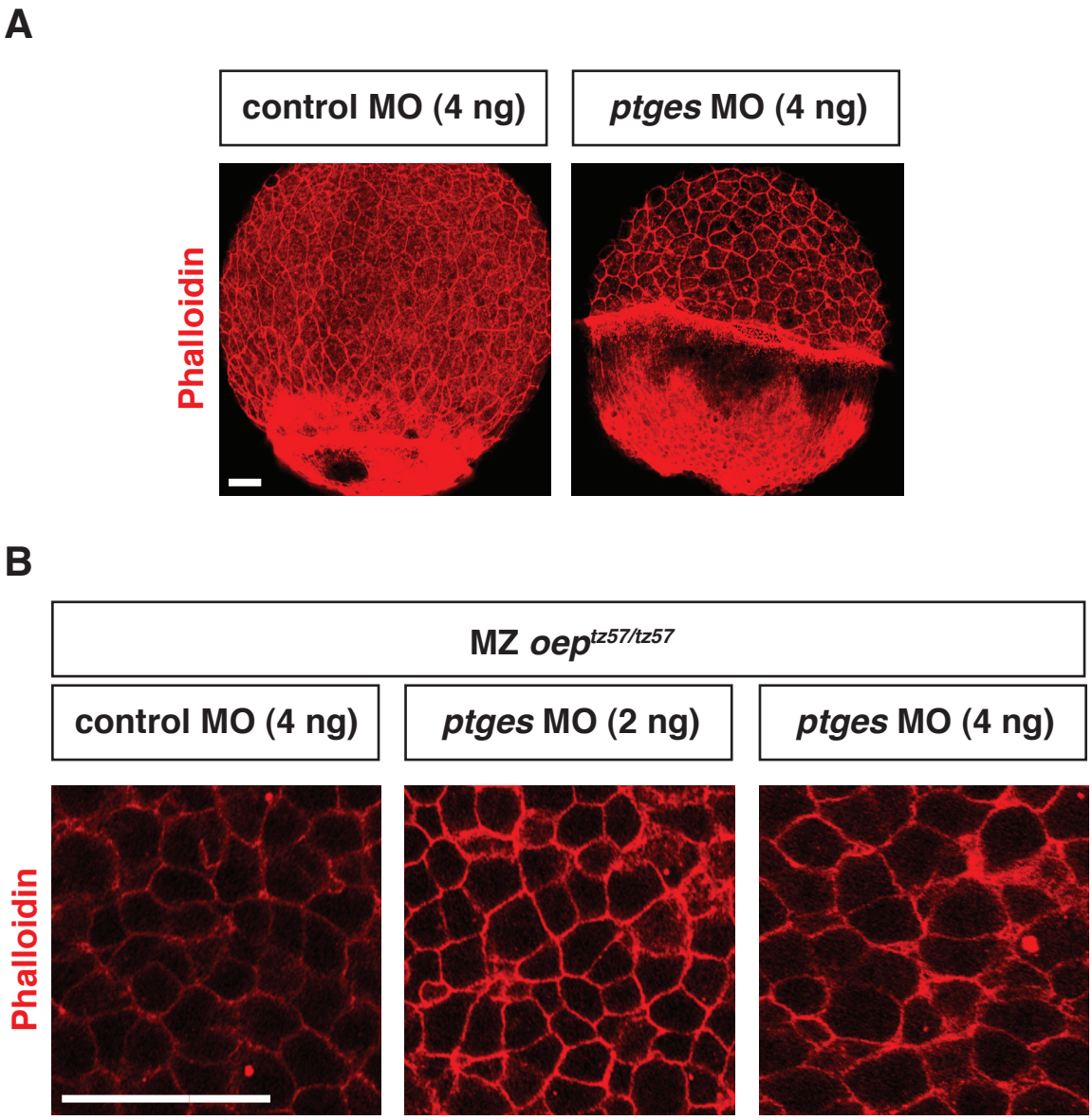

Figure 3-4. The organization of the actin cytoskeleton in *ptges* morphants. (A) *ptges* morphants at 85% epiboly stained with Phalloidin (extended focus view). (B) MZ *oep*$^{tz57/tz57}$ mutants injected with control and *ptges* MO at 65% epiboly stained with Phalloidin. Images shown represent one z-plane. Scale bar: 53 μm.

Discussion

Our results show that reduced PGE_2 signaling decreases *cas* and *sox17* expression in a MO dose-dependent manner. *sox17* expression was already decreased when expression begins, and *cas* was also decreased at the shield stage. *cas* expression is first detectable at the high stage (3.3 hpf) (Kikuchi et al., 2001), so earlier timepoints will need to be analyzed to determine the earliest manifestation of reduced endodermal markers. In addition to *cas*, other endodermal specification genes, such as *gata5*, *bon*, and *mezzo*, should be evaluated to understand the extent of the endodermal specification defect in *ptges* morphants. Whereas most of our analysis has been performed with whole-mount *in situ* hybridization, we could also obtain more accurate measurements of gene expression by qRT-PCR.

Interestingly, the extent of the deficit of endodermal cells does not correlate with a parallel loss of mesodermal cells (**Chapter 2**). However, subtle defects in mesoderm formation and/or patterning cannot be excluded at the moment and will be analyzed in the future. If mesodermal cells are normally specified in *ptges* morphants, this would suggest that Nodal signaling is intact. To test this, we analyzed *lft2* expression, and found it slightly decreased, implying that Nodal signaling is affected with reduced PGE_2 synthesis. The decline of Nodal signaling in *ptges* morphants could culminate in mesoderm fate specification with decreased endodermal specification because higher Nodal activity is required to produce endoderm than mesoderm (Peyrieras et al., 1998; Grapin-Botton and Constam, 2007). An interesting question that remains: what happens to the cells that would have contributed to the endoderm? Do they undergo cell death, or do they convert to another fate such as mesoderm? To

address this question, marginal cells in sphere stage embryos could be labeled with a lineage tracer (e.g., by uncaging of photoactivatable dye or protein), then analyzed for *tbx16* or *cas* expression by whole-mount in situ hybridization to determine the fate of uncaged cells in control and *ptges* morphants. If an increased proportion of uncaged cells are *tbx16*-positive (vs. *cas*-positive) in *ptges* morphants relative to control morphants, then that would suggest that PGE_2 mediates the mesoderm-endoderm fate decision in part by influencing Nodal signaling. That Nodal signaling is still present in the high dose *ptges* MO-injected embryos suggests that PGE_2 is not required for the expression of Nodal signaling components, but instead maintains or augments Nodal signaling activity.

Given the established roles of PGE_2 in cell survival (Sheng et al., 1998; Aoudjit et al., 2006), another possibility that should be investigated is that cells in *ptges* morphants that normally become mesendoderm die instead. Therefore, we could analyze apoptotic cell death in *ptges* and control morphants with TUNEL staining. Furthermore, we could co-inject *p53* and *ptges* MOs to test whether it can suppress the endodermal defect.

Because PGE_2 signaling limits E-cadherin expression (**Chapter 2**), one possibility is that increased cell adhesion in *ptges* morphants could underlie endoderm deficiency. The knowledge that cell adhesion and cell fate are intertwined is not new. Early experiments have shown that sponges or amphibian tissue fragments reaggregate following dissocation (Wilson, 1907; Steinberg, 1963). It was not until 1963 that the Differential Adhesion Hypothesis (DAH) was found to be a contributor to cell sorting in tissues, contributing to the sorting of differentiated cell types in culture, such as chondrogenic and liver cells

(Steinberg, 1963). These effects were later found to be mediated in part by the levels of cadherins (Foty and Steinberg, 2005). These classical experiments demonstrate that cell fate is associated with adhesion properties that are fate-specific, but does cell adhesion influence cell fate during development?

We have previously shown that PGE_2 signaling modulates cell adhesion during gastrulation (**Chapter 2**). Therefore, it is possible that the increased cell adhesion in *ptges* morphants may result in the loss of endoderm development in these embryos. For example, MZ*spg* embryos show altered, possibly decreased, cell adhesion, and also have markedly reduced endoderm (Lachnit et al., 2008). However, studies in mouse Embryonic Stem (ES) cells show that embryoid body endoderm differentiation and sorting occurs even with E-cadherin-null cells, suggesting that adherens junction-based cell adhesion is not necessary for endoderm development (Rula et al., 2007; Moore et al., 2008). However, increased cell adhesion in embryos, such as *ptges* morphants, may affect endoderm specification through an unknown mechanism. This possibility remains to be tested experimentally. An intriguing future experiment is to determine if the endoderm defect in *ptges* morphants can be suppressed by co-injection with the *e-cadherin* MO. In addition, *ptges* and *e-cadherin* MO co-injected embryos could be analyzed for *lft2* expression to determine if the decrease in Nodal signaling is suppressed. If Nodal signaling and the endoderm defect are modulated in *ptges* and *e-cadherin* MO-injected embryos, this would support the view that PGE_2 regulates Nodal signaling and, by extension, endoderm specification through the regulation of cell adhesion.

An elegant paper showed that mosaic loss-of-function or misexpression of DN-cadherin using the FLP/FRT system resulted in patterning defects in the

Drosophila ommatidium, suggesting that differential adhesion influenced the ommatidia structure without affecting cell fates (Hayashi and Carthew, 2004). Mathematical modeling of the Drosophila ommatidia, however, showed that changes in cell adhesion were insufficient to predict the patterning changes in mutants (Kafer et al., 2007). Furthermore, recent data in the zebrafish gastrula has shown that differences in cell adhesion alone cannot produce the germ layer sorting that occurs during gastrulation (Krieg et al., 2008). The DAH could not fully account for the germ layer sorting during gastrulation, as the mesoderm had the highest Cadherin expression, followed by the endoderm and ectoderm (Krieg et al., 2008). Cortical tension, which is generated by the acto-myosin contractile network in the cell cortex, and cell adhesion are opposing forces in the cell, for as a cell generates more adhesive contacts with another cell, overall cortical tension decreases through stretching of the membrane (Lecuit and Lenne, 2007). Thus, with increasing cortical tension, the surface of contact between two cells decreases, but with increasing cell adhesion, the surface contact area increases. Measurement of the cortical tension of cells in each germ layer in zebrafish gastrulae showed that the ectoderm had the highest cell tension, followed by the mesoderm and endoderm (Krieg et al., 2008). When cells were treated with drugs that disrupt the stability of the cortex, such as Blebbistatin or Cytochalasin D, the cell tension dropped to barely detectable levels, and sorting no longer occurred (Krieg et al., 2008). Interestingly, activation of Nodal signaling by exposing cell cultures to activin resulted in decreased cell tension, suggesting that Nodal signaling not only specifies mesendoderm, but also leads to mesendoderm sorting by decreasing cell tension. *ptges* morphants showed greater membrane localization of F-actin in *ptges* morphants, suggesting that

cortical tension might be increased with the loss of PGE_2 synthesis, though this notion will have to be experimentally verified. One method to quantify cell cortical tension is to measure the junctional angles between cells, as the Heisenberg group has done (Krieg et al., 2008), which generates a corollary of cortical tension. However, this remains an imperfect assay of cortical tension, as cell adhesion is also a contributor to the surface contact area.

If the increased F-actin localization in *ptges* morphants is indeed correlated to greater cortical tension, then PGE_2 may enhance the roles of Nodal signaling on endodermal specification and germ layer sorting behavior. Injection of *ptges* MO in MZ*oep*$^{tz57/tz57}$ mutants, however, did not abolish the increase of F-actin at the membrane, suggesting that PGE_2 can regulate F-actin distribution, and possibly cortical tension, through mechanisms that do not rely on Nodal signaling alone.

In summary, we have shown that PGE_2 synthesis contributes to the generation of endodermal cells, possibly through enhancement of the Nodal signaling pathway. We also presented preliminary data suggesting that reduced PGE_2 synthesis affects the intracellular distribution of F-actin via an unknown mechanism, which may ultimately affect the cortical tension of the cell.

CHAPTER IV

FUNCTIONAL CHARACTERIZATION OF A NONSENSE MUTATION IN PROSTAGLANDIN E_2 RECEPTOR 4 MUTANT

Summary

PGE_2 signaling regulates cell proliferation, apoptosis, and cell motility in vertebrates. Many of these effects occur through its GPCR EP4. Although some studies suggest that EP4 increases cAMP levels, the receptor is Pertussis toxin-sensitive, suggesting it is coupled to the $G\alpha_i$ subunit. Previous studies revealed that *ep4a* is maternally and zygotically expressed ubiquitously during early development. We have generated fish harboring a nonsense mutation in the *ep4* gene through a reverse genetics TILLING approach. Both zygotic and maternal zygotic *ep4* mutants do not show an overt phenotype, however, our additional experiments suggests that it is a null allele. There are three *ep4* paralogues in zebrafish, which might compensate for the loss of function of EP4a during gastrulation.

Introduction

Prostaglandin E_2 signaling is initiated when the lipid mediator binds its downstream GPCR, resulting in the liberation of α and βγ G proteins (Regan, 2003). There are three Prostaglandin E_2 Receptor (Ptger) subtypes; EP1, EP2, EP3, and EP4. The most well characterized are EP2 and EP4. Most studies defined the EP2 and EP4 receptors as coupled to $G\alpha_s$, leading to increased cAMP (Fujino and Regan, 2003; Regan, 2003). However, the EP4 receptor is sensitive to the Pertussis toxin, suggesting that it is coupled to $G\alpha_i$ (Fujino and Regan, 2006). Other studies show that EP4 is sensitive to agonist-mediated sensitization, and receptor activation further potentiates PGE_2 synthesis by activating *ptges* transcription in a positive feedback loop (Fujino and Regan, 2003).

Many of PGE_2's diverse physiological effects are conveyed through activation of the EP4 receptor. *Ep4* receptor knockout mice show a variety of phenotypes, including reduced immune lymphocytic responses, bone resorption and formation, severity of rheumatoid arthritis in a disease model, as well as failure of the ductus arteriosus to close after birth. The latter eventually results in neonatal death (Segi et al., 1998; Regan, 2003). Our group has shown that MOs targeting *ep4a* result in morphants with convergence and extension defects that arise in part because of the decreased speed of laterally migrating cells.

Genetic screens in the zebrafish model system are a powerful method for correlating genotype and phenotype (**Fig. 4-1**). Early screens used the forward genetics approach, whereby randomly induced mutations are identified based on the phenotypes they cause. In this approach, adult fish are exposed to the chemical mutagen *N*-ethyl-*N*-nitrosourea (ENU), an alkylating agent that in

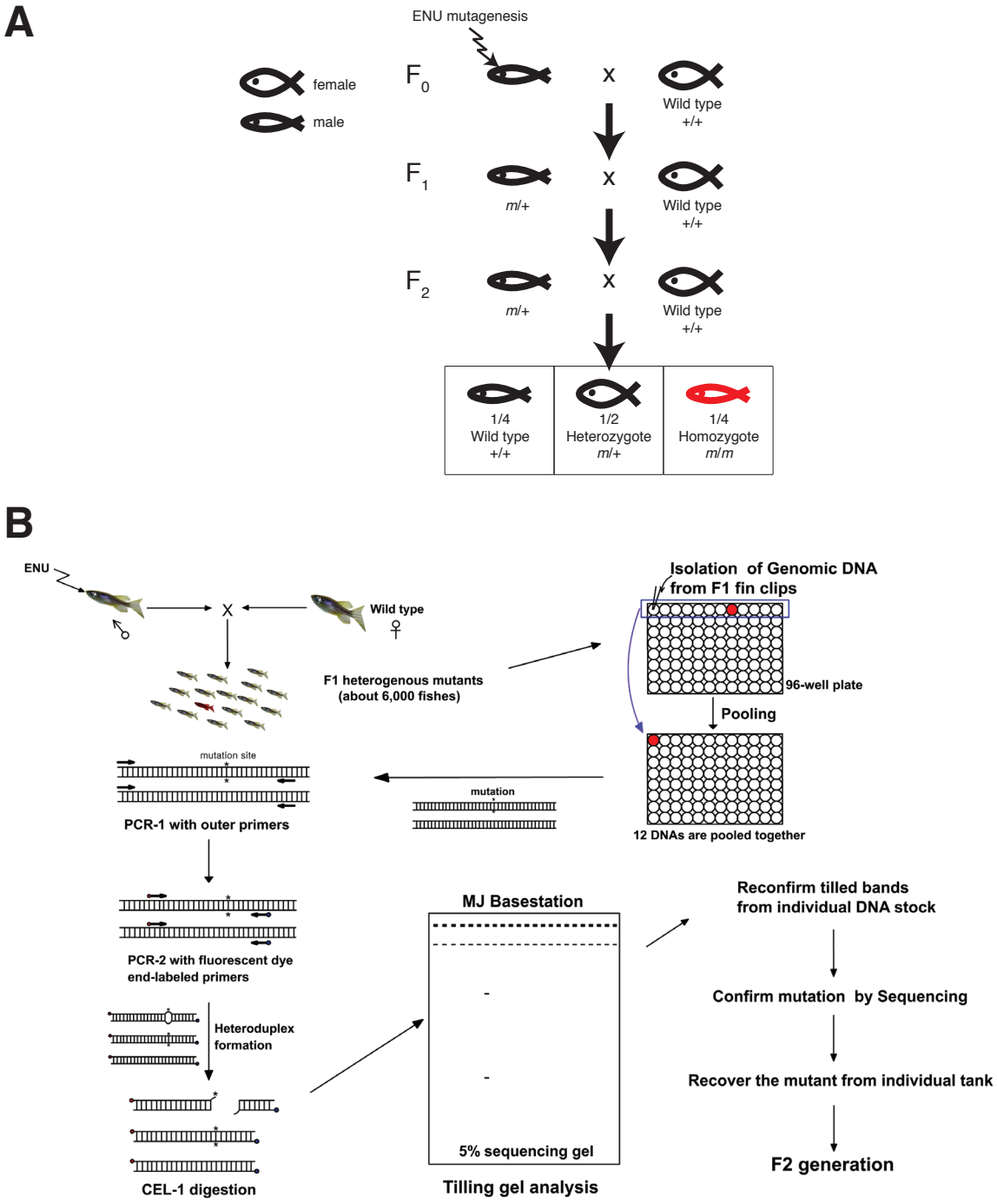

Figure 4-1. Genetic screens in zebrafish. (A) Forward genetic screens identify mutations based on a phenotype of interest (e.g., a morphological defect). In this example, recessive genetic mutations are identified based on the ratio of fish that display a phenotype. (B) Reverse genetic screens scan through target genes using a PCR and CEL-1 digestion method that displays mutations in the gene. From these mutagenized males, the mutation is recovered and confirmed by sequencing. The mutant fish are then analyzed for phenotypes related to the loss of the target gene. *Panel (B) provided courtesy of S.-H. Kim and L. Solnica-Krezel.*

zebrafish chiefly results in AT→TA transversions and AT→GC transitions. This treatment results in point mutations in the male zebrafish testes (Mullins et al., 1994; Solnica-Krezel et al., 1994). Mutagenized F0 males are outcrossed with wild-type females to generate a F1 stock, which is then incrossed to obtain F2 families that could be screened for recessive mutations by intercrossing siblings and visual inspection of the F3 progeny (**Fig. 4-1A**). The first large scale screens identified hundreds of interesting phenotypes (Driever et al., 1996; Haffter et al., 1996). Subsequent studies then molecularly characterized the affected genes using positional or candidate cloning approaches.

Reverse genetics entails finding mutations in a gene target of interest and investigating its possible function. An intriguing method that was originally developed in *Arabidopsis thaliana* and adopted for use in zebrafish is the **T**argeting **I**nduced **L**ocal **L**esions **IN G**enomes (TILLING) approach (**Fig. 4-1B**) (Henikoff et al., 2004). In this approach, genomic DNA that is isolated from F1 fish obtained from ENU mutagenesis, as described above, is then used as a template for PCR with target-specifc primers that are labeled with different dyes to distinguish the 5′ and 3′ ends (Wienholds et al., 2003). After denaturation and renaturation of the PCR amplification products, they are treated with CEL-1 enzyme, a nuclease isolated from celery that catalyzes the DNA in locations of heteroduplexes. These fragments are then resolved on sequencing gels to identify PCR product fragments that are indicative of mutations in the target gene. F1 fish are screened in pools of 12 so that a large number of fish can be efficiently screened for mutations.

TILLING by our group has yielded a nonsense mutation in the gene encoding the Ep4a receptor that we will term $ep4a^{T514A}$ (S.-H. Kim and L. Solnica-

Krezel, unpublished). The studies described in this chapter revealed that neither Zygotic nor Maternal Zygotic (MZ) mutants showed a phenotype, which is inconsistent with the gastrulation phenotype reported by our group for *ep4a* morphants (Cha et al., 2006). We describe here preliminary data indicating that the mutant form likely has no functional activity. In addition, we will discuss the presence of two other forms of Ep4 in zebrafish and suggest possible etiologies for the discrepancy between the *ep4a* morphant and mutant phenotype.

Experimental Procedures

ep4a^{T514A} mutant genotyping

DNA was isolated from fish by fin clipping. Fins from MESAB-anesthetized fish were collected in chilled PCR tubes containing 50 μL lysis buffer (10 mM Tris-HCl pH 8.0, 50 mM KCl, 0.3% Tween, 0.3% NP40). Tubes were heated at 98°C for 10 minutes, then allowed to cool before adding 4 μL Proteinase K. Fins were then incubated overnight in a 55°C waterbath. Subsequently, samples were spun down at 2000 rpm for 2 minutes, heated at 98°C for 10 minutes, and then spun again at 2000 rpm for 1 minute, before the supernatant was transferred to new tubes to exclude remaining tissue. The samples were diluted by half with ddH_2O and were prepared for PCR with *Taq*. The primers that were used for PCR and the digests which identified wild-type, heterozygotic, or homozygotic *ep4a*^{T514A} mutants are listed below.

MaeIII restriction enzyme-based genotyping.

5′ genotyping primer: 5′- GCG GGG GTC ACC CTA CT -3′

3′ genotyping primer: 5′- CAC ACC AGC ACA TTG CAG AC -3′

PCR products were digested with *MaeIII*. Wild-type alleles are 215 bp, whereas the mutant alleles generate 90 and 125 bp fragments.

Derived cleaved amplified poloymorphic sequence (dCAPS)-based genotyping.

5′ genotyping primer: 5′- TCG GCT TCG GCG AGG TGA AAA TGC AGG A -3′

3′ genotyping primer: 5′- CAC ACC AGC ACA TTG CAG AC -3′

PCR products were digested with *BamHI*. Mutant alleles are 155 bp, whereas the

wild-type alleles generate 28 and 127 bp fragments.

ep4 sequence Alignment

ep4a was used as a query sequence in Ensembl BLAST. The top two search results were *ep4b*/ *ptger4b*, which has already been annotated (Villablanca et al., 2007), and a *ep4*-like fragment that we termed *ep4c*/ *ptger4c*. Sequence were aligned using MAFFT software (v.6) (Katoh et al., 2009).

Ep4 transmembrane domain prediction

The Ep4a protein sequence was analyzed for conserved transmembrane domains using Dense Alignment Surface (DAS) method software (Cserzo et al., 1997), which generates a graphical map showing the possible transmembrane domains along the query cDNA sequence. Each possible domain is assigned a DAS profile score with loose and strict cutoffs to indicate the likelihood that the region contributes to a transmembrane domain.

EP4 fluorescent construct assay

The T514A mutation was introduced into the *ep4a-gfp* construct (Cha et al., 2006) through site-specific mutagenesis with *Pfu* polymerase (5′ primer: 5′- GGT GAA AAT GCA GTA ACC TCA AAC CTG GTG C -3′; 3′ primer: 5′- GCA CCA GGT TTG AGG TTA CTG CAT TTT CAC C 3′). Both constructs are in the pCS2 vector.

Results

Two *ep4a* TILLING mutations in F1 ENU-mutagenized fish were identified and recovered by our group (S.-H. Kim and L. Solnica-Krezel, unpublished): a missense and nonsense mutation. The nonsense mutation is a T514A transversion that results in a stop codon instead of a tyrosine reside (**Fig. 4-2**). Analysis of the protein sequence using a DAS method to predict where the transmembrane domains are located suggests that the mutation lies between the 4th and 5th transmembrane domain of the Ep4a receptor (**Fig. 4-3**).

We began characterization of the *ep4a*^{T514A} mutant by investigating the effects of the mutation in zygotic mutants generated by incrossing heterozygotes (*ep4a*$^{T514A/+}$). The homozygotes were identified by *DpnI* restriction ezyme-based genotyping. However, the mutants did not show an overt morphological phenotype (data not shown). Next, homozygotes (*ep4a*$^{T514A/T514A}$) were incrossed to generate MZ*ep4a*$^{T514A/T514A}$ mutants, but did not manifest an obvious morphological gastrulation defect.

To characterize further the outcome of the mutation on protein function, we introduced the T514A mutation into the *ep4a* cDNA tagged at the C-terminus with *gfp* cDNA (pCS2 vector). RNA was synthetically transcribed from these constructs, then embryos were injected with either the wild-type *ep4-gfp* or *ep4a*^{T514A}*-gfp* at equivalent doses (100 pg) (**Fig. 4-4**). At the tailbud stage, though embryos misexpressing Ep4-GFP showed ubiquitous fluorescence, embryos expressing Ep4^{T514A}-GFP had no detectable fluorescence, similar to the uninjected embryos (**Fig. 4-4**).

Previous studies by our group show that the gastrulation phenotypes of the *ep4a* morphants can be partially suppressed by injecting synthetic *ep4a* RNA,

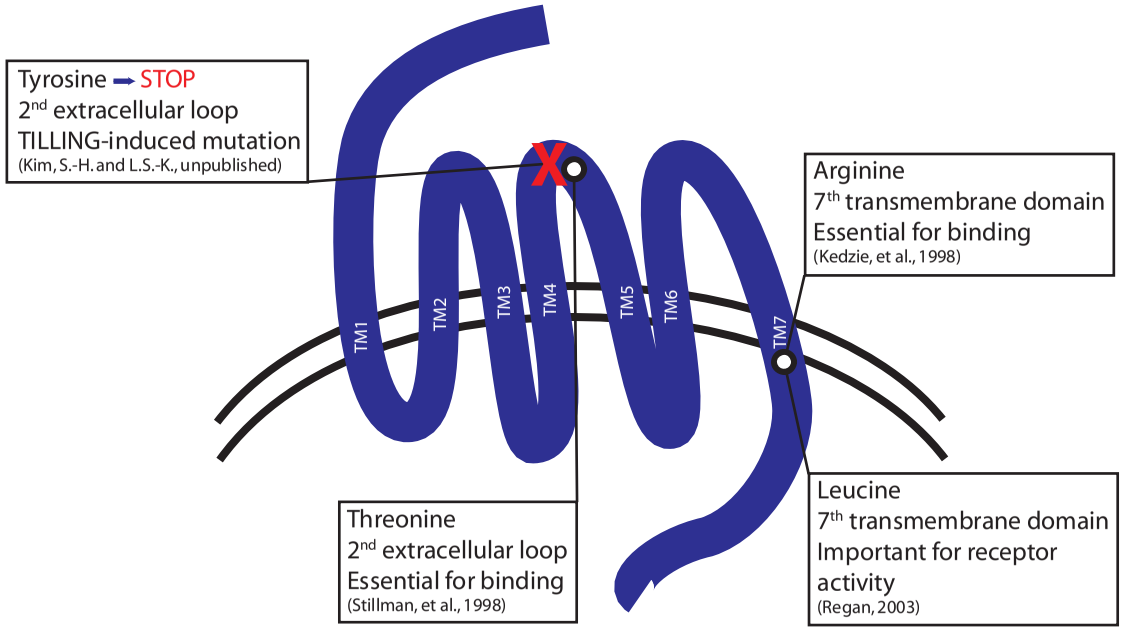

Figure 4-2. Ep4 structure-function correlation. The residues of EP4 that are important for its signaling activity in mammalian cell culture are noted. In addition, the Danio Ep4a^{T514A} is also noted on the figure (red X) to demonstrate that the TILLING Ep4a^{T514A} mutation truncates the protein upstream of the residues required for binding and signaling.

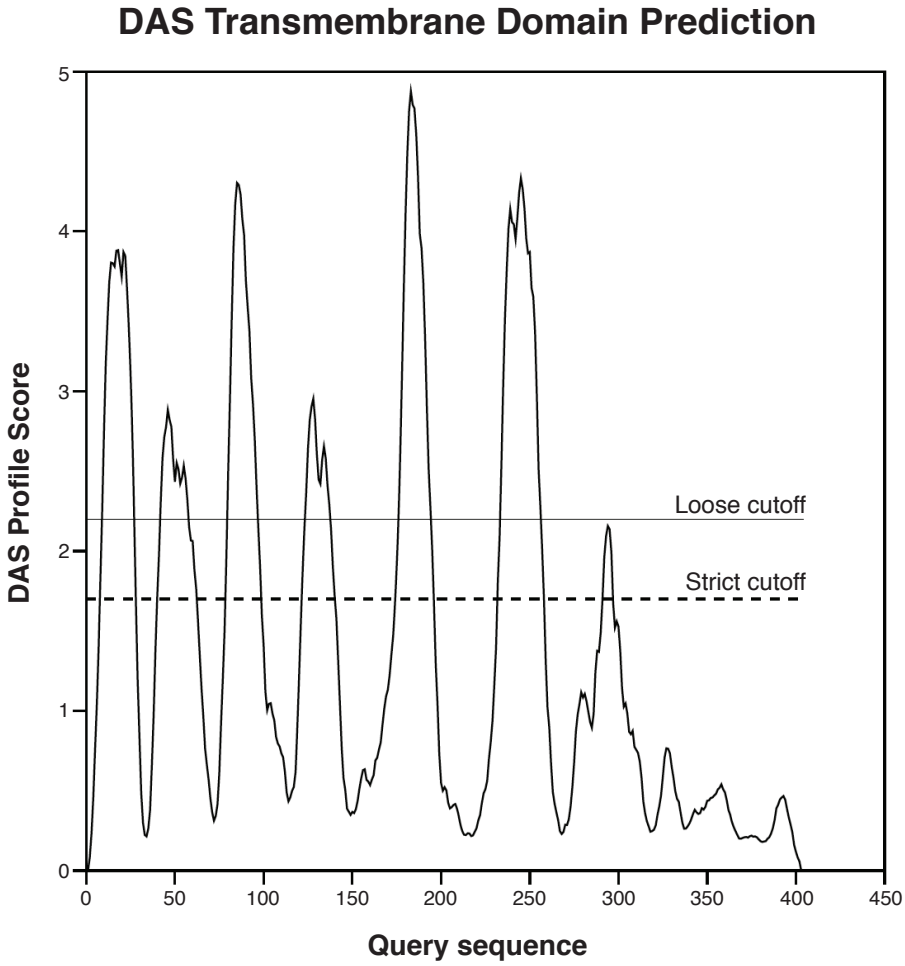

Figure 4-3. Predicted transmembrane domains of Ep4a. Each peak denotes a predicted transmembrane domain. The probability that each peak fulfills the criteria of a transmembrane domain is indicated on the left axis by the Dense Alignment Surface (DAS) profile score. The Ep4a^{T514A} stop codon is located at position 150 of the query sequence.

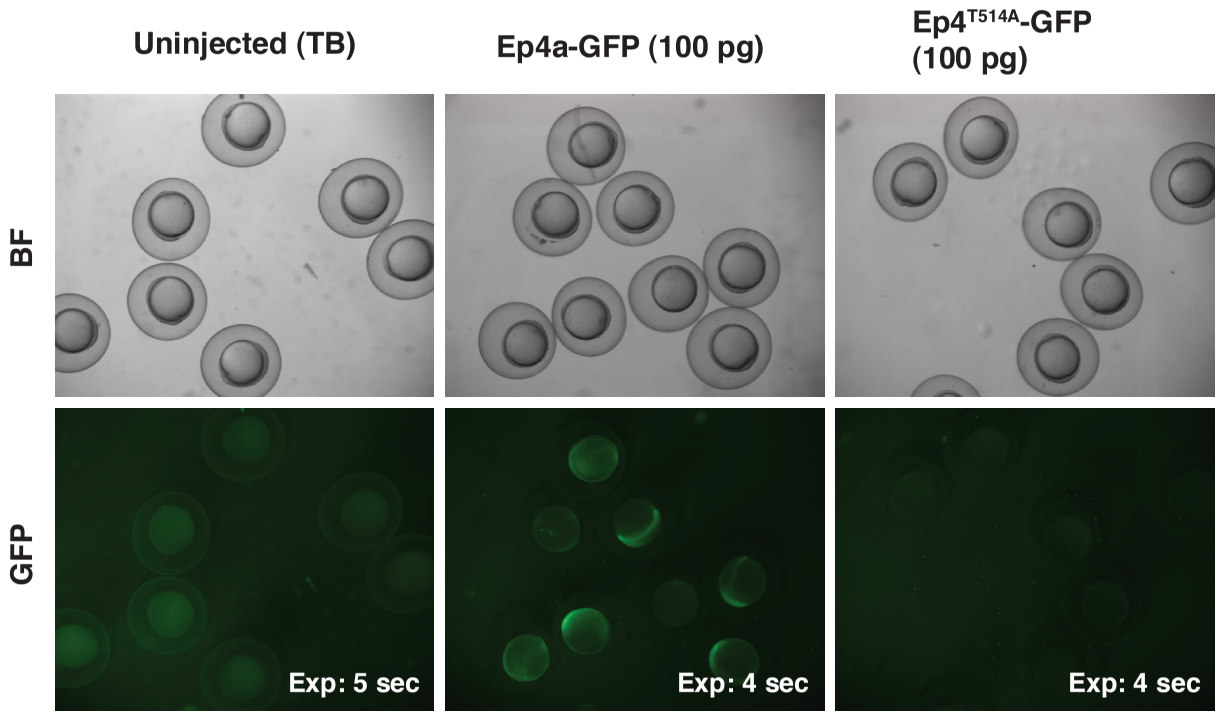

Figure 4-4. The Ep4a^{T514A}-GFP construct is not similarly expressed to the wild-type Ep4a-GFP construct. The TILLING T514A mutation was introduced into an *ep4a* cDNA construct fused to GFP at the C-terminus. Embryos were injected at the one-cell stage with equivalent levels of the construct and imaged at the TB stage using Brightfield and fluorescent illumination (exposure times are noted).

suggesting that the phenotype is specific (Cha et al., 2006). Is it possible, then, that the *ep4a* MO targets an *ep4* paralog in zebrafish, in addition to *ep4a*? Villablanca, et al., has cloned an *ep4*-like gene they annotated as *ep4b* (Villablanca et al., 2007). RT-PCR experiments show that it is expressed early in development until 48 hpf when it is downregulated, then expression reappears at 4 dpf (Villablanca et al., 2007). However, the location and dynamics of *ep4b* expression have not been investigated further by whole-mount *in situ* hybridization. We also searched Ensembl for additional paralogs of *ep4* in zebrafish, using the sequence for *Danio rerio ep4a*/*ptger4a*, which lies on Chromosome 8 (Cha et al., 2006), as the query sequence. The top search result was *ep4b*/*ptger4b* on Chromosome 5. The next search result, which we termed *ep4c* (XM_683448), was present on Chromosome 2. Alignment of *ep4a*, *ep4b*, and *ep4c* revealed that *ep4a* and *ep4b* bear more nucleic and amino acid identity than *ep4a* and *ep4c* (**Figs. 4-5, 4-6, 4-7**). Interestingly, alignment of the MO-binding site of the *ep4a* MO, the ATG start site, showed that the *ep4b* and the *ep4c* start sites had 72% and 20% sequence identity, respectively (**Figs. 4-5, 4-6**).

A

```
ptger4a     cagcagcagcatggagcccac-cgtg
ptger4b     taacagc-gcatgaaacgcacgtgtg
             * **** ***** * * ***  ***
```

B

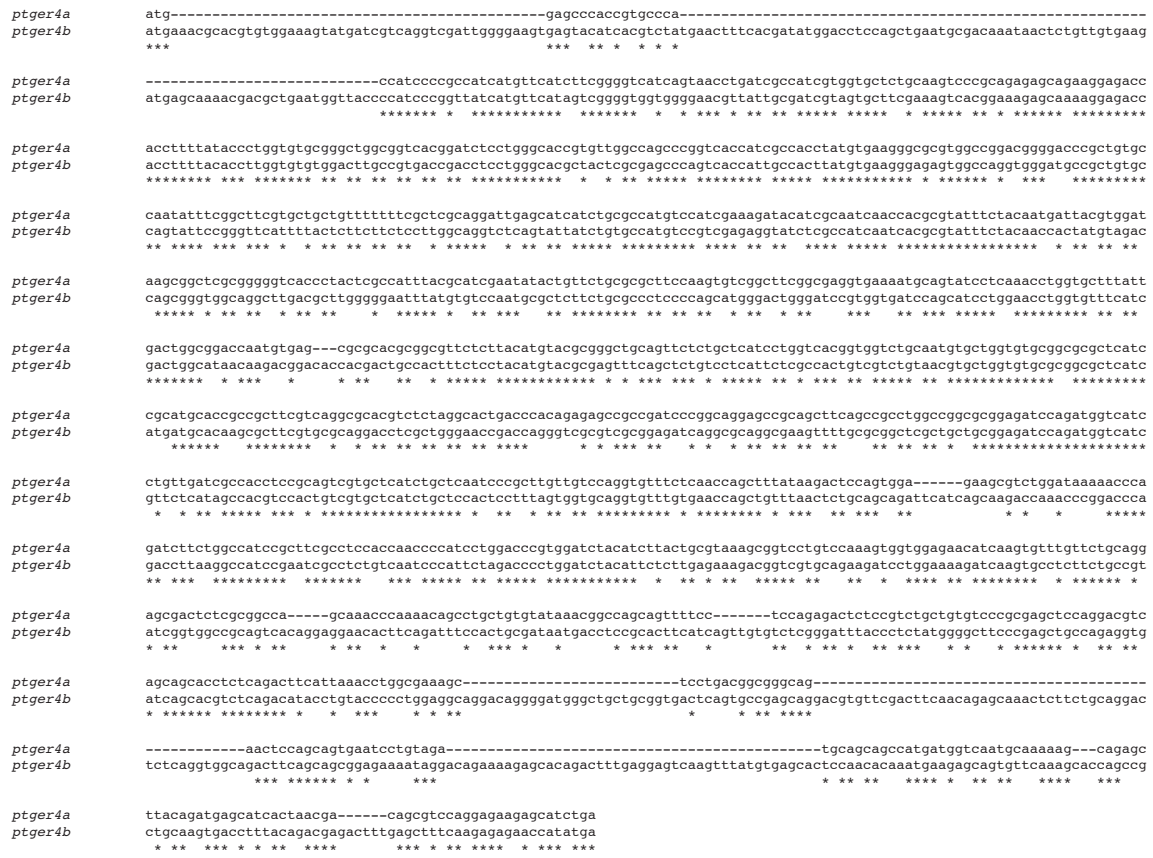

Figure 4-5. *ep4a* and *ep4b* MO-binding site and nucleic acid alignment. (A) Sequence alignment of the ATG binding site for MO2-*ep4a/ptger4a*. This genomic region of *ep4a* and *ep4b* contains 72% identity. (B) Nucleic acid sequence alignment of *ep4a* and *ep4b*.

A

```
ptger4a     cagcagcagcatggagcccaccgtg
ptger4c     tctcg----------tcacttcg
                *              ***    *
```

B

```
ptger4a     atggagcccaccgtgcccaccatccccgccatcatgttcatcttcggggtcatcagtaacctgatcgccatcgtggtgctctgcaagtcccgcagagagcagaaggagaccacctttttat
ptger4c     ----------------------------------atgtttggcgtcggagtcctcggaaaccttgtagctatcgtggtgctttgcatctccaagaaagagcagaaggagaccaccttctac
                                             *****  * **** *** ** * *****  * ** ********** ****  ***   * ********************* **

ptger4a     accctggtgtgcgggctggcggtcacggatctcctgggcaccgtgttggccagcccggtcaccatcgccacctatgtgaagggcgcgtggccggacggggacccgctgtgccaatatttc
ptger4c     actctggtgtgcgggatggccatcacagacctgctgggcacctgcttcaccagtccggttgtcatcgccacttatatcgcgggcaggtggccgggtggagcgctcctgtgccatttcttc
            ** ************ ****  **** ** ** *********   **  **** *****   ********* *** *   ****  ********  ** *  *  ******** *  ***

ptger4a     ggcttcgtgctgctgttttttttcgctcgcaggattgagcatcatctgcgccatgtccatcgaaagatacatcgcaatcaaccacgcgtatttctacaatgattacgtggataagcggctc
ptger4c     tccttttccatgctgttcttcgggtctgctgggatgtctattctgtgcgcaatgtccgtggaaagatatttggccataaaccacgcgtacttttactctcaacacgtggaccgggctatg
              ***     ******* **   *   ** **  **   **  * ***** ****** * ********  * ** ** ********** ** ***  * *  *******   *    *

ptger4a     gcgggggtcaccctactcgccatttacgcatcgaatatactgttctgcgcgcttccaagtgtcggcttcggcgaggtgaaaatgcagtatcctcaaacctggtgctttattgactggcgg
ptger4c     gctcggtttgcgctgatggcaacctatctggccaatatcgtgctgtgtatcatgcccagttttggcttcggaaagcacaagagacactttccgggaaacttggtgcttcttggactggcgc
            **  ** *  * **  * ** *  **     * *****  ** * **     * ** *** * ********  **   ** *  ** * ***   *** ********  * ********

ptger4a     accaatgtgagcgcgcacgcggcgttctcttacatgtacgcgggctgcagttctctgctcatcctggtcacggtggtctgcaatgtgctggtgtgcggcgcgctcatccgcatgcaccgc
ptger4c     gccatggactcggtcggcgcctcgtacacgtttctgtacggtggtttcatgctgctgctgatcgccgttacagtcttgtgcaatttcgccgtgtgtgcgttcactcgtcgggatgagt---
             ***  *     *    ***  *** * * *   ******  ** * **     ***** ***   ** ** **  * ****** *    *****  *  * *** ** * ***

ptger4a     cgcttcgtcaggcgcacgtctctaggcactgacccacagagagccgccgatcccggcaggagccgcagcttcagccgcctggccggcgcggagatccagatggtcatcctgttgatcgcc
ptger4c     ------------aaaatgagtcggatggtaagagcagaggtacccggacacgcagggtcaaggcgcggattcaggttaacatctgcagcggagatccagatgttctggctgttgatatta
                        * *  **           ** **  * ***   *  * **    ** *** * *****        * *  ***************  **   ********

ptger4a     acctccgcagtcgtgctcatctgctcaatcccgcttgttgtccaggtgtttctcaaccagctttata---------agactccagtggagaagcgtctggataaaaacccagatcttctg
ptger4c     atgactattgtgttcctgatatgctccatccctttagtggtgcgcatcttcgtcaaccagctgtacgatcctgcttatatttcctcaggcaaaagtccagactatcgcagtgatctcctg
            *   *    **  * ** ** ***** *****  * ** ** *   * **  ********** **          * * * *    *  **  ***  **  *   *   ***** ***

ptger4a     gccatccgcttcgcctccaccaaccccatcctggacccgtggatctacatcttactgcgtaaagcggtcctgtccaaag--------------------------------tggtggagaa
ptger4c     gctatacgattcgcctcctcaaccccatcctggatccatgggtttatattctgtgcagaaaaaaatttgttaaccaaaggctgtgcgcgactcaagcgtaccatcagacacaggaaaggg
            ** ** ** *********  *************** ** *** * ** **  *     * ***    *  *  ******                                    *   **

ptger4a     catcaagtgtttgttctg---------------caggagcgactcccgcggccagcaaacccaaaacagcc---------------------------------------tgctgtgta
ptger4c     gatcacagtcgtgttttgggttggacggatggtcaacactcacctccatcgttggta----caaagcaactgcaccagttacgcgtcactacgcacagcaatctgtagaaatgacgtggg
             ****      **** **              **  *   **  **   *   * *    **** ** *                                          **  ***

ptger4a     taaac----------ggccagcagttttcctccaga---gactctccgtctggtgtgtcccgcgagctccaggacgtca--gcagcacctctcagacttcattaaatctggcgaaagctc
ptger4c     taaacagaactgcatgaacactaaatcttatctagacttaacccttcgccaggcgtg--------------ggactttgatacagctctcgctcagtttcatc--------------ctt
            *****          *  **  *  * *  ** ***    ** ** ** * ** ***              **** *     **** *         *****               **

ptger4a     ctgacggcgggcagaactccagcagtgaatcc---tgtagatgcagcagc-----------------------------------catgatggtcaatgcaaaaagcagagcttacagat
ptger4c     tcagtgtcgagcaaaacact-gtaatgggttttgatgaagatgaagcaacatcaagtcccaaactcatcgccaagactgttatggcattaccagccactcaaatattagagaataaagct
                 * ** *** *** *  * * **  *     ** ***** **** *                                      *** *    * *  **** *  ****  ** ** *

ptger4a     g---------------------agcatcactaacgacagcgtccaggagaagagcat------ctga
ptger4c     gaaatagtgacctgcacattcagtacacctagttcttgtctatcagaaaagtgcatgagacaatga
            *                   ** *   ***      *  *    ** *** ****       ***
```

Figure 4-6. *ep4a* and *ep4c* MO-binding site and nucleic acid alignment. (A) Sequence alignment of the ATG binding site for MO2-*ep4a/ptger4a*. This genomic region of *ep4a* and *ep4c* contains 20% identity. (B) Nucleic acid sequence alignment of *ep4a* and *ep4c*.

Figure 4-7. Protein alignment of Ep4a/Ptger4a, Ep4b/Ptger4b, and Ep4c/Ptger4c. (A) Protein alignment of Ep4a and Ep4b. (B) Protein alignment of Ep4a and Ep4c. The legend (bottom) indicates the symbols for identical, strongly similar, and weakly similar amino acid residue.

Discussion

Our group has generated a mutant with a T514A transversion in the *ep4a* gene that likely introduces a stop codon between the 4th and 5th transmembrane domains. We hypothesized that this mutation results in a null allele, but there was no morphological phenotype detected in the zygotic and MZ*ep4a*$^{T514A/T514A}$ mutants, revealing a discrepancy between the *ep4a*$^{T514A/T514A}$ and the *ep4a* morphants. Interestingly, the *ep4a*^{T514A} mutation lies upstream to three residues that are important for ligand binding and signaling (**Fig. 4-2**). Studies in mammalian cell culture have indicated that a threonine in the 2nd extracellular loop and an arginine in the 7th transmembrane domain are essential for ligand binding (Kedzie et al., 1998; Stillman et al., 1998). In addition, a leucine in the 7th transmembrane domain is important for the signaling activity of the receptor (Regan, 2003) (**Fig. 4-2**). Therefore, the *ep4a*$^{T514A/T514A}$ mutants likely do not have normal ligand binding and signaling. In addition, misexpression of a C-terminus GFP-tagged form of Ep4a showed the T514A mutation likely results in a null allele, as injected embryos showed no fluorescence in comparison with the wild-type tagged construct. Therefore, it is unlikely that there is stop-codon readthrough of this mutation, a process that can occur in yeast via tightly regulated mechanisms (von der Haar and Tuite, 2007). It is possible that the truncated protein that results from the T514A mutation stimulates nonsense-mediated decay (Moens, 2000), which could be analyzed by whole-mount *in situ* hybridization. In addition, a N-terminus GFP-tagged Ep4a^{T514A} construct would address whether any protein is being synthesized in injected embryos. An important issue that remains to be addressed is whether the *ep4a*$^{T514A/T514A}$ mutants show increased sensitivity to treatment with Indomethacin or injection with the

cox1 and *ep4a* MOs than wild-type embryos. If so, this would suggest that the mutants are indeed functionally affected by the mutation, and that the lack of phenotype is owed to compensation or redundancy.

We hypothesize that the *ep4a* MO targets an *ep4* paralog that is also expressed during gastrulation. It remains to be seen whether the two search results, *ep4b* and *ep4c*, are also expressed during gastrulation, though previous study suggests that *ep4b* might be. We found that the *ep4c* ATG start site showed only 20% sequence identity, suggesting that binding of the *ep4a* MO is not likely to occur (**Fig. 4-6**). However, the *ep4b* ATG start site showed 72% sequence identity to the MO-binding site of the *ep4a* start site (**Fig. 4-5**). Although 5-6 bp mismatch morpholinos are usually used for MO controls, it is possible that because the 7 mismatched base pairs between the *ep4a* MO and the *ep4b* ATG start site are scattered throughout the sequence, there might be some MO-binding and subsequent Ep4b downregulation. This possibility could be tested by generating a GFP-tagged construct of the *ep4b* ATG start site that would be co-injected with the *ep4a* MO to test if translation of the construct is inhibited. Therefore, our analysis of this TILLING mutation may reveal an Ep4 paralog that serves a redundant function with Ep4a to regulate gastrulation movements.

CHAPTER V

DISCUSSION AND FUTURE DIRECTIONS

Prostaglandin E_2 signaling influences tumorigenesis, inflammation, reproductive fitness, and development. Our studies have focused on the roles of PGE_2 signaling during early development in zebrafish. Although previous data indicated that PGE_2 signaling components affect gastrulation movements, how it does so remained unclear. Our studies reveal that PGE_2 regulates cell adhesion and cell protrusions during gastrulation. These cell properties impinge on cell motility and their anomalies could account for the cell movement defects in Ptges-deficient embryos during development. In addition, we define the Gβγ-Gsk3β-Snail-*e-cadherin* pathway through which PGE_2 signaling modulates cell adhesion in mesendodermal progenitors. The effects of PGE_2 on cell motility and cell adhesion are also conserved in other cellular contexts, and we will discuss how our results relate to these findings as well as to the established roles for PGE_2 in cell proliferation and survival (**Fig. 5-1**). Lastly, we will review the numerous signaling networks that communicate with PGE_2 signaling, resulting in numerous cellular outcomes. One particular interaction that has been of great clinical interest is the one between PGE_2 and Wnt-β-catenin signaling. We have shown that during development, the Gβγ coupled to the EP receptor interacts with and inhibits Gsk3β. Therefore, our results provide a candidate protein for the juxtaposition of these two conserved signaling pathways that may hold

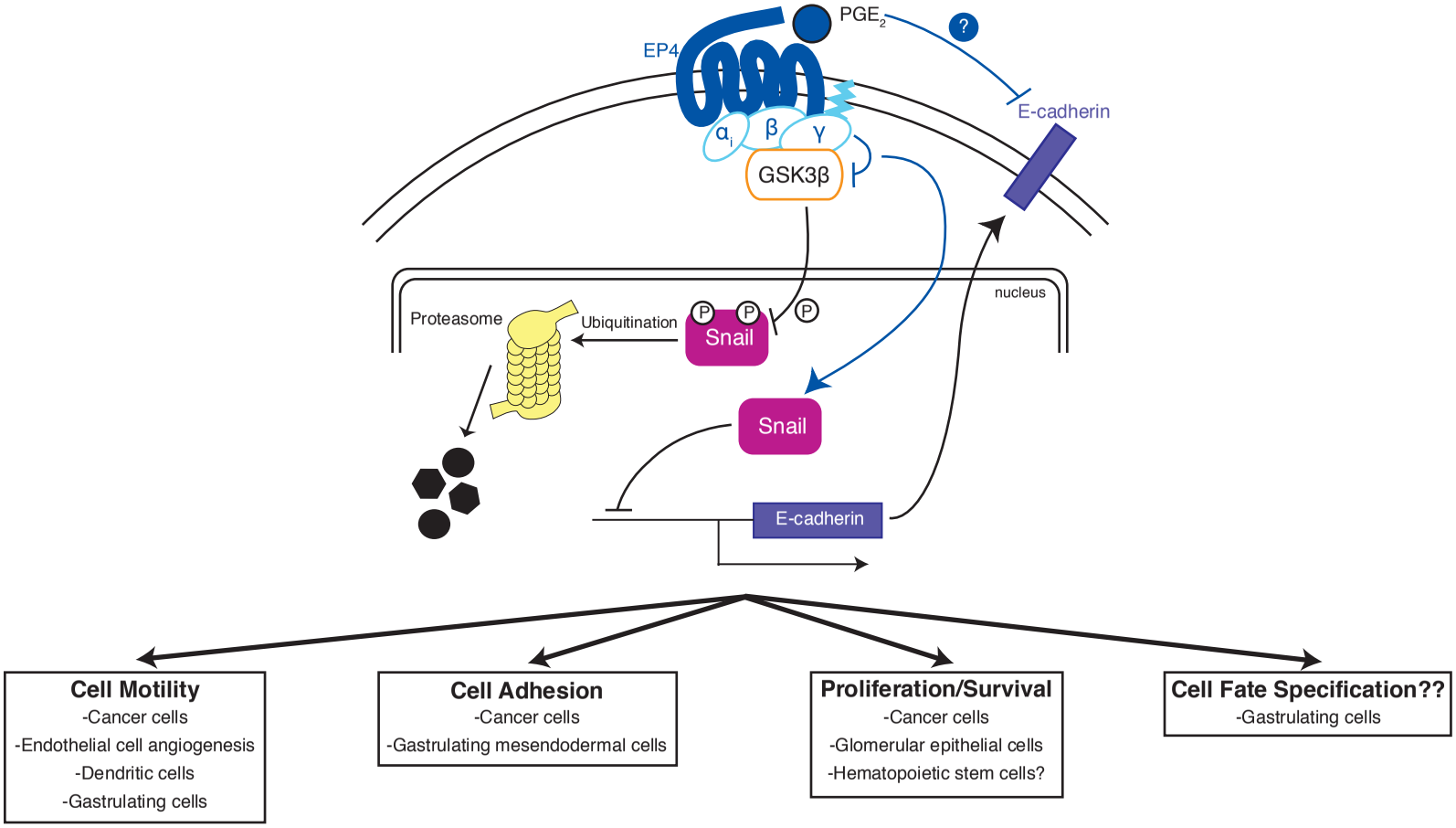

Figure 5-1. PGE_2 signaling exerts effects on many cellular properties and processes.

therapeutic potential in the pathogenesis of cancer and **h**ematopoietic **s**tem **c**ell (HSC) dysfunction.

Unifying Themes of Prostaglandin E_2 Signaling during Development and Disease

Cell motility

Tumorigenesis and Cell Metastasis

PGE_2 signaling promotes cell motility during inflammation, tumorigenesis, and embryogenesis. Most studies relevant to cell motility have focused on how PGE_2 enhances cancer cell invasion and metastasis to distant sites in the body. During metastasis, tumor cells leave the primary tumor to enter the circulation. To move to the secondary site of tumor growth, which is specific to the tumor type, the tumor cells extravasate from the vasculature and establish new growth (Buchanan et al., 2006). When treated with PGE_2, LS-174 human colon cancer cells show increased cell migration through an extracellular matrix (Sheng et al., 2001). Migration occurs within 2-4 hours post-treatment and is not seen in untreated cells. These effects are conveyed through the EP4 receptor, and consequently, treatment of cells with PGE_1 alcohol, an EP4 agonist, results in more cell migration within 1 hour than PGE_2 treatment alone. In addition, PGE_2 promotes the cell motility of cancer cells in an *in vitro* assay of cancer cell metastasis. In these experiments, PGE_2-treated or untreated cells are seeded on top of a Matrigel® (extracellular matrix components)-coated polycarbonate membrane that separates upper and lower chambers (modified Boyden chambers). After 20 hours, cells in the lower chamber represent the

number of migrated cells. PGE_2 treatment of cells increases cell motility by 2-3 fold, an effect that is abolished by either Wortmannin or LY294002, inhibitors of PIK3 (Sheng et al., 2001). These data suggest that a PGE_2-EP4-PIK3 signaling axis regulates cell motility in colorectal cancer cells. Activation of EP4 signaling in colorectal cancer cell lines also leads to the recruitment of β-arrestin 1, which acts as a scaffold, adaptor, and signal transducer in signalasome complexes that convey the signaling of GPCRs (Patel et al., 2009). β-arrestin interacts with c-Src to transactivate Epidermal Growth Factor Receptor (EGFR) and Akt, thus increasing cell migration and metastasis (Buchanan et al., 2006). LS-174 cells expressing β-arrestin also metastasize to the liver more frequently after the cells are injected into the spleen of mice, suggesting that PGE_2 and β-arrestin contribute to cell metastasis *in vivo* (Buchanan et al., 2006). Indeed, the increased cell migration of PGE_2-treated cells in the modified Boyden chamber assay is partially suppressed when the cells express a mutant β-arrestin. However, expression of the mutant β-arrestin does not prevent the stimulating effects of EGF treatment on cell migration, indicating that PGE_2 enhances cell motility upstream of EGF signaling (Buchanan et al., 2006). Moreover, combining COX-2 and EGFR inhibitors, NS-398 and AG1478, respectively, inhibits more cell motility *in vitro* than either alone, suggesting that PGE_2 and EGF signaling both control cell motility (Banu et al., 2007). EGFR signaling is also transactivated in **h**epatocellular **c**arcinoma **c**ells (HCC) by PGE_2-EP1 signaling, which leads to the phosphorylation and consequent activation of the tyrosine kinase c-Met, often associated with cancer cell invasiveness (Han et al., 2006).

In addition to EGFR and PIK3 signaling, PGE2 signaling promotes cell

motility through other mechanisms. HCC cell lines that exhibit a high level of COX2 expression also have increased expression of **M**atrix **M**etallo**p**roteinase (MMP)-2 and-9, secreted factors that enzymatically degrade ECM components to increase the efficiency of cell migration (Wu, 2006). PGE_2-induced migration is also antagonized by inhibitors of MEK/ERK, p38 MAPK, **P**rotein **K**inase **A** (PKA), and Protein Kinase C (PKC) (Wu, 2006), hinting at the complexity of the signaling mechanisms employed by PGE_2 signaling to regulate this process. Increased COX2 expression is associated with cancer cell metastasis in breast and lung cancers (Buchanan et al., 2006). Thus, the regulation of cell motility by prostaglandin signaling is likely a conserved mechanism of tumor spreading. Together, these studies indicate that PGE_2 signaling through GPCRs unleashes a diversity of signaling networks to influence cell migration during the metastasis of various tumor types.

One important aspect of tumorigenesis involves angiogenesis at the tumor site to supply it with oxygen and nutrients from the circulation. Interestingly, PGE_2 increases the cell motility of endothelial cells in primary mouse endothelial cell culture through an EP4 receptor-ERK signaling axis (Rao et al., 2007). Although PGE_2 signaling activates endothelial cell motility, the proliferation of these cells is unaffected. Therefore, PGE_2 signaling influences cell motility not only in tumor cells but also in endothelial cells, resulting in increased cell migration, ECM degradation (through MMPs), and angiogenesis, altogether promoting cancer cell metastasis.

Immune System Function

Whereas PGE_2 encourages the spread of cancer cells within the organism, it also promotes cell motility to enhance immune system function. For example, PGE_2 signaling increases the migration efficiency of **d**endritic **c**ells (DC), antigen presenting cells that participate in the organism's innate immune response. As in HCC cells, activation of the EP2 or EP4 receptors in murine bone marrow-derived DCs increases expression of MMP-9 transcript and protein through a PKA-dependent mechanism (Yen et al., 2008). Inhibition of MMP-9 reduces both DC migration in the modified Boyden chamber assay as well as the ability of MMP-9-inhibitor-treated cells to break down ECM components (Yen et al., 2008). Therefore, PGE_2 signaling advances the motility of immune cells by increasing their ability to penetrate the ECM.

Gastrulation

Grosser, et al., provided the first evidence that the inhibition of PGE_2 signaling in early zebrafish embryos halts the process of gastrulation (Grosser et al., 2002). Subsequent studies from our group demonstrated that the moderate reduction of PGE_2 signaling leads to convergence and extension defects by affecting the speed of dorsally migrating lateral mesodermal cells (Cha et al., 2006). My work has extended these studies to demonstrate that increased inhibition of PGE_2 signaling arrests all of the gastrulation cell movements. Moreover, Ptges-deficient morphant cells of the anterior mesendoderm exhibited diminished protrusion length and turnover. More severely affected embryos showed bleb-like protrusions in anterior mesendodermal cells during gastrulation.

Cellular Protrusions and Blebs: Contributions to Cell Motility

Polarized cellular filopodial protrusions are essential for efficient cell migration. For example, inhibition of Pik3 with LY294002 or expression of a dominant-negative *pik3* (*dnpik3*) mutant construct in zebrafish gastrulae impairs the protrusion formation and cell migration of anterior mesendodermal/prechordal plate cells (Montero et al., 2003). Pdgf-Pik3 signaling is also negatively regulated *in vivo* during gastrulation by another GPCR, Edg5/Miles apart, a sphingosine-1-phosphate (S1P) receptor (Kai et al., 2008). The cells from *slb* mutants that are injected with *edg5* MO move more quickly, possibly due to the increased activity of Pik3 (Kai et al., 2008). Therefore, regulators of Pik3 can affect protrusion formation in migrating cells. PGE_2 signaling activates PIK3/**P**rotein **K**inase **B** (PKB) signaling during tumorigenesis (Fujino and Regan, 2003) and likely during development (Cha et al., 2006). Thus, PGE_2 may regulate cell motility during gastrulation movements by activating Pik3/Pkb signaling.

The effects of Pik3 on cell migration led us to hypothesize that the gastrulation defects in Ptges-deficient embryos are due to decreased Pik3 function. Indeed, Pik3 activity is decreased in zebrafish gastrulae with reduced PGE_2 synthesis (Cha et al., 2006). Therefore, PGE_2 may activate Pik3 directly or via EGFR transactivation to regulate protrusion turnover in zebrafish gastrula cells. In cell culture, PIK3/PKB activation inhibits GSK3β by phosphorylation, thereby decreasing the proteasomal degradation of SNAIL/SNAI1 (Cohen and Frame, 2001). Snai1 is required during gastrulation movements and is associated with increased tumor invasiveness, as mentioned previously. Therefore, it is conceivable that activating Pik3 downstream of PGE_2 signaling stabilizes Snai1

during gastrulation because of decreased Gsk3β function. However, we found that overexpression of the GPCR βγ-coupled Pik3 isoform, Pik3γ (Leopoldt et al., 1998), did not suppress the loss of Snai1a-YFP expression in Ptges-deficient embryos. Nor could the inhibition of Pik3 with LY294002, a known inhibitor of Pik3 in zebrafish gastrulae (Montero et al., 2003), result in the consistent reduction of Snai1a-YFP in control morphants or a synergistic loss of Snai1a-YFP in *ptges* morphants. These data suggest that PGE_2 does not regulate Snai1a through Pik3 in this developmental context.

The impairment of protrusive activity in the cells of Ptges-deficient embryos could also be due to increased cell adhesion. Indeed, *e-cadherin* morphant cells have markedly blunted cellular processes at the border of the epiblast and hypoblast in gastrulae (Montero et al., 2005), which suggests that altered cell adhesion can affect cell protrusion formation or maintenance. To address this possibility, we could co-inject the *e-cadherin* and *ptges* MOs and analyze whether anterior mesendodermal cells recover their protrusive activity.

The formation of bleb-like protrusions by cells in Ptges-deficient gastrulae is rarely seen in early zebrafish wild-type gastrulae, with the exception of the primordial germ cells, which bleb during the "tumbling" phase of migration (Reichman-Fried et al., 2004). Blebs characterize amoeboid movement, which was first described in the single cell stage of *D. discoideum*. These cells are elliptical in shape and form bleb-like protrusions due to alternating expansion and contraction of the membrane (Wolf et al., 2003). *D. discoideum* cells rapidly move by propelling along paths of least resistance. To do so, they have low adhesion to the substrate that is Integrin-independent. Furthermore, they are

highly deformable, which allows them to squeeze through gaps in the ECM. Amoeboid movement also occurs in some vertebrate leukocytes and cancer cells (Wolf et al., 2003). In addition to their formation in migratory cells, cell blebs occur in apoptotic cells (Dubin-Thaler et al., 2008).

Cell migration occurs in three phases (Dubin-Thaler et al., 2008). First, early spreading occurs when the cell initially contacts the surface substrate. Next, during the middle spreading phase, the cell increases the surface area of substrate attachment. In the last phase, late spreading, the cell membrane periodically contracts, and cells form and stabilize adherens junctions. Cells have blebs during the early spreading phase.

Blebs form in a 1-minute cycle that includes the bleb extending, then pausing, and finally retracting to the baseline position of the plasma membrane (Fackler and Grosse, 2008). Blebs are triggered by intracellular and extracellular cues. Extracellular stimulants include soluble ligands such as **F**etal **C**alf **S**erum (FCS), Cholecystokinin, cAMP in *D. discoideum* cells, and GPCR ligands, such as SDF-1α, which acts during primordial germ cell migration in zebrafish (Fackler and Grosse, 2008). Intracellular cues for blebbing include RhoA activation, disruption of the actin cortex-membrane interaction, and changes in cell adhesion, particularly Integrin-based adhesion of the cell to the ECM. These triggers locally destabilize or depolymerize the cortical actin network, which increases the internal hydrostatic pressure of the cell through an unknown mechanism (Dubin-Thaler et al., 2008; Fackler and Grosse, 2008). The change in pressure within the cell forms the bleb through dissociation of the membrane from the actin cytoskeleton. Then bleb formation halts because of actin polymerization, which occurs because the bleb membrane is coated with actin

membrane cross-linker proteins (Dubin-Thaler et al., 2008; Fackler and Grosse, 2008). Thus, the disruption of actin polymerization components, such as the formin actin nucleators, impairs blebbing (Fackler and Grosse, 2008). Next, increased actin filament assembly and the recruitment of the myosin light chain to the bleb lumen activates RHOA/ROCK to phosphorylate myosin and contract the acto-myosin cytoskeleton (Dubin-Thaler et al., 2008). Acto-myosin contractility retracts the bleb, ending the cycle of bleb formation.

Amoeboid and mesenchymal movements are thought to represent the two major types of cancer cell motility (Wolf et al., 2003). Mesenchymal migration likely entails a proteolytic-dependent mechanism by which cells move via the ECM. By contrast, amoeboid movement is proteolysis-independent, and is thought to represent the preferred escape mechanism for cancer cells tested in a 3D microenvironment (Wolf et al., 2003; Fackler and Grosse, 2008). Amoeboid cells in culture showed diffuse cortical actin rims and small actin-rich punctae where collagen fibers interact (Wolf et al., 2003). Interestingly, inhibition of blebbing with either a Rock inhibitor or a Myosin inhibitor results in filopodial protrusions during the early spreading phase (Dubin-Thaler et al., 2008). Therefore, PGE_2 signaling may promote mesenchymal cell migration by increasing proteolytic enzymes, such as MMPs, and/or inhibiting the formation of plasma membrane blebs. Perhaps in Ptges-deficient embryos mesenchymal migration is lost in favor of amoeboid cell movement. Therefore, it would be interesting to test whether the inhibition of Myosin or Rock can recover the formation of filopodial protrusions in Ptges-deficient anterior mesendodermal cells.

Cell adhesion

The effects of E-cadherin on cell migration

Unbalanced cell adhesion, either in excess or deficit, cripples the cell movement of primordial germ cells in zebrafish, border cells in *D. melanogaster*, and gastrulation movements in many animals (Blaser et al., 2005; Pacquelet and Rorth, 2005; Hammerschmidt and Wedlich, 2008). For example, a Ca^{2+}-dependent cadherin-based gradient that forms because of the ventral-dorsal Bmp gradient in the zebrafish gastrula regulates the convergence movement by favoring the cell body displacement of lateral cells towards the dorsal region (von der Hardt et al., 2007). In particular, gastrulation requires appropriate levels of E-cadherin/Cadherin 1, epithelial (Cdh1) (Solnica-Krezel, 2006; Hammerschmidt and Wedlich, 2008), a Ca^{2+}-dependent component of the adherens junction that binds β-catenin and p120 (Drees et al., 2005; Hammerschmidt and Wedlich, 2008). In zebrafish, *cdh1* is maternally deposited and is expressed ubiquitously during the cleavage stages (Kane et al., 2005). By 30% epiboly, *cdh1* is expressed in a radial gradient, with the highest expression in the superficial layer, which contains the ectodermal progenitors. Expression is cleared on the dorsal side, but becomes enriched in the dorsal forerunner cells and maintained in the lateral and ventral blastoderm until late gastrulation (Kane et al., 2005). Zebrafish *cdh1*/*half baked* (*hab*) mutants or morphants manifest defects in epiboly, internalization, convergence, and extension (Babb and Marrs, 2004; Kane et al., 2005; McFarland et al., 2005; Montero et al., 2005; Shimizu et al., 2005). In addition, *hab* mutant embryos exhibit irregular blastoderm surfaces as well as blastodermal cell shedding (Shimizu et al., 2005).

hab mutant cells in both the ectodermal (superficial layer) and mesendodermal (deep layer) progenitors have a rounder shape than wild-type cells, and the boundary between the superficial and deep layers is considerably less distinct (Kane et al., 2005). *cdh1*/*hab* mutations also impair the migration of the dorsal forerunner cells, which eventually decouple from the EVL-DEL margin, breaking up into discrete clusters that are rarely seen in wild-type gastrulae (Kane et al., 2005; Lin et al., 2009). The requirement for E-cadherin during gastrulation is cell-autonomous, as the mosaic transplantation of *hab* mutant cells to wild-type host embryos show a similarly rounded shape typical of cells within the *hab* mutant embryos. In addition, *hab* mutant donor cells contribute preferentially to the deep blastoderm, in contrast to the wild-type donor cells, which contribute largely to the superficial blastoderm, indicating that E-cadherin is required for the normal radial intercalation of cells within the blastoderm during gastrulation (Kane et al., 2005). MO-targeting of *cdh1* disrupts adhesion between the EVL and deep cells, which was discernable by electron microscopy (Shimizu et al., 2005). Similarly to *hab* mutants, *cdh1* morphants exhibit epiboly, convergence, and extension defects as well as cell shedding and the defective animalward migration of mesendodermal cells (Babb and Marrs, 2004; Montero et al., 2005).

Snail

The presence of several direct and indirect inhibitors of E-cadherin; Snail, $G_{\alpha 12/13}$, Wnt11, and p38, underscores the importance of precisely and dynamically regulating cell adhesion for normal gastrulation movements (Lin et al., 2005; Ulrich et al., 2005; Zohn et al., 2006). Snai1 is a transcriptional repressor of E-cadherin that binds E-box domains within the *cdh1* promoter. In addition to

repressing E-cadherin-based cell adhesion during mesenchymal cell migration, Snai1 is the canonical promoter of the Epithelial-Mesenchymal Transition (EMT), which occurs during development and disease. EMT entails the downregulation of epithelial markers (*e.g.*, E-cadherin, Claudins, Occludins, Cytokeratins) as well as the upregulation of mesenchymal markers (Fibronectin, Vitronectin). Snai1 also influences cell proliferation, motility/invasiveness, and survival (Barrallo-Gimeno and Nieto, 2005).

During early development, Snail is required for normal gastrulation movements in Drosophila and sea urchin (Barrallo-Gimeno and Nieto, 2005; Wu and McClay, 2007). Snai1 conditional mouse mutants show defective formation of the mesoderm layer because of persistent epithelial morphology as well as impaired anterior migration of mesodermal cells (Carver et al., 2001). During gastrulation, zebrafish embryos express two genes encoding Snai1, *snai1a* and *snai1b*. MO-targeting of both *snai1* genes delays the anterior migration of prechordal plate cells (Yamashita et al., 2004; Blanco et al., 2007). Interestingly, *snai1a*, *e-cadherin*, and *snai1b* are expressed in mutually exclusive domains along the anterior mesendodermal axis as well as during convergence and extension movements (Blanco et al., 2007). As previously mentioned, E-cadherin function is required for the anterior migration of prechordal plate cells. An elegant study by the Nieto group shows that *snai1a*-positive cells lead the migration of a domain of E-cadherin-expressing prechordal plate cells that will become the future hatching gland. As such, Snai1a function during gastrulation determines the anterior limit of the hatching gland (Blanco et al., 2007). By contrast, *snai1b*-positive cells lie posterior to the hatching gland anlage, actively migrating anteriorly to define the posterior limit of the hatching gland. Therefore, the *snai1*

genes are required during gastrulation for normal anterior migration of mesendodermal cells. In addition, *snai1b* morphants display convergence and extension defects (Blanco et al., 2007). All together, these data imply that Snai1a and Snai1b are required for the gastrulation movements.

Snail nuclear localization is also regulated downstream of Stat3 signaling in prospective prechordal mesoderm cells during early zebrafish gastrulation by Liv1/Solute carrier family 39, member 6/Slc39a6, a zinc transporter-related protein that is also an oncogene during breast cancer metastasis (Yamashita et al., 2004). During gastrulation, *liv1* is expressed in the prechordal plate progenitors at the margin in shield stage embryos, and continues to be expressed as prechordal plate cells migrate anteriorly to the animal pole (Yamashita et al., 2004). The axial mesoderm of *liv1* morphants was shorter and slightly wider, revealing a requirement for *liv1* in convergence and extension movements. Furthermore, cell transplantation experiments established that Liv1 is required in prechordal plate cells for anterior migration (Yamashita et al., 2004). These results are consistent with the convergence and extension defects in *snai1b* morphants. Indeed, Liv1-deficient embryos show Snai1a-YFP mislocalization to the cytoplasm, in contrast to the nuclear localization observed in wild-type gastrulae. Therefore, Liv1 regulates anterior migration, convergence, and extension in zebrafish gastrulae by promoting Snail activity, which likely regulates cell adhesion in prechordal plate cells (Yamashita et al., 2004; Blanco et al., 2007).

We have demonstrated here that Ptges-deficient embryos have decreased Snail activity due to increased Snail degradation. Therefore, how do our results relate to what is already known about Snail function during gastrulation

movements? Ptges-deficient embryos exhibit more severe gastrulation movement defects than interference with either *liv1* or *snai1* (Yamashita et al., 2004; Blanco et al., 2007). Therefore, it is likely that PGE_2 regulates targets during gastrulation besides Snai1 and E-cadherin. Because Ptges-deficient embryos manifest defective anterior migration of prechordal plate cells, like those in *snai1* and *liv1* morphants, it is possible that this phenotype in *ptges* morphants can be suppressed by overexpressing Snai1a or Snai1b, though this remains to be experimentally tested. In addition, *cdh1* MO co-injection in *ptges* morphants could rescue the anterior migration defect of prechordal plate cells, though we have not yet analyzed this particular movement in co-injected embryos.

Snail has been implicated in the tumorigenesis of breast, gastric, hepatocellular, colon, and synovial cancers (Barrallo-Gimeno and Nieto, 2005). In addition, SNAI1 expression levels are positively correlated with mammary tumor recurrence in a HER2/neu-induced mammary tumor mouse model (Moody et al., 2005). Most of these effects are proposed to occur through the inhibition of E-cadherin. Indeed, decreasing E-cadherin expression with **s**mall **h**airpin **RNA** (shRNA) in breast cancer cell lines activates β-catenin through dephosphorylation, possibly by modulating the activity of GSK3β (Onder et al., 2008). Thus, Snail expression could promote tumorigenesis by activating β–catenin through the loss of E-cadherin. In addition, the expression of TWIST and *TCF8/ZEB-1*, additional repressors of E-cadherin, is increased when E-cadherin is downregulated, which possibly sets up a positive feedback loop that maintains the loss of E-cadherin, activates β–catenin, and advances the mesenchymal, motile state (Onder et al., 2008).

PGE_2 can limit E-cadherin-based cell adhesion by increasing *SNAIL* transcription. For example, PGE_2 boosts *SNAI1* and *ZEB* transcript in **n**on-**s**mall **c**ell **l**ung **c**ancer (NSCLC) cell lines (Dohadwala et al., 2006). *COX2*-sense-transfected NSCLC cells and PGE_2-treated cells show decreased E-cadherin levels, whereas *COX2* antisense-transfected cells and cells treated with the COX2 inhibitor Celecoxib result in increased E-cadherin expression. Downregulation of SNAIL or ZEB using **s**mall **i**nterfering **RNA** (siRNA) constructs resulted in a diminished effect of PGE_2 treatment on E-cadherin expression. It is therefore feasible that PGE_2 regulates *snai1a* transcription during gastrulation. However, our experiments showed that decreased PGE_2 synthesis curtails Snail protein stability without significantly altering the transcript levels of *snai1a* and *snai1b* genes. The proven ability of PGE_2 to affect Snail expression either by increasing transcription or protein stability suggets that modulating cell adhesion is an important function of the PGE_2 signaling pathway. Although our results indicate that PGE_2 does not influence *snai1a* transcription during zebrafish gastrulation movements, it is intriguing that the regulation of Snai1 through both of these mechanisms simultaneously, within a single cell type, might have a potent effect on cell adhesion.

How does PGE_2 activate Snai1 during gastrulation movements, if not through transcription? Snai1 protein can be functionally silenced in two ways (**Fig. 5-2**). First, the transcriptional activity of SNAI1 can be repressed by nuclear exportation through CRM1 (Dominguez et al., 2003). In addition, SNAI1 contains two serine-rich domains that can be phosphorylated by GSK3β. In cell culture, the phosphorylation of these domains recruits the ubiquitin ligase β-

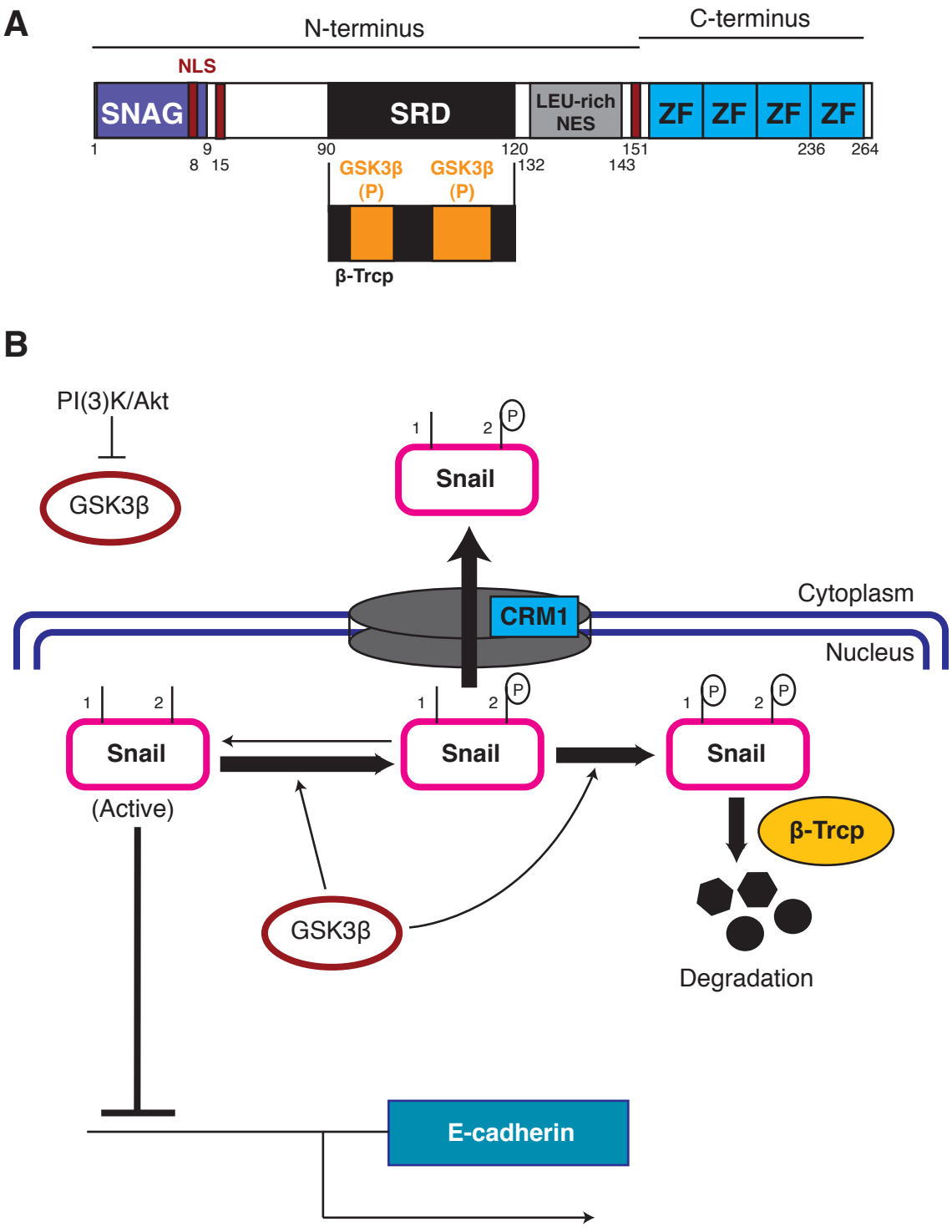

Figure 5-2. Snail protein domain schematic and regulation mechanism. (A) Protein domain structure of Snail. The N-terminus SNAG domain is required for the repressive function of Snail in mammals. Snail can be regulated by nuclear export (through its NES) or by phosphorylation of its Serine Rich Domain (SRD) by Gsk3β. (B) Gsk3β can phosphorylate Snail at one of two domains to induce its nuclear export and proteasomal degradation.

TRCP, targeting SNAI1 to the proteasome for degradation (Zhou et al., 2004). To answer this question in a developmental context, we have delineated a novel mechanism whereby the PGE_2-associated GPCR βγ subunits stabilize Snai1a by interacting with and inhibiting Gsk3β function (see ***Wnt-β-catenin***, below). This results in the decreased ability of Gsk3β to target Snai1a to the proteasome for degradation, and allows Snail to repress *e-cadherin* and cell adhesion.

E-cadherin regulation in ectodermal progenitors

PGE_2-deficient embryos show clusters of cells with upregulated E-cadherin expression in the animal pole at the shield stage, where *snai1a* is not expressed (Hammerschmidt and Nusslein-Volhard, 1993). We also observed this "patchy" E-cadherin expression in *ptges* MO-injected MZ*oep*$^{tz57/tz57}$ mutants, which lack most of the mesendodermal progenitors and exhibit diminished *snai1a* expression (Gritsman et al., 1999). This "patchy" expression of E-cadherin starkly contrasts with the ubiquitous upregulation seen in the mesendoderm, suggesting that PGE_2 regulates E-cadherin by distinct mechanisms that are germ layer-specific. Moreover, PGE_2 can modulate cell adhesion by enhancing Snail protein stability, as well as governing E-cadherin protein through a Snai1a-independent mechanism.

Because Gsk3β is such a prominent target of PGE_2 in the mesendoderm, we hypothesized that PGE_2 may also regulate E-cadherin protein in the ectoderm by inhibiting Gsk3β. GSK3β can phosphorylate cadherin cytoplasmic domains at serine residues to increase interaction with β-catenin (Huber and Weis, 2001; Nelson, 2008). To address this hypothesis experimentally, we inhibited Gsk3β with BIO or overexpressed Gsk3β in *ptges* morphants to determine if the cell

clumping phenotype in the ectoderm could be suppressed or worsened, respectively. However, we found no changes to the cell clumping, suggesting that Gsk3β is not the sole target gene of PGE_2 signaling to modulate cell adhesion. We are continuing these experiments to determine if inhibiting or overexpressing Gsk3β can alter E-cadherin expression in the embryo. However, continued work needs to be done to determine how PGE_2 regulates E-cadherin in the ectoderm. Some studies suggest that cAMP can regulate E-cadherin expression, though differing conclusions about its effects are drawn. In Schwann cells, the activation of PKA by cAMP stabilizes E-cadherin expression, which may occur through potentiation of E-cadherin expression or through decreased degradation (Crawford et al., 2008). However, in intestinal epithelial cells, cAMP decreases E-cadherin expression in adherens junctions through the phosphorylation of a serine residue (Boucher et al., 2005). These data suggest that GPCR activation can regulate cell adhesion through cAMP. Therefore, PGE_2 could regulate E-cadherin protein directly through a cAMP-dependent mechanism. It is still unknown whether Ep4a in zebrafish is coupled to $G\alpha_i$ or $G\alpha_s$. Therefore, current experiments are testing whether $G\alpha_{i/s}$ overexpression can regulate Snai1a expression similarly to $G\beta\gamma$.

We speculate that the variegated expression of E-cadherin in the ectoderm may be caused by artifactual genetic noise or an intrinsic sorting capability of Cadherin-expressing cells. Firstly, there is a considerable amount of fluctuation, or noise, in protein expression in prokaryotic and eukaryotic systems (Raj and van Oudenaarden, 2008). Interestingly, even if two populations of cells have the same mean protein levels, they can vary tremendously in the amount of noise

from cell to cell depending on the coupling of the transcription and translation rates. If one population has a high transcription rate with a low translation rate, there will be small fluctuations in the protein level from cell to cell. If, however, a population has a low transcription rate with a high translation rate, there are larger protein fluctuations that lead to variability in the amount of protein expressed in each cell (Ozbudak et al., 2002; Raj and van Oudenaarden, 2008). Therefore, could increasing E-cadherin translation in the ectoderm through the loss of PGE_2 signaling, coupled to an unchanged level of transcription, result in the "patchy" expression pattern in the ectoderm? That this does not occur in the mesendoderm suggests that this idea is implausible, but perhaps there are permissive conditions in the ectoderm that are not present in the mesendoderm that contribute to this effect. Secondly, and perhaps more tenably, the "patchy" expression of various Cadherins in the mouse and chicken brain results in the sorting of neuronal cell populations, which then leads to functional organization and specialized connectivity based on the molecular signature (Heyers et al., 2003; Hertel et al., 2008). The sorting of cell types based on cell adhesion molecules is not a novel concept and demonstrates the Differential Adhesion Hypothesis (Hayashi and Carthew, 2004; Lecuit and Lenne, 2007). This possibility would imply a role for cadherins in the sorting and specialization of cell populations that may be inhibited by PGE_2 signaling because of the importance of maintaining synchronicity in gastrulating cells. This possibility is especially interesting as it is still unknown how PGE_2 signals in the embryo, and how widely it can travel to exert its signaling effects. To address the signaling "range" of PGE_2 in the gastrula, wild-type cells could be transplanted at the sphere stage into *ptges* morphants expressing Snai1a-YFP. As previously

demonstrated, *ptges* morphant cells will not express Snai1a-YFP unless they are stimulated by PGE_2 secreted from the transplanted wild-type cells. Hence, one would expect to see patches of Snai1a-YFP-expressing cells around transplanted cells that could be quantified to approximate the signaling range of PGE_2. Furthermore, are there extracellular modifiers that degrade or otherwise inhibit PGE_2 and limit the diffusibility of the molecule, as Lft does to Sqt? Or are there factors that stabilize PGE_2 and increase the range of the signal? These experiments would contribute much to the understanding of how lipids signal *in vivo*.

Other inhibitors of E-cadherin

Wnt11/Silberblick (Slb) and Wnt5/Pipetail activate the non-canonical Wnt-Planar Cell Polarity (PCP) signaling pathway during zebrafish convergence and extension movements. *slb* mutant gastrulae prechordal plate cells have decreased cell protrusion alignment, directed movement, and overall cell speed (Ulrich et al., 2003). In addition, Wnt11 helps Rab5c, a regulator of early endocytosis, in the endocytosis and recycling of E-cadherin (Ulrich et al., 2005). Another inhibitor of E-cadherin during gastrulation is P38/Mapk14. The *P38-Interacting Protein* (*P38ip*) mouse mutant shows internalization movement defects during gastrulation because cells cannot downregulate E-cadherin and migrate away from the primitive streak (Zohn et al., 2006). P38IP is required for the activation and function of P38, and together they limit E-cadherin protein expression without affecting *Snail* transcription. Thus, could PGE_2 signaling regulate E-cadherin in ectodermal precursors via P38? PGE_2 signaling activates and phosphorylates P38 in kidney and cardiac cell culture (Jin et al., 2007; Miyatake et al., 2007). In addition, activating P38 function potentiates the

production of prostaglandins (Shoji et al., 2007). In zebrafish, inhibiting P38 with a dominant-negative mutant form results in early cleavage defects on the future dorsal side of the embryo (Fujii et al., 2000). However, we found that inhibiting P38 function by treatment with SB203580 did not result in a cleavage or gastrulation phenotype, even at high doses (C.K. Speirs and L. Solnica-Krezel, unpublished observations). This could mean that either PGE_2 does not function through P38 in this developmental context, or that treatment with SB203580, whereas specific against mouse p38 (Zohn et al., 2006), does not inhibit zebrafish P38. In future experiments, a zebrafish *p38* dominant-negative construct could be employed to downregulate P38 activity to test for an interaction between PGE_2 and P38 (Fujii et al., 2000).

In summary, our studies provide further support that gastrulation cell movements require the dynamic regulation of E-cadherin. The rapid and large-scale movements require coordination between tissues that are becoming increasingly specialized with progressively disparate cell properties and behaviors. The internalization movement, in particular, aptly demonstrates the orchestration that is required to manage this complexity in the gastrula. Internalization at the shield requires the transient downregulation of cell junctions as ingressing cells delaminate from epibolizing neighbors. Then once they reach the deeper mesendodermal progenitor layer, cell junctions are rapidly reestablished so that cells retain their associations with their new neighbors (Montero et al., 2005). Meanwhile, with all of this activity, both cell layers continue to undergo epiboly towards the vegetal pole. Therefore, it will be intriguing to test whether PGE_2 signaling interacts with these known regulators

of E-cadherin during gastrulation to accomplish the rapid changes in E-cadherin expression and/or distribution that are required for cell migration.

Endodermal development

Ptges-deficient embryos show a MO dose-dependent decrease of endodermal cells. Although we did find that Nodal signaling was slightly decreased in these embryos, suggesting that endodermal specification may be affected (see **Cell fate specification**, below), we cannot rule out the possibility that altered cell adhesion may also contribute to these effects. Downregulation of E-cadherin in mouse embryoid bodies does not affect the development of the three germ layers (Rula et al., 2007), but it is difficult to predict the effects of increasing cell adhesion on endodermal specification. Co-injecting *ptges* and *e-cadherin* MOs would determine if the endoderm deficiency phenotype is suppressed. If decreasing cell adhesion in the Ptges-deficient embryos does rescue endodermal formation, the next step would be to determine if the decreased numbers of endodermal cells are due to impaired specification, or if it results from a movement defect, in which cells cannot be specified correctly because they are not in the right environment at the proper time.

Stem cell maintenance

PGE_2 signaling also maintains the **h**ematopoietic **s**tem **c**ell (HSC) population in both developing and adult zebrafish and mice. Although PGE_2 has been proposed to regulate proliferation and survival in stem cells, it is conceivable that PGE_2 could also alter cell adhesion, as it does in other cell types, to influence stem cell development. Indeed, cell adhesion is required for the normal infrastructure of the stem cell niche in Drosophila. The stem cell niche in the Drosophila gonad is composed of a hub of twelve nondividing somatic cells

that are anchored to the surrounding anterior testis tip by attachment to the ECM (Wang et al., 2006). The hub signals to the attached stem cells, regulating their division such that one daughter cell retains germline stem cell qualities while the other is displaced from the hub and undergoes differentiation when it enters spermatogenesis (Van Doren, 2007). Drosophila with mutations in *Gef26*, a PDZ domain **G**uanine nucleotide **E**xchange **F**actor (GEF) for Rap 1, are sterile because of a loss of germline stem cells (Wang et al., 2006). Rap1 is a tumor suppressor GTPase that competes for an effector component of Ras signaling, thereby undermining it. Recent data also suggests that it regulates adherens junctions through a RAP1 GTPase, DOCK4. Indeed, *Gef26* mutants have impaired adherens junctions, and as a result, the germline stem cells move away from the niche and lose their stem cell identity (Wang et al., 2006). This study suggests that adherens junctions maintain the position of germline stem cells within the niche. Other adhesion factors regulate the maintainence and generation of stem cells. Adult Drosophila *mysopheroid*^{XG43} (*mys*^{XG43}) mutants have a mutation in the gene that encodes for the βPS Integrin subunit. Consequently, *mys*^{XG43} mutants have mislocated testis stem cell hubs and misoriented spindle orientation within the hub (Tanentzapf et al., 2007). Integrins are heterodimeric transmembrane receptors composed of α and β subunits that are required for adhesion of the cell to the ECM. *mys*^{XG43} mutants also show the decreased recruitment of ECM components, suggesting that Integrin organizes the ECM for the attachment of the stem cell hub. Depletion of Talin, an Integrin-associated protein, results in a testis with only differentiated sperm and a gradually disappearing hub (Tanentzapf et al., 2007). Together, these results imply that cell adhesion

proteins are essential for the structure and function of the stem cell niche, and that regulating cell adhesion is paramount to the maintenance of the stem cell identity. It is therefore tempting to speculate that PGE_2 signaling may also influence the generation, maintenance, and differentiation of HSCs in vertebrates by modulating cell adhesion in the AGM. However, this possibility remains to be experimentally addressed.

Vascular tube development

As previously discussed, COX inhibition results in posterior vascular tube defects as well as impaired intersomitic vessel development. In particular, the posterior vascular cord forms a vascular tube that becomes the **d**orsal **a**orta (DA) and **p**osterior **c**ardinal **v**ein (PCV). In the absence of prostaglandin synthesis from the 24-26 somite stages, the vascular cord does not lumenize to form a tube, and retains only arterial markers. PGE_2 could suppress this phenotype, but how it regulates vascular tube development remains unclear. A recent study showed that many cadherin family members are upregulated in the ferret brain during the peak of vascular development, suggesting that cadherins may regulate angiogenesis (Krishna and Redies, 2009). Cell junctions are assembled in the vascular tube of zebrafish starting at 17 hpf, which is shortly before Cox1 function is required in the vascular tube (Cha et al., 2005). The downregulation of VE-cadherin, one of the major cadherins in endothelial cells, in zebrafish embryos results in hemorrhages of the cranial vasculature and some trunk vasculature (Montero-Balaguer et al., 2009). In addition, VE-cadherin appears to be important in the development of the lumen during vascular development in zebrafish, so PGE_2 may modulate cell adhesion during vascular development as well as gastrulation (Montero-Balaguer et al., 2009). These data suggest that

major remodeling of the vasculature occurs during its development in part because of the dynamic turnover of cell adhesion. Therefore, it would be worthwhile to determine whether markers of cell adhesion fluctuate in the DA and PCV with the loss of prostaglandin signaling. Indeed, the adhesion complexes in endothelial cells resemble epithelial cells with conservation of many of the same components (Baldessari and Mione, 2008), so it is possible that PGE_2 regulates both cancer cell and endothelial cell adhesion.

Proliferation/Survival

Apoptosis

As previously mentioned, PGE_2 signaling has been implicated in the proliferation and survival of cells in multiple contexts. Human colon cancer cells show increased apoptosis when treated with SC-58125, a COX2 inhibitor. The increased apoptotic cell death is reversed with PGE_2 treatment, suggesting that PGE_2 promotes cell survival (Sheng et al., 1998). Increased apoptosis in SC-58125-treated cells is accompanied by elevated levels of BCL-2, which is an anti-apoptotic factor that affects **m**itochondrial **o**uter **m**embrane **p**ermeabilization (MOMP). CASPASE3/CASP3 is one of the terminal effectors of apoptosis, and its elevated expression is reversed by PGE_2 treatment in a rat model of **P**uromycin **A**minonucleoside **N**ephrosis (PAN) in rat glomerular epithelial cell culture, an effect that was mediated by cAMP (Aoudjit et al., 2006). Levels of the apoptotic factor BAX are increased and of the anti-apoptotic factor BCL-XL are decreased in PAN-induced glomerular epithelial cells. These molecular changes, which are characteristic of increased apoptosis, are also be suppressed with PGE_2 treatment (Aoudjit et al., 2006).

Anoikis

Normal cells are anchorage-dependent and undergo anoikis, a type of apoptosis that is induced when cells become detached from the ECM. Interactions between integrin and the ECM result in the activation of pro-survival pathways such as ERK, JNK, and AKT, as well as the inhibition of pro-apoptotic proteins (Chiarugi and Giannoni, 2008). Therefore, the loss of this pro-survival signal initiates the extrinsic and intrinsic apoptotic pathways (Chiarugi and Giannoni, 2008). Transfection of the EP4 receptor into colon cancer cells results in anchorage independence and evasion of anoikis (Chell et al., 2006). As the effector pathways of anoikis are the same as those in other apoptotic cells, PGE_2 likely promotes survival in these cells through the mechanisms described above.

Cell proliferation

The induction of COX2 with Ponasterone A in GECs increases the incorporation of BrDU and ^{3}H-thymidine (Aoudjit et al., 2006). The activation of cell proliferation by PGE_2 potentially occurs through an EP4-PIK3-ERK-EGR-1 signaling axis, as EGR-1 activates *Cyclin D1*, a cell cycle regulator, in **c**hinese **h**amster **o**vary (CHO) cells (Guillemot et al., 2001; Fujino et al., 2003; Shao et al., 2005).

Does PGE_2 also regulate cell proliferation during development? An intriguing study has linked cell cycle, apoptosis, and the gastrulation movements in zebrafish (Liu et al., 2009). Cdt1 is a DNA replication initiation factor that activates DNA synthesis, and can be antagonized by binding to Geminin/Gmnn. *gmnn* morphants are shorter than control embryos, and transplanted *gmnn* morphant shield cells into wild-type hosts exhibit impaired migration to the

animal pole, suggesting that Gmnn is required cell autonomously in the anterior mesendodermal progenitors for gastrulation movements (Liu et al., 2009). *gmnn* morphants also have increased H3P-expressing cells, suggesting increased mitotic activity. By contrast, apoptosis in Gmnn-deficient embryos is decreased. These effects are reversed in embryos that misexpress Gmnn, which have fewer mitotically active cells than the control morphants, and more apoptotic cells. Interestingly, expression of Nf-κb/Nfkb, an antiapoptotic factor that activates the Bcl-2 antiapoptotic genes, is correlated to the incidence of apoptosis in the embryo. Correspondingly, Gmnn-deficient embryos show decreased Nf-κb expression. Nf-κb can bind the *snai1a* promoter to activate transcription and possibly regulate gastrulation movements, which may contribute to the gastrulation defects in *gmnn* morphants. Interestingly, *gmnn* morphants show decreased **C**hloramphenicol **A**cetyl**t**ransferase (CAT) activity when injected with a CAT construct driven by the *snai1a* promoter. The effects of Gmnn on Snai1a may contribute to the defective mesendodermal delamination and endodermal migration in Gmnn-deficient embryos. In particular, the authors argue that Gmnn and Cdt1 form a critical balance that determines the cell cycle in the zebrafish gastrula, and that this balance affects genes that regulate gastrulation movements (Liu et al., 2009). Therefore, it is tempting to hypothesize that PGE_2 participates at this tipping point by regulating cell movement, proliferation, and apoptosis simultaneously during gastrulation. However, testing this hypothesis requires assaying the proliferation and apoptosis in Ptges-deficient gastrulae. SNAI1 represses *CYCLIN D1* expression in cell culture (Vega et al., 2004), so if PGE_2 signaling does enhance cell proliferation during development, it likely

occurs through a Snail–independent mechanism.

Cell fate specification

Ptges-deficient embryos show a MO dose-dependent decrease of endodermal cell numbers. We found that Nodal signaling was slightly decreased in these embryos. As endodermal cells require the highest levels of Nodal signaling to become specified (Peyrieras et al., 1998; Grapin-Botton and Constam, 2007), it is possible that this diminution of the Nodal signaling strength ultimately results in the loss of endodermal specification. To address the possibility of PGE_2 regulating Nodal signaling, we will investigate other Nodal genes such as *cyc* and *sqt*, to determine if the ligands are decreased or if signaling itself cannot be efficiently maintained in *ptges* morphants. In addition, we will overexpress Cyc in the *ptges* morphants to attempt to suppress the endoderm defect phenotype.

We confirmed the loss of endodermal cells in Ptges-deficient embryos with the markers *casanova* and *sox17*. We interpret the reduced expression of both genes, which was already detectable by the shield stage, to mean that PGE_2 affects endodermal specification at or before this time in development. In addition, Cas induces endodermal differentiation by activating *sox17* transcription. *cas* expression is first detected at the high stage, and future experiments will need to address when *cas* expression is first affected in *ptges* morphants. We will also investigate other endodermal markers downstream of Nodal signaling that function to activate Cas, such as *gata5*, *bon*, and *mezzo/og9x*, to investigate the possibility that PGE_2 affects genes downstream of Nodal signaling to promote endodermal specification. The regulation of Nodal

signaling or endodermal development by PGE_2 is a completely novel concept in any cellular context, and therefore, testing these possibilities would make an exciting and promising future project.

Interaction with other signaling pathways

EGF

PGE_2 signaling has been shown to interact with other signaling pathways, including EGF, Hedgehog, and Wnt signaling (**Fig. 5-3**). In addition to the examples mentioned earlier, **E**pidermal **G**rowth **F**actor **R**eceptor (EGFR) signaling activates *SNAI1* to repress *15-PGDH* transcription in colorectal cancer cells, resulting in the increased stability of PGE_2 (Mann et al., 2006). EGFR autocrine signaling results in COX2 and PGE_2 upregulation and is important for the downstream transformation of cells through a Ras-dependent mechanism (Repasky et al., 2007). In addition, the combination of an EGFR blocker and a COX2 inhibitor decreases colorectal cancer cell motility (Banu et al., 2007). These results suggest that EGF signaling may not only function in PGE_2 signal transduction, but may also activate and stabilize PGE_2 synthesis.

Wnt-β-catenin

There are many reports in the literature about the interaction of PGE_2 with the Wnt-β-catenin pathway (**Fig. 5-3**). Mutations in the **A**denomatous **P**olyposis **C**oli (APC) gene are associated with a confluence of intestinal tumors in 100% of human carriers due to the loss of heterozygosity, resulting in the disease **F**amilial **A**denomatous **P**olyposis (FAP) (Moser et al., 1990; Su et al., 1992). There are multiple mouse models of FAP. The most common is the Apc^{min}, or the $Apc^{\Delta 850}$,

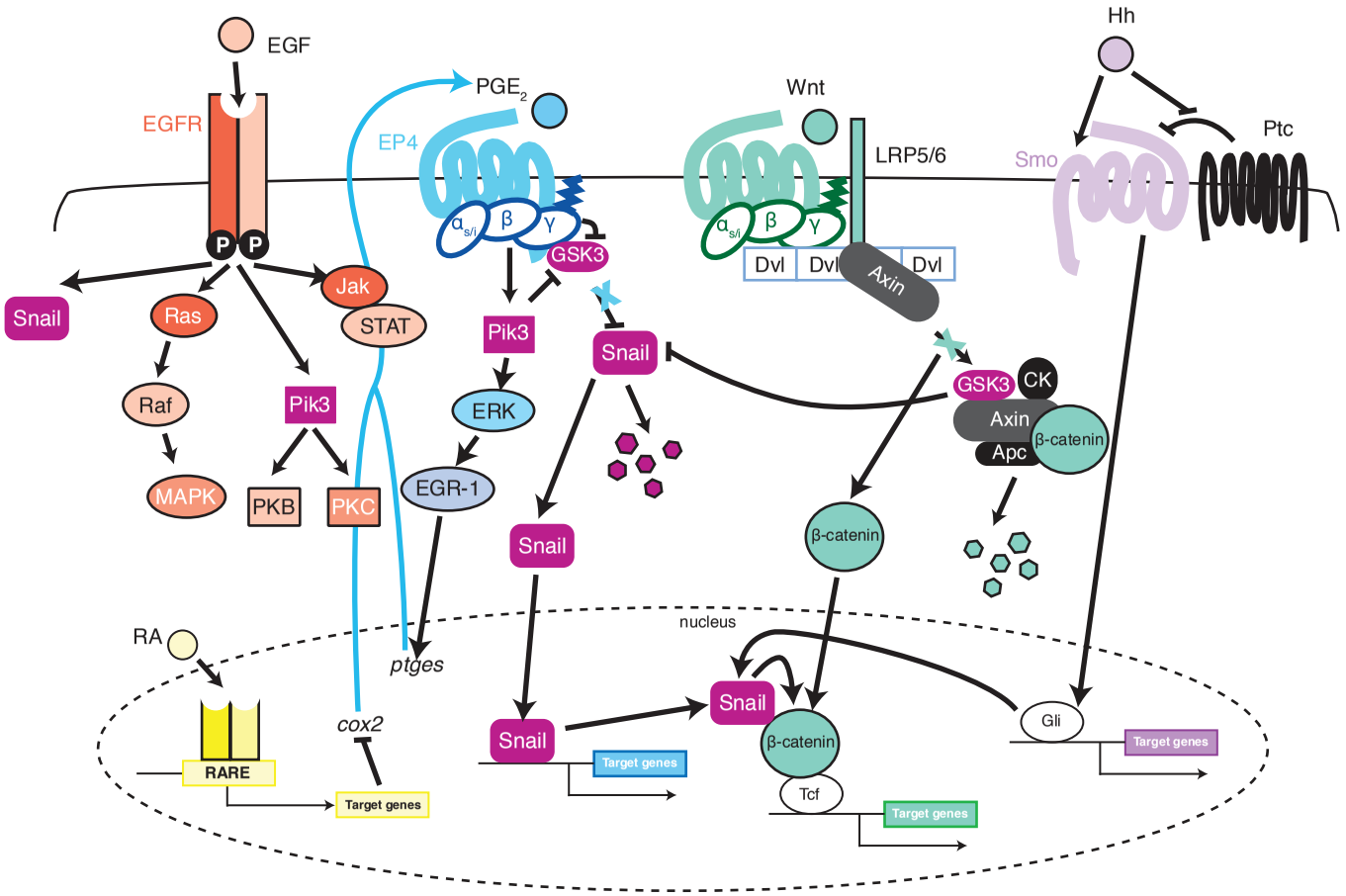

Figure 5-3. PGE_2 signaling impinges on many other conserved signaling pathways in the cell. This schematic is representative of a portion of the interactions that have been described between PGE_2 and the EGF, Wnt, Hh, and RA signaling pathways. Genes that are conserved from one pathway to another are noted (pink).

mouse, which is a result of chemical carcinogenesis (Moser et al., 1990; Su et al., 1992). There are also two homologous recombination mutants, the *Apc*$^{\Delta 716}$ and the *Apc*$^{\Delta 1368}$ mutants (Oshima et al., 1995; Oshima et al., 2001). Mice homozygous for the disrupted alleles are embryonic lethal, however the heterozygous mice are models for FAP. The *Apc*$^{\Delta 716}$ mice show increased expression of the EP2 and EP4 receptors. Notably, they have a 7-fold reduction in intestinal polyposis when treated with a COX2 inhibitor. In addition, *Apc*$^{\Delta 716}$;*Cox2* transheterozygotes also show decreased intestinal polyposis, suggesting that PGE_2 and Wnt signaling functionally converge during tumorigenesis (Oshima et al., 2001). PGE_2 treatment of **h**uman **e**mbryonic **k**idney (HEK) cells transfected with the EP2 and EP4 receptors increases Tcf/Lef-responsive luciferase expression, a transcriptional output of β-catenin activation (Fujino et al., 2002). In addition, the GSK3α phosphorylation (**Table 1-1**) increases following PGE_2 treatment, though phosphorylation of GSK3β remains unchanged. Phosphorylation and inhibition of GSK3α decreases the degradation of β-catenin by the proteasome, suggesting that PGE_2 stabilizes β-catenin. Inhibition of PIK3 with Wortmannin abolishes GSK3α phosphorylation and reverses activation of Tcf/Lef signaling, which implies that PGE_2 signaling regulates GSK3α in this context via PIK3 (Fujino et al., 2002). These effects are also seen in PGE_2-treated colon cancer cells, in addition to the decreased phosphorylation and increased nuclear localization of β-catenin (Castellone et al., 2005). The EP2 G protein $G_{\alpha s}$ was reported to interact with Axin through its **R**egulator of **G**-protein **S**ignaling (RGS) domain, which displaces GSK3β from its binding site with Axin, and thus stabilizes β-catenin. Indeed, the binding domain in Axin for GSK3β is required to enhance TOP/FOP

reporter expression, suggesting that PGE_2 needs GSK3β to potentiate Wnt signaling. The activation of these pathways displaces GSK3β from the β-catenin degradation complex and stabilizes β-catenin, allowing it to exert its effects on TCF and LEF gene expression and ultimately, cell growth (Castellone et al., 2005). In addition, VEGF transcript and protein, as well as CYCLIN D1 protein, were increased in colon cancer cells following PGE_2 stimulation (Shao et al., 2005). CYCLIN D1 and VEGF were also induced following the PGE_2 treatment of *Apc*^{min} mice. These results show that PGE_2 and Wnt signaling converge on cell cycle and apoptotic factors to promote cell growth and survival. However, other signaling pathways may also affect the interactions between PGE_2 and Wnt signaling, complicating the cellular signaling networks involved. For example, studies in colon cancer cell line and zebrafish show that Retinoic Acid antagonizes the stabilization of β-catenin by PGE_2 by modulating COX2 levels (Eisinger et al., 2006) (**Fig. 5-3**). These studies suggest that PGE_2 and Wnt are oncogenic signaling pathways that must be tightly controlled to prevent the initiation and spread of cancer, possibly in part through inhibiting GSK3β and, by extension, activating Snail function.

Our data show that inhibition of Gsk3β function occurs downstream of PGE_2 GPCR activation. As previously mentioned, Snail is negatively regulated by GSK3β. Since Wnt signaling inhibits the function of GSK3β in targeting β-catenin to the proteasome, so it protects SNAI1 from GSK3β-mediated phosphorylation, stabilizing SNAI1 levels in the embryo (Yook et al., 2005). Furthermore, activation of the β-catenin/TCF signaling cascade in transfected MCF cell lines induces *Axin2* expression. AXIN2 then acts as a chaperone for

GSK3β, exporting it from the nucleus, thereby stabilizing SNAI1 (Yook et al., 2006). In addition, SNAI1 can directly interact with β-catenin to enhance the expression of Wnt target genes in human embryonic kidney 293T cells (Stemmer et al., 2008). Therefore, our data suggests that PGE_2 signaling activates Wnt-β-catenin by inhibiting Gsk3β, a notion that has powerful implications for the understanding of how and when these signals function during development, as well as how to treat the disease processes that are influenced by these signaling mediators.

We show in transfected cells that Gsk3β can be detected in immunoprecipitates that were purified from cultured mammalian cells by antibodies against tagged $G\beta_1\gamma_2$. Additionally, this effect could be abolished by β-ark transfection, arguing that binding of these components is specific. Direct interaction of Gβγ with GSK3β is also suggested by studies in the frog and cell culture that show that $G\beta_1\gamma_2$ can be pulled down by purified MBP-GSK3 protein (Jernigan and Lee). Furthermore, the authors suggest that in their experiments, Gβγ recruits GSK3β to the membrane, which activates its phosphorylation of LRP6 to ultimately inhibit β-catenin activity (Jernigan and Lee).

We have yet to determine the precise mechanism by which Ep Gβγ inhibits Gsk3β function through its association. Sequestering Gsk3β to the membrane by interaction with the βγ subunits may keep it from inhibiting Snai1a in the nucleus (Jernigan and Lee, ; Yook et al., 2005; Yook et al., 2006). To address this possibility, we have used two GSK3β antibodies to address whether membrane localization is increased in *ptges* morphants. Although some preliminary results show that there is a change in the membrane:cytoplasm

localization of total and phosphorylated Gsk3β (data not shown), these results were not consistent with both antibodies, so future experiments will need to be done to confirm these findings. Another possibility is that Gsk3β is phosphorylated and silenced at the Ser9 position, which occurs through PIK3-mediated phosphorylation in cell lines (Cohen and Frame, 2001). As *ep4* morphants had decreased Pik3/Akt activity, we hypothesized that Gsk3β phosphorylation is decreased in *ptges* morphants, which would lead to increased Gsk3β function, particularly in the inhibtion of Snai1. We have tested the phosphorylation of Gsk3β, but do not find that *ptges* morphants have changes in the levels of phosphorylated Gsk3β in zebrafish gastrulae. We have also performed immunoblotting with Gsk3α in control and *ptges* morphant gastrulae, but could not detect Gsk3α during gastrulation, suggesting that Gsk3α may not be expressed during this phase of development. Moreover, our results indicate that Pik3 likely does not regulate Snai1 protein during gastrulation. Therefore, more work remains to be done to determine the manner in which PGE_2 inhibits Gsk3β function, as this would shed more light on the mechanism by which PGE_2 restricts E-cadherin and cell adhesion to consequently promote gastrulation movements. Furthermore, interaction between the Gβγ subunits and GSK3β has never been described previously, and therefore, this interaction also reveals how GPCR effector subunits can directly influence signaling components without using second messengers.

Our results also suggest a possible function for PGE_2 during **m**icro**t**ubule (MT) assembly. In cell culture, GSK3β phosphorylates **c**ytoplasmic **l**inker-**as**sociated **p**roteins (CLASPs), which link lamella MT to adhesion sites. CLASPs

may function to polarize cell migration, as they are enriched in the cell cortex towards the direction of migration (Kumar et al., 2009). When phosphorylated by GSK3β, CLASP function is repressed, which may have subsequent effects on cell migration. Indeed, expression of GSK3β in cell culture results in cells that move more slowly and have a less dense network of lamellar MTs (Kumar et al., 2009). Phosphorylation-resistant CLASP2 mutants were rendered insensitive to the effects of GSK3β on the lamellar MT network and cell migration. This data suggests that the function of GSK3β contributes to turnover of the microtubule network and may have implications for the regulation of cell motility by PGE_2 signaling. Therefore, it would be interesting to analyze the dynamics of the microtubule network in the cells of Ptges-deficient embryos. What also remains to be determined are the possible developmental functions of PGE_2 and Wnt signaling interaction, and how Wnt and PGE_2 signaling might be regulated temporally and spatially during development to optimize their interaction.

Wnt signaling may also converge with PGE_2 signaling later in development, during HSC generation and maintenance. Overexpression of β-catenin in murine HSC culture results in the expansion of the HSC population, as well as the activated expression of *HoxB4* and *Notch*, which enhance the self-renewal and proliferation of HSCs, respectively (Reya et al., 2003). Inhibition of Wnt signaling in the HSC culture with Axin decreases growth of the HSC cell population and curtails reconsititution of the HSCs in irradiated mice (Reya et al., 2003). Inhibition of GSK3 using CHIR-911 increases the HSC population in mouse and human cells (Trowbridge et al., 2006). In the intestinal epithelium, where the crypts represent an adult stem cell niche, the inducible loss of β-

catenin in adult mice results in the loss of stem cell markers and the terminal differentiation of crypt cells (Fevr et al., 2007). The terminal differentiation of intestinal cells blocks intestinal function because of increased Caspase-3-dependent apoptosis, which eventually leads to the death of mutants 6 days following the induced loss of β-catenin (Fevr et al., 2007). Additionally, Wnt10b is upregulated in regenerating HSCs within the bone marrow following injury, suggesting that Wnt-β-catenin signaling supports HSC generation and renewal in adult animals (Congdon et al., 2008). These effects of β-catenin may be conveyed by TCF3, as its expression is seen in proliferating, unspecified embryonic progenitors in the mouse epidermis and is lost in differentiated skin cells (Nguyen et al., 2006). These results show the enormous importance of Wnt signaling in the proliferation and maintenance of stem cells in the adult animal.

PGE_2 inhibition with Indomethacin in zebrafish embryos results in decreased TOP:dGFP expression in the AGM, where HSCs are generated (Goessling et al., 2009). Indeed, Indomethacin treatment decreases numbers of HSCs while increasing TUNEL-positive cells, an index of apoptosis. Indomethacin also reverses the increased cell proliferation that occurrs with Wnt8 misexpression in zebrafish embryos, suggesting that PGE_2 supports HSC proliferation in the zebrafish through interaction with the Wnt signaling pathway. Potentiation of Wnt activity by PGE_2 signaling in this process is mediated by cAMP, and results in the enhanced repopulation of HSCs in irradiated zebrafish and mice. Lastly, liver regeneration is enhanced in $Apc^{+/-}$ mutants, however, this effect is abolished by treating $Apc^{+/-}$ zebrafish with Indomethacin (Goessling et al., 2009). Decreased regeneration with

Indomethacin is accompanied by decreased Cyclin D1/Ccnd1 expression in the liver. This study demonstrated that the Wnt and PGE_2 signaling pathways cooperate in the generation and function of HSCs in vertebrates.

We are interested in applying these findings to our work on zebrafish gastrulation to determine whether PGE_2 activates Wnt-β-catenin during gastrulation, similarly to HSC development and maintenance. To address this question, we are currently analyzing the effects of the loss of PGE2 synthesis on β-catenin in gastrulation. We have analyzed α- and β-catenin immunohistochemistry in 60% epiboly gastrula that are injected with control or *ptges* MO, but found no significant changes in protein localization. However, these results are preliminary and need to be repeated. In addition, we are analyzing the nuclear localization of β-catenin in *ptges* morphants at the sphere stage to determine if Wnt-β-catenin is affected by the loss of Ptges before the commencement of gastrulation. We are also analyzing control and *ptges* morphants for the expression of Wnt-β-catenin downstream targets, including *boz*, *gsc*, and *nkd1*. Lastly, it would be interesting to test whether *ptges* morphants and mutants that show decreased β-catenin function, such as *ichabod*, demonstrate genetic interactions. Or we could determine whether *ptges* morphants are more or less sensitive to β-catenin-mediated axis duplication. The results of these current and upcoming experiments will determine if there is functional interaction between PGE_2 and Wnt signaling during early zebrafish embryogenesis.

Hedgehog

SNAI1 is also induced downstream of GLI, the effectors of Hedgehog (Hh)

signaling, in **B**asal **C**ell **C**arcinoma (BCC) and **N**euro**e**ndocrine **T**umor (NET) ileum cell culture (Li et al., 2006; Fendrich et al., 2007; Li et al., 2007) (**Fig. 5-3**). In skin cancer cell lines, GLI function activates β-catenin signaling by inducing SNAI1, which in turn decreases E-cadherin transcript (Li et al., 2007). This diminution of E-cadherin expression decreases the amount of β-catenin binding in the adherens junctions, allowing its relocalization to the nucleus. Indeed, *Gli1*-transgenic mice show higher levels of active, unphosphorylated β-catenin. Therefore, PGE_2 signaling and Hh signaling could synergistically activate Wnt-β-catenin by converging on Snail during development.

Perspective

The body of literature suggests that PGE_2 signaling regulates morphogenesis, survival, and tumorigenesis in vertebrates. These effects occur through multiple mechanisms, and reveal the growing importance of lipid signaling in the regulation of cell adhesion, motility, and survival. Are there qualities of lipid signaling that make lipid mediators favorable for these roles, particularly to promote the gastrulation movements? Lipids are widespread, quickly generated, short acting, and generally signal through autocrine or paracrine mechanisms (Wymann and Schneiter, 2008). Both PGE_2 and S1P and their GPCRs have been implicated in regulating cell motility during gastrulation, though they have contradictory effects. In addition, studies in medaka have uncovered the importance of membrane microdomains enriched in glycolipids and glycoproteins for the normal gastrulation movements, as chemical disruption of these microdomains resulted in epiboly defects that could be

suppressed by cholesterol treatment (Adachi et al., 2007). These membrane microdomains were found to contain localized E-cadherin, cSrc, β-catenin, and Plcγ, suggesting that these microdomains serve as a platform for both cell adhesion and signaling (Adachi et al., 2009). Therefore, lipids regulate gastrulation movements as structural and signaling components, but much work needs to be done before their role is fully elucidated.

Our work has contributed to the understanding of how a secreted molecule such as PGE_2 regulates multiple movements during zebrafish gastrulation. PGE_2 signaling promotes cell motility and survival, and inhibits cell adhesion in cancer cells, and our results suggest that it also regulates gastrulation movements through an assortment of mechanisms. PGE_2 modulates cell adhesion by regulating adherens and tight junction proteins in the ectoderm. In the mesendoderm, the loss of PGE_2 synthesis results in the global upregulation of E-cadherin due to decreased Snail function. PGE_2 signaling stabilizes Snail by inhibiting Gsk3β through interaction with EP receptor Gβγ subunits. In addition, loss of PGE_2 synthesis increases bleb formation in cells of the anterior mesendoderm, which may hamper mesenchymal cell motility. We also show that the inhibition of PGE_2 synthesis impairs endodermal development, possibly by interactions between PGE_2 and Nodal signaling. Lastly, we present preliminary characterization of a TILLING *ep4a* nonsense mutation that may reveal redundant *ep4* genes in zebrafish gastrulae. Our data contributes to a better understanding of the many faces of PGE_2, but it also is a reminder of how little we know about lipid biology during development. How far does the PGE_2 signal travel? How does a ubiquitously expressed lipid have such diverse, cell

type-specific effects in the embryo? Why are endodermal cells so sensitive to the loss of PGE_2? These remaining questions reveal exciting new directions for future studies of lipid signaling in cell fate specification and movements during vertebrate gastrulation.

REFERENCES

Abdelilah, S., Solnica-Krezel, L., Stainier, D. Y. and Driever, W. (1994). Implications for dorsoventral axis determination from the zebrafish mutation janus. *Nature* **370**, 468-71.

Adachi, T., Sato, C., Kishi, Y., Totani, K., Murata, T., Usui, T. and Kitajima, K. (2009). Membrane microdomains from early gastrula embryos of medaka, Oryzias latipes, are a platform of E-cadherin- and carbohydrate-mediated cell-cell interactions during epiboly. *Glycoconj J* **26**, 285-99.

Adachi, T., Sato, C. and Kitajima, K. (2007). Membrane microdomain formation is crucial in epiboly during gastrulation of medaka. *Biochem Biophys Res Commun* **358**, 848-53.

Alexander, J. and Stainier, D. Y. (1999). A molecular pathway leading to endoderm formation in zebrafish. *Curr Biol* **9**, 1147-57.

Amatruda, J. F. and Zon, L. I. (1999). Dissecting hematopoiesis and disease using the zebrafish. *Dev Biol* **216**, 1-15.

Amsterdam, A. and Hopkins, N. (2006). Mutagenesis strategies in zebrafish for identifying genes involved in development and disease. *Trends Genet* **22**, 473-8.

Anderson, G. J. and Darshan, D. (2008). Small-molecule dissection of BMP signaling. *Nat Chem Biol* **4**, 15-6.

Aoki, T. O., Mathieu, J., Saint-Etienne, L., Rebagliati, M. R., Peyrieras, N. and Rosa, F. M. (2002). Regulation of nodal signalling and mesendoderm formation by TARAM-A, a TGFbeta-related type I receptor. *Dev Biol* **241**, 273-88.

Aoudjit, L., Potapov, A. and Takano, T. (2006). Prostaglandin E2 promotes cell survival of glomerular epithelial cells via the EP4 receptor. *Am J Physiol Renal Physiol*.

Babb, S. G. and Marrs, J. A. (2004). E-cadherin regulates cell movements and tissue formation in early zebrafish embryos. *Dev Dyn* **230**, 263-77.

Backlund, M. G., Mann, J. R. and Dubois, R. N. (2005). Mechanisms for the prevention of gastrointestinal cancer: the role of prostaglandin E2. *Oncology* **69 Suppl 1**, 28-32.

Backlund, M. G., Mann, J. R., Holla, V. R., Shi, Q., Daikoku, T., Dey, S. K. and DuBois, R. N. (2008). Repression of 15-hydroxyprostaglandin dehydrogenase involves histone deacetylase 2 and snail in colorectal cancer. *Cancer Res* **68**, 9331-7.

Bahary, N. and Zon, L. I. (1998). Use of the zebrafish (Danio rerio) to define hematopoiesis. *Stem Cells* **16**, 89-98.

Baldessari, D. and Mione, M. (2008). How to create the vascular tree? (Latest) help from the zebrafish. *Pharmacol Ther* **118**, 206-30.

Banu, N., Buda, A., Chell, S., Elder, D., Moorghen, M., Paraskeva, C., Qualtrough, D. and Pignatelli, M. (2007). Inhibition of COX-2 with NS-398 decreases colon cancer cell motility through blocking epidermal growth factor receptor transactivation: possibilities for combination therapy. *Cell Prolif* **40**, 768-79.

Barrallo-Gimeno, A. and Nieto, M. A. (2005). The Snail genes as inducers of cell movement and survival: implications in development and cancer. *Development* **132**, 3151-61.

Bellipanni, G., Varga, M., Maegawa, S., Imai, Y., Kelly, C., Myers, A. P., Chu, F., Talbot, W. S. and Weinberg, E. S. (2006). Essential and opposing roles of zebrafish beta-catenins in the formation of dorsal axial structures and neurectoderm. *Development* **133**, 1299-309.

Bischof, J. and Driever, W. (2004). Regulation of hhex expression in the yolk syncytial layer, the potential Nieuwkoop center homolog in zebrafish. *Dev Biol* **276**, 552-62.

Blader, P., Rastegar, S., Fischer, N. and Strahle, U. (1997). Cleavage of the BMP-4 antagonist chordin by zebrafish tolloid. *Science* **278**, 1937-40.

Blanco, M. J., Barrallo-Gimeno, A., Acloque, H., Reyes, A. E., Tada, M., Allende, M. L., Mayor, R. and Nieto, M. A. (2007). Snail1a and Snail1b cooperate in the anterior migration of the axial mesendoderm in the zebrafish embryo. *Development* **134**, 4073-81.

Blaser, H., Eisenbeiss, S., Neumann, M., Reichman-Fried, M., Thisse, B., Thisse, C. and Raz, E. (2005). Transition from non-motile behaviour to directed migration during early PGC development in zebrafish. *J Cell Sci* **118**, 4027-38.

Boucher, M. J., Laprise, P. and Rivard, N. (2005). Cyclic AMP-dependent protein kinase A negatively modulates adherens junction integrity and differentiation of intestinal epithelial cells. *J Cell Physiol* **202**, 178-90.

Braun, M. M., Etheridge, A., Bernard, A., Robertson, C. P. and Roelink, H. (2003). Wnt signaling is required at distinct stages of development for the induction of the posterior forebrain. *Development* **130**, 5579-87.

Brouxhon, S., Kyrkanides, S., O'Banion, M. K., Johnson, R., Pearce, D. A., Centola, G. M., Miller, J. N., McGrath, K. H., Erdle, B., Scott, G., Schneider, S., VanBuskirk, J. and Pentland, A. P. (2007). Sequential down-regulation of E-cadherin with squamous cell carcinoma progression: loss of E-cadherin via a prostaglandin E2-EP2 dependent posttranslational mechanism. *Cancer Res* **67**, 7654-64.

Buchanan, F. G. and Dubois, R. N. (2006). Connecting COX-2 and Wnt in cancer. *Cancer Cell* **9**, 6-8.

Buchanan, F. G., Gorden, D. L., Matta, P., Shi, Q., Matrisian, L. M. and Dubois, R. N. (2006). Role of {beta}-arrestin 1 in the metastatic progression of colorectal cancer. *Proc Natl Acad Sci U S A*.

Buchanan, F. G., Gorden, D. L., Matta, P., Shi, Q., Matrisian, L. M. and DuBois, R. N. (2006). Role of beta-arrestin 1 in the metastatic progression of colorectal cancer. *Proc Natl Acad Sci U S A* **103**, 1492-7.

Caneparo, L., Huang, Y. L., Staudt, N., Tada, M., Ahrendt, R., Kazanskaya, O., Niehrs, C. and Houart, C. (2007). Dickkopf-1 regulates gastrulation movements by coordinated modulation of Wnt/beta catenin and Wnt/PCP activities, through interaction with the Dally-like homolog Knypek. *Genes Dev* **21**, 465-80.

Carmany-Rampey, A. and Schier, A. F. (2001). Single-cell internalization during zebrafish gastrulation. *Curr Biol* **11**, 1261-5.

Carver, E. A., Jiang, R., Lan, Y., Oram, K. F. and Gridley, T. (2001). The mouse snail gene encodes a key regulator of the epithelial-mesenchymal transition. *Mol Cell Biol* **21**, 8184-8.

Castellone, M. D., Teramoto, H., Williams, B. O., Druey, K. M. and Gutkind, J. S. (2005). Prostaglandin E2 promotes colon cancer cell growth through a Gs-axin-beta-catenin signaling axis. *Science* **310**, 1504-10.

Cha, Y. I., Kim, S. H., Sepich, D., Buchanan, F. G., Solnica-Krezel, L. and Dubois, R. N. (2006). Cyclooxygenase-1-derived PGE2 promotes cell motility via the G-protein-coupled EP4 receptor during vertebrate gastrulation. *Genes Dev* **20**, 77-86.

Cha, Y. I., Kim, S. H., Solnica-Krezel, L. and Dubois, R. N. (2005). Cyclooxygenase-1 signaling is required for vascular tube formation during development. *Dev Biol* **282**, 274-83.

Cha, Y. I., Solnica-Krezel, L. and Dubois, R. N. (2006). Fishing for prostanoids: Deciphering the developmental functions of cyclooxygenase-derived prostaglandins. *Dev Biol* **289**, 263-72.

Chaw, R. C., Vance, E. and Black, S. D. (2007). Gastrulation in the spider Zygiella x-notata involves three distinct phases of cell internalization. *Dev Dyn* **236**, 3484-95.

Chell, S. D., Witherden, I. R., Dobson, R. R., Moorghen, M., Herman, A. A., Qualtrough, D., Williams, A. C. and Paraskeva, C. (2006). Increased EP4 receptor expression in colorectal cancer progression promotes cell growth and anchorage independence. *Cancer Res* **66**, 3106-13.

Chen, Y. and Schier, A. F. (2001). The zebrafish Nodal signal Squint functions as a morphogen. *Nature* **411**, 607-10.

Chen, Y. and Schier, A. F. (2002). Lefty proteins are long-range inhibitors of squint-mediated nodal signaling. *Curr Biol* **12**, 2124-8.

Cheng, A. M., Thisse, B., Thisse, C. and Wright, C. V. (2000). The lefty-related factor Xatv acts as a feedback inhibitor of nodal signaling in mesoderm induction and L-R axis development in xenopus. *Development* **127**, 1049-61.

Chiarugi, P. and Giannoni, E. (2008). Anoikis: a necessary death program for anchorage-dependent cells. *Biochem Pharmacol* **76**, 1352-64.

Clements, D. and Woodland, H. R. (2000). Changes in embryonic cell fate produced by expression of an endodermal transcription factor, Xsox17. *Mech Dev* **99**, 65-70.

Cohen, P. and Frame, S. (2001). The renaissance of GSK3. *Nat Rev Mol Cell Biol* **2**, 769-76.

Congdon, K. L., Voermans, C., Ferguson, E. C., DiMascio, L. N., Uqoezwa, M., Zhao, C. and Reya, T. (2008). Activation of Wnt signaling in hematopoietic regeneration. *Stem Cells* **26**, 1202-10.

Corey, D. R. and Abrams, J. M. (2001). Morpholino antisense oligonucleotides: tools for investigating vertebrate development. *Genome Biol* **2**, REVIEWS1015.

Crawford, A. T., Desai, D., Gokina, P., Basak, S. and Kim, H. A. (2008). E-cadherin expression in postnatal Schwann cells is regulated by the cAMP-dependent protein kinase a pathway. *Glia* **56**, 1637-47.

Cserzo, M., Wallin, E., Simon, I., von Heijne, G. and Elofsson, A. (1997). Prediction of transmembrane alpha-helices in prokaryotic membrane proteins: the dense alignment surface method. *Protein Eng* **10**, 673-6.

Davison, J. M., Akitake, C. M., Goll, M. G., Rhee, J. M., Gosse, N., Baier, H., Halpern, M. E., Leach, S. D. and Parsons, M. J. (2007). Transactivation from Gal4-VP16 transgenic insertions for tissue-specific cell labeling and ablation in zebrafish. *Dev Biol* **304**, 811-24.

Dick, A., Hild, M., Bauer, H., Imai, Y., Maifeld, H., Schier, A. F., Talbot, W. S., Bouwmeester, T. and Hammerschmidt, M. (2000). Essential role of Bmp7 (snailhouse) and its prodomain in dorsoventral patterning of the zebrafish embryo. *Development* **127**, 343-54.

Dickinson, K., Leonard, J. and Baker, J. C. (2006). Genomic profiling of mixer and Sox17beta targets during Xenopus endoderm development. *Dev Dyn* **235**, 368-81.

Dinchuk, J. E., Car, B. D., Focht, R. J., Johnston, J. J., Jaffee, B. D., Covington, M. B., Contel, N. R., Eng, V. M., Collins, R. J., Czerniak, P. M. and et al. (1995). Renal abnormalities and an altered inflammatory response in mice lacking cyclooxygenase II. *Nature* **378**, 406-9.

Dohadwala, M., Yang, S. C., Luo, J., Sharma, S., Batra, R. K., Huang, M., Lin, Y., Goodglick, L., Krysan, K., Fishbein, M. C., Hong, L., Lai, C., Cameron, R. B., Gemmill, R. M., Drabkin, H. A. and Dubinett, S. M. (2006). Cyclooxygenase-2-dependent regulation of E-cadherin: prostaglandin E(2) induces transcriptional repressors ZEB1 and snail in non-small cell lung cancer. *Cancer Res* **66**, 5338-45.

Doitsidou, M., Reichman-Fried, M., Stebler, J., Koprunner, M., Dorries, J., Meyer, D., Esguerra, C. V., Leung, T. and Raz, E. (2002). Guidance of primordial germ cell migration by the chemokine SDF-1. *Cell* **111**, 647-59.

Dominguez, D., Montserrat-Sentis, B., Virgos-Soler, A., Guaita, S., Grueso, J., Porta, M., Puig, I., Baulida, J., Franci, C. and Garcia de Herreros, A. (2003). Phosphorylation regulates the subcellular location and activity of the snail transcriptional repressor. *Mol Cell Biol* **23**, 5078-89.

Dosch, R. and Niehrs, C. (2000). Requirement for anti-dorsalizing morphogenetic protein in organizer patterning. *Mech Dev* **90**, 195-203.

Drees, F., Pokutta, S., Yamada, S., Nelson, W. J. and Weis, W. I. (2005). Alpha-catenin is a molecular switch that binds E-cadherin-beta-catenin and regulates actin-filament assembly. *Cell* **123**, 903-15.

Driever, W., Solnica-Krezel, L., Schier, A. F., Neuhauss, S. C., Malicki, J., Stemple, D. L., Stainier, D. Y., Zwartkruis, F., Abdelilah, S., Rangini, Z., Belak, J. and Boggs, C. (1996). A genetic screen for mutations affecting embryogenesis in zebrafish. *Development* **123**, 37-46.

Dubin-Thaler, B. J., Hofman, J. M., Cai, Y., Xenias, H., Spielman, I., Shneidman, A. V., David, L. A., Dobereiner, H. G., Wiggins, C. H. and Sheetz, M. P. (2008). Quantification of cell edge velocities and traction forces reveals distinct motility modules during cell spreading. *PLoS One* **3**, e3735.

Eisinger, A. L., Nadauld, L. D., Shelton, D. N., Peterson, P. W., Phelps, R. A., Chidester, S., Stafforini, D. M., Prescott, S. M. and Jones, D. A. (2006). The adenomatous polyposis coli tumor suppressor gene regulates expression of cyclooxygenase-2 by a mechanism that involves retinoic acid. *J Biol Chem* **281**, 20474-82.

Erter, C. E., Solnica-Krezel, L. and Wright, C. V. (1998). Zebrafish nodal-related 2 encodes an early mesendodermal inducer signaling from the extraembryonic yolk syncytial layer. *Dev Biol* **204**, 361-72.

Erter, C. E., Wilm, T. P., Basler, N., Wright, C. V. and Solnica-Krezel, L. (2001). Wnt8 is required in lateral mesendodermal precursors for neural posteriorization in vivo. *Development* **128**, 3571-83.

Fackler, O. T. and Grosse, R. (2008). Cell motility through plasma membrane blebbing. *J Cell Biol* **181**, 879-84.

Fekany, K., Yamanaka, Y., Leung, T., Sirotkin, H. I., Topczewski, J., Gates, M. A., Hibi, M., Renucci, A., Stemple, D., Radbill, A., Schier, A. F., Driever, W., Hirano, T., Talbot, W. S. and Solnica-Krezel, L. (1999). The zebrafish bozozok locus encodes Dharma, a homeodomain protein essential for induction of gastrula organizer and dorsoanterior embryonic structures. *Development* **126**, 1427-38.

Fekany-Lee, K., Gonzalez, E., Miller-Bertoglio, V. and Solnica-Krezel, L. (2000). The homeobox gene bozozok promotes anterior neuroectoderm formation in zebrafish through negative regulation of BMP2/4 and Wnt pathways. *Development* **127**, 2333-45.

Feldman, B., Concha, M. L., Saude, L., Parsons, M. J., Adams, R. J., Wilson, S. W. and Stemple, D. L. (2002). Lefty antagonism of Squint is essential for normal gastrulation. *Curr Biol* **12**, 2129-35.

Feldman, B., Dougan, S. T., Schier, A. F. and Talbot, W. S. (2000). Nodal-related signals establish mesendodermal fate and trunk neural identity in zebrafish. *Curr Biol* **10**, 531-4.

Feldman, B., Gates, M. A., Egan, E. S., Dougan, S. T., Rennebeck, G., Sirotkin, H. I., Schier, A. F. and Talbot, W. S. (1998). Zebrafish organizer development and germ-layer formation require nodal-related signals. *Nature* **395**, 181-5.

Fendrich, V., Waldmann, J., Esni, F., Ramaswamy, A., Mullendore, M., Buchholz, M., Maitra, A. and Feldmann, G. (2007). Snail and Sonic Hedgehog activation in neuroendocrine tumors of the ileum. *Endocr Relat Cancer* **14**, 865-74.

Fevr, T., Robine, S., Louvard, D. and Huelsken, J. (2007). Wnt/beta-catenin is essential for intestinal homeostasis and maintenance of intestinal stem cells. *Mol Cell Biol* **27**, 7551-9.

Foty, R. A. and Steinberg, M. S. (2005). The differential adhesion hypothesis: a direct evaluation. *Dev Biol* **278**, 255-63.

Fujii, R., Yamashita, S., Hibi, M. and Hirano, T. (2000). Asymmetric p38 activation in zebrafish: its possible role in symmetric and synchronous cleavage. *J Cell Biol* **150**, 1335-48.

Fujino, H. and Regan, J. W. (2003). Prostanoid receptors and phosphatidylinositol 3-kinase: a pathway to cancer? *Trends Pharmacol Sci* **24**, 335-40.

Fujino, H. and Regan, J. W. (2006). EP(4) prostanoid receptor coupling to a pertussis toxin-sensitive inhibitory G protein. *Mol Pharmacol* **69**, 5-10.

Fujino, H., West, K. A. and Regan, J. W. (2002). Phosphorylation of glycogen synthase kinase-3 and stimulation of T-cell factor signaling following activation of EP2 and EP4 prostanoid receptors by prostaglandin E2. *J Biol Chem* **277**, 2614-9.

Fujino, H., Xu, W. and Regan, J. W. (2003). Prostaglandin E2 induced functional expression of early growth response factor-1 by EP4, but not EP2, prostanoid receptors via the phosphatidylinositol 3-kinase and extracellular signal-regulated kinases. *J Biol Chem* **278**, 12151-6.

Funayama, N., Fagotto, F., McCrea, P. and Gumbiner, B. M. (1995). Embryonic axis induction by the armadillo repeat domain of beta-catenin: evidence for intracellular signaling. *J Cell Biol* **128**, 959-68.

Gimlich, R. L. and Gerhart, J. C. (1984). Early cellular interactions promote embryonic axis formation in Xenopus laevis. *Dev Biol* **104**, 117-30.

Goessling, W., North, T. E., Loewer, S., Lord, A. M., Lee, S., Stoick-Cooper, C. L., Weidinger, G., Puder, M., Daley, G. Q., Moon, R. T. and Zon, L. I. (2009). Genetic interaction of PGE2 and Wnt signaling regulates developmental specification of stem cells and regeneration. *Cell* **136**, 1136-47.

Gore, A. V., Maegawa, S., Cheong, A., Gilligan, P. C., Weinberg, E. S. and Sampath, K. (2005). The zebrafish dorsal axis is apparent at the four-cell stage. *Nature* **438**, 1030-5.

Grapin-Botton, A. and Constam, D. (2007). Evolution of the mechanisms and molecular control of endoderm formation. *Mech Dev* **124**, 253-78.

Gritsman, K., Zhang, J., Cheng, S., Heckscher, E., Talbot, W. S. and Schier, A. F. (1999). The EGF-CFC protein one-eyed pinhead is essential for nodal signaling. *Cell* **97**, 121-32.

Grosser, T., Yusuff, S., Cheskis, E., Pack, M. A. and FitzGerald, G. A. (2002). Developmental expression of functional cyclooxygenases in zebrafish. *Proc Natl Acad Sci U S A* **99**, 8418-23.

Grunwald, D. J. and Streisinger, G. (1992). Induction of recessive lethal and specific locus mutations in the zebrafish with ethyl nitrosourea. *Genet Res* **59**, 103-16.

Guillemot, L., Levy, A., Raymondjean, M. and Rothhut, B. (2001). Angiotensin II-induced transcriptional activation of the cyclin D1 gene is mediated by Egr-1 in CHO-AT(1A) cells. *J Biol Chem* **276**, 39394-403.

Habas, R. and Dawid, I. B. (2005). Dishevelled and Wnt signaling: is the nucleus the final frontier? *J Biol* **4**, 2.

Haffter, P., Granato, M., Brand, M., Mullins, M. C., Hammerschmidt, M., Kane, D. A., Odenthal, J., van Eeden, F. J., Jiang, Y. J., Heisenberg, C. P., Kelsh, R. N., Furutani-Seiki, M., Vogelsang, E., Beuchle, D., Schach, U., Fabian, C. and Nusslein-Volhard, C. (1996). The identification of genes with unique and essential functions in the development of the zebrafish, Danio rerio. *Development* **123**, 1-36.

Hammerschmidt, M. and Nusslein-Volhard, C. (1993). The expression of a zebrafish gene homologous to Drosophila snail suggests a conserved function in invertebrate and vertebrate gastrulation. *Development* **119**, 1107-18.

Hammerschmidt, M., Pelegri, F., Mullins, M. C., Kane, D. A., van Eeden, F. J., Granato, M., Brand, M., Furutani-Seiki, M., Haffter, P., Heisenberg, C. P., Jiang, Y. J., Kelsh, R. N., Odenthal, J., Warga, R. M. and Nusslein-Volhard, C. (1996). dino and mercedes, two genes regulating dorsal development in the zebrafish embryo. *Development* **123**, 95-102.

Hammerschmidt, M. and Wedlich, D. (2008). Regulated adhesion as a driving force of gastrulation movements. *Development* **135**, 3625-41.
Han, C., Michalopoulos, G. K. and Wu, T. (2006). Prostaglandin E2 receptor EP1 transactivates EGFR/MET receptor tyrosine kinases and enhances invasiveness in human hepatocellular carcinoma cells. *J Cell Physiol* **207**, 261-70.
Hartsock, A. and Nelson, W. J. (2008). Adherens and tight junctions: structure, function and connections to the actin cytoskeleton. *Biochim Biophys Acta* **1778**, 660-9.
Hayashi, T. and Carthew, R. W. (2004). Surface mechanics mediate pattern formation in the developing retina. *Nature* **431**, 647-52.
Heisenberg, C. P. and Tada, M. (2002). Zebrafish gastrulation movements: bridging cell and developmental biology. *Semin Cell Dev Biol* **13**, 471-9.
Henikoff, S., Till, B. J. and Comai, L. (2004). TILLING. Traditional mutagenesis meets functional genomics. *Plant Physiol* **135**, 630-6.
Hertel, N., Krishna, K., Nuernberger, M. and Redies, C. (2008). A cadherin-based code for the divisions of the mouse basal ganglia. *J Comp Neurol* **508**, 511-28.
Heyers, D., Kovjanic, D. and Redies, C. (2003). Cadherin expression coincides with birth dating patterns in patchy compartments of the developing chicken telencephalon. *J Comp Neurol* **460**, 155-66.
Hizaki, H., Segi, E., Sugimoto, Y., Hirose, M., Saji, T., Ushikubi, F., Matsuoka, T., Noda, Y., Tanaka, T., Yoshida, N., Narumiya, S. and Ichikawa, A. (1999). Abortive expansion of the cumulus and impaired fertility in mice lacking the prostaglandin E receptor subtype EP(2). *Proc Natl Acad Sci U S A* **96**, 10501-6.
Hla, T. (2005). Genomic insights into mediator lipidomics. *Prostaglandins Other Lipid Mediat* **77**, 197-209.
Ho, C. Y., Houart, C., Wilson, S. W. and Stainier, D. Y. (1999). A role for the extraembryonic yolk syncytial layer in patterning the zebrafish embryo suggested by properties of the hex gene. *Curr Biol* **9**, 1131-4.
Ho, R. K. and Kane, D. A. (1990). Cell-autonomous action of zebrafish spt-1 mutation in specific mesodermal precursors. *Nature* **348**, 728-30.
Hoggatt, J., Singh, P., Sampath, J. and Pelus, L. M. (2009). Prostaglandin E2 enhances hematopoietic stem cell homing, survival, and proliferation. *Blood* **113**, 5444-55.
Houart, C., Caneparo, L., Heisenberg, C., Barth, K., Take-Uchi, M. and Wilson, S. (2002). Establishment of the telencephalon during gastrulation by local antagonism of Wnt signaling. *Neuron* **35**, 255-65.
Hsia, N. and Zon, L. I. (2005). Transcriptional regulation of hematopoietic stem cell development in zebrafish. *Exp Hematol* **33**, 1007-14.
Huber, A. H. and Weis, W. I. (2001). The structure of the beta-catenin/E-cadherin complex and the molecular basis of diverse ligand recognition by beta-catenin. *Cell* **105**, 391-402.
Hwang, S. P., Tsou, M. F., Lin, Y. C. and Liu, C. H. (1997). The zebrafish BMP4 gene: sequence analysis and expression pattern during embryonic development. *DNA Cell Biol* **16**, 1003-11.
Inbal, A., Topczewski, J. and Solnica-Krezel, L. (2006). Targeted gene expression in the zebrafish prechordal plate. *Genesis* **44**, 584-8.

Jernigan, K. K., Cselenyi, C. S., Thorne, C., Hajicek, N., Oldham, W. M., Lee, L. A., Hamm, H. E., Hepler, J. R., Kozasa, T., Linder, M. E. and Lee, E. Gβγ promotes LRP6 mediated β-catenin/TCF signaling by stimulating plasma membrane localization and activation of GSK3. *To be submitted*.

Jernigan, K. K. and Lee, E. personal communications.

Jessen, J. R. and Solnica-Krezel, L. (2005). Axis formation--beta-catenin catches a Wnt. *Cell* **120**, 736-7.

Jessen, J. R., Topczewski, J., Bingham, S., Sepich, D. S., Marlow, F., Chandrasekhar, A. and Solnica-Krezel, L. (2002). Zebrafish trilobite identifies new roles for Strabismus in gastrulation and neuronal movements. *Nat Cell Biol* **4**, 610-5.

Jin, S. W., Beis, D., Mitchell, T., Chen, J. N. and Stainier, D. Y. (2005). Cellular and molecular analyses of vascular tube and lumen formation in zebrafish. *Development* **132**, 5199-209.

Jin, Y., Wang, Z., Zhang, Y., Yang, B. and Wang, W. H. (2007). PGE2 inhibits apical K channels in the CCD through activation of the MAPK pathway. *Am J Physiol Renal Physiol* **293**, F1299-307.

Kafer, J., Hayashi, T., Maree, A. F., Carthew, R. W. and Graner, F. (2007). Cell adhesion and cortex contractility determine cell patterning in the Drosophila retina. *Proc Natl Acad Sci U S A* **104**, 18549-54.

Kai, M., Heisenberg, C. P. and Tada, M. (2008). Sphingosine-1-phosphate receptors regulate individual cell behaviours underlying the directed migration of prechordal plate progenitor cells during zebrafish gastrulation. *Development* **135**, 3043-51.

Kane, D. A., McFarland, K. N. and Warga, R. M. (2005). Mutations in half baked/E-cadherin block cell behaviors that are necessary for teleost epiboly. *Development* **132**, 1105-16.

Kaplan, D. D., Meigs, T. E. and Casey, P. J. (2001). Distinct regions of the cadherin cytoplasmic domain are essential for functional interaction with Galpha 12 and beta-catenin. *J Biol Chem* **276**, 44037-43.

Katoh, K., Asimenos, G. and Toh, H. (2009). Multiple alignment of DNA sequences with MAFFT. *Methods Mol Biol* **537**, 39-64.

Kawahara, A., Wilm, T., Solnica-Krezel, L. and Dawid, I. B. (2000). Antagonistic role of vega1 and bozozok/dharma homeobox genes in organizer formation. *Proc Natl Acad Sci U S A* **97**, 12121-6.

Kedzie, K. M., Donello, J. E., Krauss, H. A., Regan, J. W. and Gil, D. W. (1998). A single amino-acid substitution in the EP2 prostaglandin receptor confers responsiveness to prostacyclin analogs. *Mol Pharmacol* **54**, 584-90.

Keller, P. J., Schmidt, A. D., Wittbrodt, J. and Stelzer, E. H. (2008). Reconstruction of zebrafish early embryonic development by scanned light sheet microscopy. *Science* **322**, 1065-9.

Kelly, C., Chin, A. J., Leatherman, J. L., Kozlowski, D. J. and Weinberg, E. S. (2000). Maternally controlled (beta)-catenin-mediated signaling is required for organizer formation in the zebrafish. *Development* **127**, 3899-911.

Kelly, G. M., Erezyilmaz, D. F. and Moon, R. T. (1995). Induction of a secondary embryonic axis in zebrafish occurs following the overexpression of beta-catenin. *Mech Dev* **53**, 261-73.

Kelly, G. M., Greenstein, P., Erezyilmaz, D. F. and Moon, R. T. (1995). Zebrafish wnt8 and wnt8b share a common activity but are involved in distinct developmental pathways. *Development* **121**, 1787-99.

Kikuchi, Y., Agathon, A., Alexander, J., Thisse, C., Waldron, S., Yelon, D., Thisse, B. and Stainier, D. Y. (2001). casanova encodes a novel Sox-related protein necessary and sufficient for early endoderm formation in zebrafish. *Genes Dev* **15**, 1493-505.

Kim, S. H., Shin, J., Park, H. C., Yeo, S. Y., Hong, S. K., Han, S., Rhee, M., Kim, C. H., Chitnis, A. B. and Huh, T. L. (2002). Specification of an anterior neuroectoderm patterning by Frizzled8a-mediated Wnt8b signalling during late gastrulation in zebrafish. *Development* **129**, 4443-55.

Kimmel, C. B., Ballard, W. W., Kimmel, S. R., Ullmann, B. and Schilling, T. F. (1995). Stages of embryonic development of the zebrafish. *Dev Dyn* **203**, 253-310.

Kimmel, C. B. and Law, R. D. (1985). Cell lineage of zebrafish blastomeres. II. Formation of the yolk syncytial layer. *Dev Biol* **108**, 86-93.

Kishimoto, Y., Lee, K. H., Zon, L., Hammerschmidt, M. and Schulte-Merker, S. (1997). The molecular nature of zebrafish swirl: BMP2 function is essential during early dorsoventral patterning. *Development* **124**, 4457-66.

Kominami, T. and Takata, H. (2004). Gastrulation in the sea urchin embryo: a model system for analyzing the morphogenesis of a monolayered epithelium. *Dev Growth Differ* **46**, 309-26.

Koos, D. S. and Ho, R. K. (1999). The nieuwkoid/dharma homeobox gene is essential for bmp2b repression in the zebrafish pregastrula. *Dev Biol* **215**, 190-207.

Krieg, M., Arboleda-Estudillo, Y., Puech, P. H., Kafer, J., Graner, F., Muller, D. J. and Heisenberg, C. P. (2008). Tensile forces govern germ-layer organization in zebrafish. *Nat Cell Biol* **10**, 429-36.

Krishna, K. and Redies, C. (2009). Expression of cadherin superfamily genes in brain vascular development. *J Cereb Blood Flow Metab* **29**, 224-9.

Kumar, P., Lyle, K. S., Gierke, S., Matov, A., Danuser, G. and Wittmann, T. (2009). GSK3beta phosphorylation modulates CLASP-microtubule association and lamella microtubule attachment. *J Cell Biol* **184**, 895-908.

Lachnit, M., Kur, E. and Driever, W. (2008). Alterations of the cytoskeleton in all three embryonic lineages contribute to the epiboly defect of Pou5f1/Oct4 deficient MZspg zebrafish embryos. *Dev Biol* **315**, 1-17.

Langenbach, R., Morham, S. G., Tiano, H. F., Loftin, C. D., Ghanayem, B. I., Chulada, P. C., Mahler, J. F., Lee, C. A., Goulding, E. H., Kluckman, K. D., Kim, H. S. and Smithies, O. (1995). Prostaglandin synthase 1 gene disruption in mice reduces arachidonic acid-induced inflammation and indomethacin-induced gastric ulceration. *Cell* **83**, 483-92.

Lawson, N. D., Scheer, N., Pham, V. N., Kim, C. H., Chitnis, A. B., Campos-Ortega, J. A. and Weinstein, B. M. (2001). Notch signaling is required for arterial-venous differentiation during embryonic vascular development. *Development* **128**, 3675-83.

Lecuit, T. and Lenne, P. F. (2007). Cell surface mechanics and the control of cell shape, tissue patterns and morphogenesis. *Nat Rev Mol Cell Biol* **8**, 633-44.

Lekven, A. C., Thorpe, C. J., Waxman, J. S. and Moon, R. T. (2001). Zebrafish wnt8 encodes two wnt8 proteins on a bicistronic transcript and is required for mesoderm and neurectoderm patterning. *Dev Cell* **1**, 103-14.

Leopoldt, D., Hanck, T., Exner, T., Maier, U., Wetzker, R. and Nurnberg, B. (1998). Gbetagamma stimulates phosphoinositide 3-kinase-gamma by direct interaction with two domains of the catalytic p110 subunit. *J Biol Chem* **273**, 7024-9.

Leung, T., Bischof, J., Soll, I., Niessing, D., Zhang, D., Ma, J., Jackle, H. and Driever, W. (2003). bozozok directly represses bmp2b transcription and mediates the earliest dorsoventral asymmetry of bmp2b expression in zebrafish. *Development* **130**, 3639-49.

Li, X., Deng, W., Lobo-Ruppert, S. M. and Ruppert, J. M. (2007). Gli1 acts through Snail and E-cadherin to promote nuclear signaling by beta-catenin. *Oncogene* **26**, 4489-98.

Li, X., Deng, W., Nail, C. D., Bailey, S. K., Kraus, M. H., Ruppert, J. M. and Lobo-Ruppert, S. M. (2006). Snail induction is an early response to Gli1 that determines the efficiency of epithelial transformation. *Oncogene* **25**, 609-21.

Lin, F., Chen, S., Sepich, D. S., Panizzi, J. R., Clendenon, S. G., Marrs, J. A., Hamm, H. E. and Solnica-Krezel, L. (2009). Galpha12/13 regulate epiboly by inhibiting E-cadherin activity and modulating the actin cytoskeleton. *J Cell Biol* **184**, 909-21.

Lin, F., Sepich, D. S., Chen, S., Topczewski, J., Yin, C., Solnica-Krezel, L. and Hamm, H. (2005). Essential roles of G{alpha}12/13 signaling in distinct cell behaviors driving zebrafish convergence and extension gastrulation movements. *J Cell Biol* **169**, 777-87.

Little, S. C. and Mullins, M. C. (2009). Bone morphogenetic protein heterodimers assemble heteromeric type I receptor complexes to pattern the dorsoventral axis. *Nat Cell Biol* **11**, 637-43.

Liu, X., Huang, S., Ma, J., Li, C., Zhang, Y. and Luo, L. (2009). NF-kappaB and Snail1a coordinate the cell cycle with gastrulation. *J Cell Biol* **184**, 805-15.

Logan, C. Y. and Nusse, R. (2004). The Wnt signaling pathway in development and disease. *Annu Rev Cell Dev Biol* **20**, 781-810.

Long, S., Ahmad, N. and Rebagliati, M. (2003). The zebrafish nodal-related gene southpaw is required for visceral and diencephalic left-right asymmetry. *Development* **130**, 2303-16.

Lord, A. M., North, T. E. and Zon, L. I. (2007). Prostaglandin E2: making more of your marrow. *Cell Cycle* **6**, 3054-7.

Lorenz, M., Slaughter, H. S., Wescott, D. M., Carter, S. I., Schnyder, B., Dinchuk, J. E. and Car, B. D. (1999). Cyclooxygenase-2 is essential for normal recovery from 5-fluorouracil-induced myelotoxicity in mice. *Exp Hematol* **27**, 1494-502.

Lu, Z., Ghosh, S., Wang, Z. and Hunter, T. (2003). Downregulation of caveolin-1 function by EGF leads to the loss of E-cadherin, increased transcriptional activity of beta-catenin, and enhanced tumor cell invasion. *Cancer Cell* **4**, 499-515.

Lunde, K., Belting, H. G. and Driever, W. (2004). Zebrafish pou5f1/pou2, homolog of mammalian Oct4, functions in the endoderm specification cascade. *Curr Biol* **14**, 48-55.

Mann, J. R., Backlund, M. G., Buchanan, F. G., Daikoku, T., Holla, V. R., Rosenberg, D. W., Dey, S. K. and DuBois, R. N. (2006). Repression of prostaglandin dehydrogenase by epidermal growth factor and snail increases prostaglandin E2 and promotes cancer progression. *Cancer Res* **66**, 6649-56.

Mao, J., Wang, J., Liu, B., Pan, W., Farr, G. H., 3rd, Flynn, C., Yuan, H., Takada, S., Kimelman, D., Li, L. and Wu, D. (2001). Low-density lipoprotein receptor-related protein-5 binds to Axin and regulates the canonical Wnt signaling pathway. *Mol Cell* **7**, 801-9.

Martinez-Barbera, J. P., Toresson, H., Da Rocha, S. and Krauss, S. (1997). Cloning and expression of three members of the zebrafish Bmp family: Bmp2a, Bmp2b and Bmp4. *Gene* **198**, 53-9.

McCrea, P. D., Brieher, W. M. and Gumbiner, B. M. (1993). Induction of a secondary body axis in Xenopus by antibodies to beta-catenin. *J Cell Biol* **123**, 477-84.

McFarland, K. N., Warga, R. M. and Kane, D. A. (2005). Genetic locus half baked is necessary for morphogenesis of the ectoderm. *Dev Dyn* **233**, 390-406.

Meigs, T. E., Fedor-Chaiken, M., Kaplan, D. D., Brackenbury, R. and Casey, P. J. (2002). Galpha12 and Galpha13 negatively regulate the adhesive functions of cadherin. *J Biol Chem* **277**, 24594-600.

Meigs, T. E., Fields, T. A., McKee, D. D. and Casey, P. J. (2001). Interaction of Galpha 12 and Galpha 13 with the cytoplasmic domain of cadherin provides a mechanism for beta -catenin release. *Proc Natl Acad Sci U S A* **98**, 519-24.

Melby, A. E., Beach, C., Mullins, M. and Kimelman, D. (2000). Patterning the early zebrafish by the opposing actions of bozozok and vox/vent. *Dev Biol* **224**, 275-85.

Meno, C., Gritsman, K., Ohishi, S., Ohfuji, Y., Heckscher, E., Mochida, K., Shimono, A., Kondoh, H., Talbot, W. S., Robertson, E. J., Schier, A. F. and Hamada, H. (1999). Mouse Lefty2 and zebrafish antivin are feedback inhibitors of nodal signaling during vertebrate gastrulation. *Mol Cell* **4**, 287-98.

Miller-Bertoglio, V. E., Fisher, S., Sanchez, A., Mullins, M. C. and Halpern, M. E. (1997). Differential regulation of chordin expression domains in mutant zebrafish. *Dev Biol* **192**, 537-50.

Miyagi, C., Yamashita, S., Ohba, Y., Yoshizaki, H., Matsuda, M. and Hirano, T. (2004). STAT3 noncell-autonomously controls planar cell polarity during zebrafish convergence and extension. *J Cell Biol* **166**, 975-81.

Miyatake, S., Manabe-Kawaguchi, H., Watanabe, K., Hori, S., Aikawa, N. and Fukuda, K. (2007). Prostaglandin E2 induces hypertrophic changes and suppresses alpha-skeletal actin gene expression in rat cardiomyocytes. *J Cardiovasc Pharmacol* **50**, 548-54.

Mizuno, T., Yamaha, E., Kuroiwa, A. and Takeda, H. (1999). Removal of vegetal yolk causes dorsal deficencies and impairs dorsal-inducing ability of the yolk cell in zebrafish. *Mech Dev* **81**, 51-63.

Moens, C. B. (2000). Reduced levels of mutant mRNAs in zebrafish mutants may not be due to loss of positive autoregulation. *The Zebrafish Science Monitor* **7**.

Montero, J. A., Carvalho, L., Wilsch-Brauninger, M., Kilian, B., Mustafa, C. and Heisenberg, C. P. (2005). Shield formation at the onset of zebrafish gastrulation. *Development* **132**, 1187-98.
Montero, J. A. and Heisenberg, C. P. (2004). Gastrulation dynamics: cells move into focus. *Trends Cell Biol* **14**, 620-7.
Montero, J. A., Kilian, B., Chan, J., Bayliss, P. E. and Heisenberg, C. P. (2003). Phosphoinositide 3-kinase is required for process outgrowth and cell polarization of gastrulating mesendodermal cells. *Curr Biol* **13**, 1279-89.
Montero-Balaguer, M., Swirsding, K., Orsenigo, F., Cotelli, F., Mione, M. and Dejana, E. (2009). Stable vascular connections and remodeling require full expression of VE-cadherin in zebrafish embryos. *PLoS One* **4**, e5772.
Moody, S. E., Perez, D., Pan, T. C., Sarkisian, C. J., Portocarrero, C. P., Sterner, C. J., Notorfrancesco, K. L., Cardiff, R. D. and Chodosh, L. A. (2005). The transcriptional repressor Snail promotes mammary tumor recurrence. *Cancer Cell* **8**, 197-209.
Moore, R., Cai, K. Q. and Xu, X. X. (2008). Patterning of the mouse embryonic germ layers: The Townes and Holtfreter cell sorting experiments revisited. *Dev Biol* **319**, 507.
Moser, A. R., Pitot, H. C. and Dove, W. F. (1990). A dominant mutation that predisposes to multiple intestinal neoplasia in the mouse. *Science* **247**, 322-4.
Mullins, M. C., Hammerschmidt, M., Haffter, P. and Nusslein-Volhard, C. (1994). Large-scale mutagenesis in the zebrafish: in search of genes controlling development in a vertebrate. *Curr Biol* **4**, 189-202.
Mullins, M. C., Hammerschmidt, M., Kane, D. A., Odenthal, J., Brand, M., van Eeden, F. J., Furutani-Seiki, M., Granato, M., Haffter, P., Heisenberg, C. P., Jiang, Y. J., Kelsh, R. N. and Nusslein-Volhard, C. (1996). Genes establishing dorsoventral pattern formation in the zebrafish embryo: the ventral specifying genes. *Development* **123**, 81-93.
Murakami, M., Nakatani, Y., Tanioka, T. and Kudo, I. (2002). Prostaglandin E synthase. *Prostaglandins Other Lipid Mediat* **68-69**, 383-99.
Myers, D. C., Sepich, D. S. and Solnica-Krezel, L. (2002). Convergence and extension in vertebrate gastrulae: cell movements according to or in search of identity? *Trends Genet* **18**, 447-55.
Nair, S. and Schilling, T. F. (2008). Chemokine signaling controls endodermal migration during zebrafish gastrulation. *Science* **322**, 89-92.
Nelson, W. J. (2008). Regulation of cell-cell adhesion by the cadherin-catenin complex. *Biochem Soc Trans* **36**, 149-55.
Nguyen, H., Rendl, M. and Fuchs, E. (2006). Tcf3 governs stem cell features and represses cell fate determination in skin. *Cell* **127**, 171-83.
Nieuwkoop, P. D. (1977). Origin and establishment of embryonic polar axes in amphibian development. *Curr Top Dev Biol* **11**, 115-32.
Nojima, H., Shimizu, T., Kim, C. H., Yabe, T., Bae, Y. K., Muraoka, O., Hirata, T., Chitnis, A., Hirano, T. and Hibi, M. (2004). Genetic evidence for involvement of maternally derived Wnt canonical signaling in dorsal determination in zebrafish. *Mech Dev* **121**, 371-86.
North, T. E., Goessling, W., Walkley, C. R., Lengerke, C., Kopani, K. R., Lord, A. M., Weber, G. J., Bowman, T. V., Jang, I. H., Grosser, T., Fitzgerald, G. A., Daley, G. Q., Orkin, S. H. and Zon, L. I. (2007). Prostaglandin E2

regulates vertebrate haematopoietic stem cell homeostasis. *Nature* **447**, 1007-11.

Nusse, R. (2005). Wnt signaling in disease and in development. *Cell Res* **15**, 28-32.

Onder, T. T., Gupta, P. B., Mani, S. A., Yang, J., Lander, E. S. and Weinberg, R. A. (2008). Loss of E-cadherin promotes metastasis via multiple downstream transcriptional pathways. *Cancer Res* **68**, 3645-54.

Orkin, S. H. and Zon, L. I. (1997). Genetics of erythropoiesis: induced mutations in mice and zebrafish. *Annu Rev Genet* **31**, 33-60.

Orkin, S. H. and Zon, L. I. (2002). Hematopoiesis and stem cells: plasticity versus developmental heterogeneity. *Nat Immunol* **3**, 323-8.

Oshima, M., Murai, N., Kargman, S., Arguello, M., Luk, P., Kwong, E., Taketo, M. M. and Evans, J. F. (2001). Chemoprevention of intestinal polyposis in the Apcdelta716 mouse by rofecoxib, a specific cyclooxygenase-2 inhibitor. *Cancer Res* **61**, 1733-40.

Oshima, M., Oshima, H., Kitagawa, K., Kobayashi, M., Itakura, C. and Taketo, M. (1995). Loss of Apc heterozygosity and abnormal tissue building in nascent intestinal polyps in mice carrying a truncated Apc gene. *Proc Natl Acad Sci U S A* **92**, 4482-6.

Ozbudak, E. M., Thattai, M., Kurtser, I., Grossman, A. D. and van Oudenaarden, A. (2002). Regulation of noise in the expression of a single gene. *Nat Genet* **31**, 69-73.

Pacquelet, A. and Rorth, P. (2005). Regulatory mechanisms required for DE-cadherin function in cell migration and other types of adhesion. *J Cell Biol* **170**, 803-12.

Parker, L. H., Schmidt, M., Jin, S. W., Gray, A. M., Beis, D., Pham, T., Frantz, G., Palmieri, S., Hillan, K., Stainier, D. Y., De Sauvage, F. J. and Ye, W. (2004). The endothelial-cell-derived secreted factor Egfl7 regulates vascular tube formation. *Nature* **428**, 754-8.

Pasquini, M. C. (2008). Impact of graft-versus-host disease on survival. *Best Pract Res Clin Haematol* **21**, 193-204.

Patel, P. A., Tilley, D. G. and Rockman, H. A. (2009). Physiologic and cardiac roles of beta-arrestins. *J Mol Cell Cardiol* **46**, 300-8.

Peyrieras, N., Strahle, U. and Rosa, F. (1998). Conversion of zebrafish blastomeres to an endodermal fate by TGF-beta-related signaling. *Curr Biol* **8**, 783-6.

Pezeron, G., Mourrain, P., Courty, S., Ghislain, J., Becker, T. S., Rosa, F. M. and David, N. B. (2008). Live analysis of endodermal layer formation identifies random walk as a novel gastrulation movement. *Curr Biol* **18**, 276-81.

Pongracz, J. E. and Stockley, R. A. (2006). Wnt signalling in lung development and diseases. *Respir Res* **7**, 15.

Poole, T. J., Finkelstein, E. B. and Cox, C. M. (2001). The role of FGF and VEGF in angioblast induction and migration during vascular development. *Dev Dyn* **220**, 1-17.

Raj, A. and van Oudenaarden, A. (2008). Nature, nurture, or chance: stochastic gene expression and its consequences. *Cell* **135**, 216-26.

Rao, R., Redha, R., Macias-Perez, I., Su, Y., Hao, C., Zent, R., Breyer, M. D. and Pozzi, A. (2007). Prostaglandin E2-EP4 receptor promotes endothelial cell migration via ERK activation and angiogenesis in vivo. *J Biol Chem* **282**, 16959-68.

Reese, J., Paria, B. C., Brown, N., Zhao, X., Morrow, J. D. and Dey, S. K. (2000). Coordinated regulation of fetal and maternal prostaglandins directs successful birth and postnatal adaptation in the mouse. *Proc Natl Acad Sci U S A* **97**, 9759-64.

Regan, J. W. (2003). EP2 and EP4 prostanoid receptor signaling. *Life Sci* **74**, 143-53.

Reichman-Fried, M., Minina, S. and Raz, E. (2004). Autonomous modes of behavior in primordial germ cell migration. *Dev Cell* **6**, 589-96.

Reim, G., Mizoguchi, T., Stainier, D. Y., Kikuchi, Y. and Brand, M. (2004). The POU domain protein spg (pou2/Oct4) is essential for endoderm formation in cooperation with the HMG domain protein casanova. *Dev Cell* **6**, 91-101.

Repasky, G. A., Zhou, Y., Morita, S. and Der, C. J. (2007). Ras-mediated intestinal epithelial cell transformation requires cyclooxygenase-2-induced prostaglandin E2 signaling. *Mol Carcinog* **46**, 958-70.

Reya, T., Duncan, A. W., Ailles, L., Domen, J., Scherer, D. C., Willert, K., Hintz, L., Nusse, R. and Weissman, I. L. (2003). A role for Wnt signalling in self-renewal of haematopoietic stem cells. *Nature* **423**, 409-14.

Roberts, D. M., Slep, K. C. and Peifer, M. (2007). It takes more than two to tango: Dishevelled polymerization and Wnt signaling. *Nat Struct Mol Biol* **14**, 463-5.

Rocca, B., Spain, L. M., Pure, E., Langenbach, R., Patrono, C. and FitzGerald, G. A. (1999). Distinct roles of prostaglandin H synthases 1 and 2 in T-cell development. *J Clin Invest* **103**, 1469-77.

Rula, M. E., Cai, K. Q., Moore, R., Yang, D. H., Staub, C. M., Capo-Chichi, C. D., Jablonski, S. A., Howe, P. H., Smith, E. R. and Xu, X. X. (2007). Cell autonomous sorting and surface positioning in the formation of primitive endoderm in embryoid bodies. *Genesis* **45**, 327-38.

Ryu, S. L., Fujii, R., Yamanaka, Y., Shimizu, T., Yabe, T., Hirata, T., Hibi, M. and Hirano, T. (2001). Regulation of dharma/bozozok by the Wnt pathway. *Dev Biol* **231**, 397-409.

Saloman, D. S., Bianco, C., Ebert, A. D., Khan, N. I., De Santis, M., Normanno, N., Wechselberger, C., Seno, M., Williams, K., Sanicola, M., Foley, S., Gullick, W. J. and Persico, G. (2000). The EGF-CFC family: novel epidermal growth factor-related proteins in development and cancer. *Endocr Relat Cancer* **7**, 199-226.

Sampath, K., Rubinstein, A. L., Cheng, A. M., Liang, J. O., Fekany, K., Solnica-Krezel, L., Korzh, V., Halpern, M. E. and Wright, C. V. (1998). Induction of the zebrafish ventral brain and floorplate requires cyclops/nodal signalling. *Nature* **395**, 185-9.

Scheer, N. and Campos-Ortega, J. A. (1999). Use of the Gal4-UAS technique for targeted gene expression in the zebrafish. *Mech Dev* **80**, 153-8.

Schier, A. F., Neuhauss, S. C., Helde, K. A., Talbot, W. S. and Driever, W. (1997). The one-eyed pinhead gene functions in mesoderm and endoderm formation in zebrafish and interacts with no tail. *Development* **124**, 327-42.

Schier, A. F. and Shen, M. M. (2000). Nodal signalling in vertebrate development. *Nature* **403**, 385-9.

Schier, A. F. and Talbot, W. S. (2005). Molecular Genetics of Axis Formation in Zebrafish. *Annu Rev Genet* **39**, 561-613.

Schmid, B., Furthauer, M., Connors, S. A., Trout, J., Thisse, B., Thisse, C. and Mullins, M. C. (2000). Equivalent genetic roles for bmp7/snailhouse and bmp2b/swirl in dorsoventral pattern formation. *Development* **127**, 957-67.

Segi, E., Sugimoto, Y., Yamasaki, A., Aze, Y., Oida, H., Nishimura, T., Murata, T., Matsuoka, T., Ushikubi, F., Hirose, M., Tanaka, T., Yoshida, N., Narumiya, S. and Ichikawa, A. (1998). Patent ductus arteriosus and neonatal death in prostaglandin receptor EP4-deficient mice. *Biochem Biophys Res Commun* **246**, 7-12.

Sepich, D. S., Calmelet, C., Kiskowski, M. and Solnica-Krezel, L. (2005). Initiation of convergence and extension movements of lateral mesoderm during zebrafish gastrulation. *Dev Dyn* **234**, 279-92.

Shao, J., Jung, C., Liu, C. and Sheng, H. (2005). Prostaglandin E2 Stimulates the beta-catenin/T cell factor-dependent transcription in colon cancer. *J Biol Chem* **280**, 26565-72.

Sheng, H., Shao, J., Morrow, J. D., Beauchamp, R. D. and DuBois, R. N. (1998). Modulation of apoptosis and Bcl-2 expression by prostaglandin E2 in human colon cancer cells. *Cancer Res* **58**, 362-6.

Sheng, H., Shao, J., Washington, M. K. and DuBois, R. N. (2001). Prostaglandin E2 increases growth and motility of colorectal carcinoma cells. *J Biol Chem* **276**, 18075-81.

Shimizu, T., Yabe, T., Muraoka, O., Yonemura, S., Aramaki, S., Hatta, K., Bae, Y. K., Nojima, H. and Hibi, M. (2005). E-cadherin is required for gastrulation cell movements in zebrafish. *Mech Dev* **122**, 747-63.

Shoji, T., Yoshida, S., Mitsunari, M., Miyake, N., Tsukihara, S., Iwabe, T., Harada, T. and Terakawa, N. (2007). Involvement of p38 MAP kinase in lipopolysaccharide-induced production of pro- and anti-inflammatory cytokines and prostaglandin E(2) in human choriodecidua. *J Reprod Immunol* **75**, 82-90.

Smith, C. J., Morrow, J. D., Roberts, L. J., 2nd and Marnett, L. J. (1993). Differentiation of monocytoid THP-1 cells with phorbol ester induces expression of prostaglandin endoperoxide synthase-1 (COX-1). *Biochem Biophys Res Commun* **192**, 787-93.

Solnica-Krezel, L. (2003). Vertebrate development: taming the nodal waves. *Curr Biol* **13**, R7-9.

Solnica-Krezel, L. (2005). Conserved patterns of cell movements during vertebrate gastrulation. *Curr Biol* **15**, R213-28.

Solnica-Krezel, L. (2006). Gastrulation in zebrafish -- all just about adhesion? *Curr Opin Genet Dev* **16**, 433-41.

Solnica-Krezel, L., Schier, A. F. and Driever, W. (1994). Efficient recovery of ENU-induced mutations from the zebrafish germline. *Genetics* **136**, 1401-20.

Spemann, H. and Mangold, H. (1924). Über induktion von embryonalagen durch implantation artfremder organisatoren. *Roux' Arch Entw Mech* **100**, 599-638.

Stachel, S. E., Grunwald, D. J. and Myers, P. Z. (1993). Lithium perturbation and goosecoid expression identify a dorsal specification pathway in the pregastrula zebrafish. *Development* **117**, 1261-74.

Stainier, D. Y., Weinstein, B. M., Detrich, H. W., 3rd, Zon, L. I. and Fishman, M. C. (1995). Cloche, an early acting zebrafish gene, is required by both the endothelial and hematopoietic lineages. *Development* **121**, 3141-50.

Steinberg, M. S. (1963). Reconstruction of tissues by dissociated cells. Some morphogenetic tissue movements and the sorting out of embryonic cells may have a common explanation. *Science* **141**, 401-8.

Stemmer, V., de Craene, B., Berx, G. and Behrens, J. (2008). Snail promotes Wnt target gene expression and interacts with beta-catenin. *Oncogene* **27**, 5075-80.

Stickney, H. L., Imai, Y., Draper, B., Moens, C. and Talbot, W. S. (2007). Zebrafish bmp4 functions during late gastrulation to specify ventroposterior cell fates. *Dev Biol* **310**, 71-84.

Stillman, B. A., Audoly, L. and Breyer, R. M. (1998). A conserved threonine in the second extracellular loop of the human EP2 and EP4 receptors is required for ligand binding. *Eur J Pharmacol* **357**, 73-82.

Su, L. K., Kinzler, K. W., Vogelstein, B., Preisinger, A. C., Moser, A. R., Luongo, C., Gould, K. A. and Dove, W. F. (1992). Multiple intestinal neoplasia caused by a mutation in the murine homolog of the APC gene. *Science* **256**, 668-70.

Sugimoto, Y., Yamasaki, A., Segi, E., Tsuboi, K., Aze, Y., Nishimura, T., Oida, H., Yoshida, N., Tanaka, T., Katsuyama, M., Hasumoto, K., Murata, T., Hirata, M., Ushikubi, F., Negishi, M., Ichikawa, A. and Narumiya, S. (1997). Failure of parturition in mice lacking the prostaglandin F receptor. *Science* **277**, 681-3.

Tanentzapf, G., Devenport, D., Godt, D. and Brown, N. H. (2007). Integrin-dependent anchoring of a stem-cell niche. *Nat Cell Biol* **9**, 1413-8.

Thompson, M. A., Ransom, D. G., Pratt, S. J., MacLennan, H., Kieran, M. W., Detrich, H. W., 3rd, Vail, B., Huber, T. L., Paw, B., Brownlie, A. J., Oates, A. C., Fritz, A., Gates, M. A., Amores, A., Bahary, N., Talbot, W. S., Her, H., Beier, D. R., Postlethwait, J. H. and Zon, L. I. (1998). The cloche and spadetail genes differentially affect hematopoiesis and vasculogenesis. *Dev Biol* **197**, 248-69.

Tingaud-Sequeira, A., Andre, M., Forgue, J., Barthe, C. and Babin, P. J. (2004). Expression patterns of three estrogen receptor genes during zebrafish (Danio rerio) development: evidence for high expression in neuromasts. *Gene Expr Patterns* **4**, 561-8.

Trede, N. S. and Zon, L. I. (1998). Development of T-cells during fish embryogenesis. *Dev Comp Immunol* **22**, 253-63.

Trinh, L. A., Meyer, D. and Stainier, D. Y. (2003). The Mix family homeodomain gene bonnie and clyde functions with other components of the Nodal signaling pathway to regulate neural patterning in zebrafish. *Development* **130**, 4989-98.

Trinkaus, J. P. (1984). Mechanism of *Fundulus* epiboly-- a current view. *Amer Zool* **24**, 673-88.

Trowbridge, J. J., Xenocostas, A., Moon, R. T. and Bhatia, M. (2006). Glycogen synthase kinase-3 is an in vivo regulator of hematopoietic stem cell repopulation. *Nat Med* **12**, 89-98.

Ulrich, F., Concha, M. L., Heid, P. J., Voss, E., Witzel, S., Roehl, H., Tada, M., Wilson, S. W., Adams, R. J., Soll, D. R. and Heisenberg, C. P. (2003).

Slb/Wnt11 controls hypoblast cell migration and morphogenesis at the onset of zebrafish gastrulation. *Development* **130**, 5375-84.

Ulrich, F., Krieg, M., Schotz, E. M., Link, V., Castanon, I., Schnabel, V., Taubenberger, A., Mueller, D., Puech, P. H. and Heisenberg, C. P. (2005). Wnt11 functions in gastrulation by controlling cell cohesion through Rab5c and E-cadherin. *Dev Cell* **9**, 555-64.

Van Doren, M. (2007). Much HUBbub about stem-cell niches. *Nat Cell Biol* **9**, 1344-5.

Van Raay, T. J., Coffey, R. J. and Solnica-Krezel, L. (2007). Zebrafish Naked1 and Naked2 antagonize both canonical and non-canonical Wnt signaling. *Dev Biol* **309**, 151-68.

Vega, S., Morales, A. V., Ocana, O. H., Valdes, F., Fabregat, I. and Nieto, M. A. (2004). Snail blocks the cell cycle and confers resistance to cell death. *Genes Dev* **18**, 1131-43.

Villablanca, E. J., Pistocchi, A., Court, F. A., Cotelli, F., Bordignon, C., Allende, M. L., Traversari, C. and Russo, V. (2007). Abrogation of prostaglandin E2/EP4 signaling impairs the development of rag1+ lymphoid precursors in the thymus of zebrafish embryos. *J Immunol* **179**, 357-64.

Vogeli, K. M., Jin, S. W., Martin, G. R. and Stainier, D. Y. (2006). A common progenitor for haematopoietic and endothelial lineages in the zebrafish gastrula. *Nature* **443**, 337-9.

von der Haar, T. and Tuite, M. F. (2007). Regulated translational bypass of stop codons in yeast. *Trends Microbiol* **15**, 78-86.

von der Hardt, S., Bakkers, J., Inbal, A., Carvalho, L., Solnica-Krezel, L., Heisenberg, C. P. and Hammerschmidt, M. (2007). The Bmp gradient of the zebrafish gastrula guides migrating lateral cells by regulating cell-cell adhesion. *Curr Biol* **17**, 475-87.

Wang, D. and Dubois, R. N. (2006). Prostaglandins and cancer. *Gut* **55**, 115-22.

Wang, H., Singh, S. R., Zheng, Z., Oh, S. W., Chen, X., Edwards, K. and Hou, S. X. (2006). Rap-GEF signaling controls stem cell anchoring to their niche through regulating DE-cadherin-mediated cell adhesion in the Drosophila testis. *Dev Cell* **10**, 117-26.

Warga, R. M., Kane, D. A. and Ho, R. K. (2009). Fate mapping embryonic blood in zebrafish: multi- and unipotential lineages are segregated at gastrulation. *Dev Cell* **16**, 744-55.

Warga, R. M. and Nusslein-Volhard, C. (1999). Origin and development of the zebrafish endoderm. *Development* **126**, 827-38.

Wienholds, E., van Eeden, F., Kosters, M., Mudde, J., Plasterk, R. H. and Cuppen, E. (2003). Efficient target-selected mutagenesis in zebrafish. *Genome Res* **13**, 2700-7.

Williams, N. and Jackson, H. (1980). Limitation of macrophage production in long-term marrow cultures containing prostaglandin E. *J Cell Physiol* **103**, 239-46.

Willot, V., Mathieu, J., Lu, Y., Schmid, B., Sidi, S., Yan, Y. L., Postlethwait, J. H., Mullins, M., Rosa, F. and Peyrieras, N. (2002). Cooperative action of ADMP- and BMP-mediated pathways in regulating cell fates in the zebrafish gastrula. *Dev Biol* **241**, 59-78.

Wilson, H. V. (1907). A New Method by Which Sponges May Be Artificially Reared. *Science* **25**, 912-915.

Wise, S. B. and Stock, D. W. (2006). Conservation and divergence of Bmp2a, Bmp2b, and Bmp4 expression patterns within and between dentitions of teleost fishes. *Evol Dev* **8**, 511-23.

Wolf, K., Mazo, I., Leung, H., Engelke, K., von Andrian, U. H., Deryugina, E. I., Strongin, A. Y., Brocker, E. B. and Friedl, P. (2003). Compensation mechanism in tumor cell migration: mesenchymal-amoeboid transition after blocking of pericellular proteolysis. *J Cell Biol* **160**, 267-77.

Wu, S. Y. and McClay, D. R. (2007). The Snail repressor is required for PMC ingression in the sea urchin embryo. *Development* **134**, 1061-70.

Wu, T. (2006). Cyclooxygenase-2 in hepatocellular carcinoma. *Cancer Treat Rev* **32**, 28-44.

Wymann, M. P. and Schneiter, R. (2008). Lipid signalling in disease. *Nat Rev Mol Cell Biol* **9**, 162-76.

Yamanaka, Y., Mizuno, T., Sasai, Y., Kishi, M., Takeda, H., Kim, C. H., Hibi, M. and Hirano, T. (1998). A novel homeobox gene, dharma, can induce the organizer in a non-cell-autonomous manner. *Genes Dev* **12**, 2345-53.

Yamashita, S., Miyagi, C., Fukada, T., Kagara, N., Che, Y. S. and Hirano, T. (2004). Zinc transporter LIVI controls epithelial-mesenchymal transition in zebrafish gastrula organizer. *Nature* **429**, 298-302.

Yap, A. S., Crampton, M. S. and Hardin, J. (2007). Making and breaking contacts: the cellular biology of cadherin regulation. *Curr Opin Cell Biol* **19**, 508-14.

Yen, J. H., Khayrullina, T. and Ganea, D. (2008). PGE2-induced metalloproteinase-9 is essential for dendritic cell migration. *Blood* **111**, 260-70.

Yook, J. I., Li, X. Y., Ota, I., Fearon, E. R. and Weiss, S. J. (2005). Wnt-dependent regulation of the E-cadherin repressor snail. *J Biol Chem* **280**, 11740-8.

Yook, J. I., Li, X. Y., Ota, I., Hu, C., Kim, H. S., Kim, N. H., Cha, S. Y., Ryu, J. K., Choi, Y. J., Kim, J., Fearon, E. R. and Weiss, S. J. (2006). A Wnt-Axin2-GSK3beta cascade regulates Snail1 activity in breast cancer cells. *Nat Cell Biol* **8**, 1398-406.

Yoshimatsu, K., Golijanin, D., Paty, P. B., Soslow, R. A., Jakobsson, P. J., DeLellis, R. A., Subbaramaiah, K. and Dannenberg, A. J. (2001). Inducible microsomal prostaglandin E synthase is overexpressed in colorectal adenomas and cancer. *Clin Cancer Res* **7**, 3971-6.

Zhou, B. P., Deng, J., Xia, W., Xu, J., Li, Y. M., Gunduz, M. and Hung, M. C. (2004). Dual regulation of Snail by GSK-3beta-mediated phosphorylation in control of epithelial-mesenchymal transition. *Nat Cell Biol* **6**, 931-40.

Zhu, T., Gobeil, F., Vazquez-Tello, A., Leduc, M., Rihakova, L., Bossolasco, M., Bkaily, G., Peri, K., Varma, D. R., Orvoine, R. and Chemtob, S. (2006). Intracrine signaling through lipid mediators and their cognate nuclear G-protein-coupled receptors: a paradigm based on PGE2, PAF, and LPA1 receptors. *Can J Physiol Pharmacol* **84**, 377-91.

Zohn, I. E., Li, Y., Skolnik, E. Y., Anderson, K. V., Han, J. and Niswander, L. (2006). p38 and a p38-interacting protein are critical for downregulation of E-cadherin during mouse gastrulation. *Cell* **125**, 957-69.

Zon, L. I. (1995). Developmental biology of hematopoiesis. *Blood* **86**, 2876-91.

Zorn, A. M. and Wells, J. M. (2007). Molecular basis of vertebrate endoderm development. *Int Rev Cytol* **259**, 49-111.